Combustion Behavior of Lumpy Coke Particle under Shaft Kiln Conditions

Dissertation

Zur Erlangung des akasdemischen Grades

Doktoringenieur

(Dr. Ing.)

vorgelegt von

M.Sc. Nyein Nyein Linn

geb. am 07.01.1985

in Namtu, Shan state, Myanmar

genehmigt durch die
Fakultat fur Verfahrens- und Systemtechnik
der Otto-von-Guericke-Universität Magdeburg

Gutachter:

Prof. Dr.-Ing. Eckehard Specht
Institute of Fluid Dynamics and Thermodynamics,
Otto-von-Guericke- Universität Magdeburg.

Prof. Dr-Ing. Fabian Herz

Hochschule Anhalt, Köthen.

JProf. Dr.-Ing. Benoît Fond
Institute of Fluid Dynamics and Thermodynamics,
Otto-von-Guericke- Universität Magdeburg.

Eingereicht am : 28.06.2017

Promotionskolloquium am : 26.09.2017

Preface

This dissertation is submitted to Otto von Guericke University, Magdeburg for the degree of Doctor of Philosophy. The research described herein was conducted under the supervision of **Prof. Eckehard Specht** between April 2014 and June 2017. To the best of my knowledge, this work is original, except where suitable references are made to pervious works. Neither this, nor any substantially similar dissertation has been submitted for degree, diploma or qualification at any other university or institution.

Nyein Nyein Linn

Magdeburg, 21.03.2018

Acknowledgement

I would like to show my sincere gratitude to my enthusiastic supervisor **Prof. E. Specht** for providing me the opportunity to work with him and pursue a doctoral degree. He has been supportive since the first day of my Ph.D student life in Germany. He continuously encouraged me to finish this work successfully and discussed about the problems in shaft kiln applications. I appreciate all his contributions of time, patience, insightful discussion.I could not imagine me without him, I would not have this day. It has been an honor to be his student.

Besides my advisor, I would like to thanks my thesis committee member, **Prof. Dr.-Ing. Fabian Herz** and **JProf. Dr.-Ing. Benoît Fond** for their insightful comments and elaborated review.

Dr.-Ing H. Woche provided his guidance during my study. I would like to thank **Herr Bassem,** especially for his support along with for the experimental part of the work with his friendly nature and supportive behavior during experiments. I would love to thank our secretary **Frau Hasemann** for her continuous support for the administration part of the work.

I would like to personally thank all my colleagues for their encouragement and understanding. I had wonderful time with **Dr.-Ing. Nallathambi**, **Dr.-Ing. Pavan Penumakala** and **Gaurav** in office for the whole Ph.D study. **Dr. –Ing. Nallathambi** is a great and best friend. His unconditional support for both personal and professional life has been essential all these years, through which my motivation towards the research has been enhanced. Further, I extend my sincere thanks to my dearest (colleague), Tino, Aina, Sabariman, Abdul, Adnan, Ali, Kamyar, Fang, Jie, Nil and Jacob. Similarly, Arputha, Divya and Nimmy always encouraged me to complete the dissertation. I got lot of support and

inspiration from them.
One word thank you is not sufficient to my dearest friend **Soe Myat Htwe and Saya Ngin**, who motivated (forced) me to pursue research in Germany. **Phyu Phyu Win** who is always with me from the day we first met, who stands as an example of a friend and I learned a lot from her. I would say, one of the best persons I have ever seen.

I have an amazing family, unique in many ways, and their support has been unconditional all these years. Especially, I thank my parents, who believe me and encourage me all the time. I would like to thank my brother and sister: Myo Thant Linn, Paing Paing, Noe Noe and Apukyu, Ma Line, Ma Chawsu, Catherine and Matthias, Marei's family, Jugern, Markus and Jana, Ragu, Alpha, Sonalini, Chandu, Monika, Gauri, Prakash, Ashkey and Prabhu for their continuous encouragement and support. I specially thank my teachers whose wish to see me as a Doctor Engineer.

I also personally thank all my Myanmar friends Ko Stephen, Fau members, Ma Amy family, Aunty Maw family, Aunty Mar family, Aunty Kyin Than family, Win, Suan, and Ma Mon family. I would have missed a lot if I didn't meet them.

Finally, I would like to express my sincere thanks to every individual German citizen for contributing either directly or indirectly. During my stay in Germany, I learned self-discipline, punctuality and time management from the fellow citizens of Germany.

I would like to acknowledge the financial support provided by the DAAD (German Exchange Service).

Abstract

The main focus of the current research work is to understand the combustion behavior of coke in shaft kilns and cupola furnaces. A mathematical model has been developed for the combustion inside the shaft kiln which includes the situation of counter current flow and the variation in excess air number. Numerical analyses are reported to describe the importance of Boudouard reaction during the combustion process where the value of excess air number is less than 1. Both the experimental and numerical results reported in the present study suggest that Boudouard reaction has an influence in the low temperature process.

The reaction with oxygen is dominated by mass transfer. The reaction with carbon dioxide (Boudouard reaction) is dominated by the chemical kinetics. To determine this, spherical coke particles with 30-40mm diameter were gasified with carbon dioxide and nitrogen mixtures in a tube furnace. The influence of the Boudouard reaction on the combustion time and the length of combustion zone in mixed feed shaft kilns are discussed. The function of excess air number, temperature of coke and size of coke are investigated. By using the experimental results, the reaction coefficient of coke has been determined. Experiments show that the reaction coefficient is dependent on the type of coke. The weight loss of coke reaches maximum 30% during the gasification with carbon dioxide. Reaction coefficient influences the process temperature significantly.

Simulation of coke particle size distribution has been conducted using a steady state model that is coupled with the chemical reactions. A model is proposed in current research, which is capable to involve the particle size distribution. It is remarkable that the particle size distribution resulting from the model is close to reality.

The set of equations describes chemical reactions, heat and mass transfer between gas and solid phases. The model predicts the temperature of gas, coke,

conversion degree, mass flow rate, gas concentrations and rate of change of mass.

Zusammenfassung

Der Schwerpunkt der aktuellen Forschung besteht in der Untersuchung des Verbrennungsverhaltens von Koks in Schacht- und Kuppelöfen. Es wurde ein mathematisches Modell für die Verbrennung innerhalb des Schachtofens entwickelt, das Gegenstromfluss sowie eine variierende Luftüberschusszahl berücksichtigt. Numerische Analysen werden durchgeführt, um die Bedeutung der Boudouard-Reaktion während des Verbrennungsprozesses zu beschreiben, wobei die Luftüberschusszahl kleiner als 1 ist. Sowohl die experimentellen als auch die numerischen Ergebnisse, die in der vorliegenden Studie präsentiert werden, deuten darauf hin, dass die Boudouard-Reaktion einen Einfluss auf den Niedrigtemperaturprozess ausübt.

Die Reaktion mit Sauerstoff beruht hauptsächlich auf Stoffübertragung. Die Reaktion mit Kohlendioxid (Boudouard-Reaktion) wird von chemischer Kinetik bestimmt. Um dies zu untersuchen, wurden sphärische Kokspartikel mit einem Durchmesser von 30-40 mm mit einem Kohlendioxid-Stickstoff-Gemisch in einem Röhrenofen vergast. Die Auswirkung der Boudouard-Reaktion auf die Verbrennungszeit und die Ausdehnung der Verbrennungszone in Mischförderschachtöfen werden diskutiert und der Einfluss der Luftüberschusszahl, der Temperatur und Größe des Koks werden untersucht. Unter Verwendung der experimentellen Ergebnisse wurde der Reaktionskoeffizient von Koks bestimmt. Versuche zeigen, dass der Reaktionskoeffizient von der Art des Kokses abhängig ist. Der Gewichtsverlust von Koks erreicht bei der Vergasung mit Kohlendioxid maximal 30% und der Reaktionskoeffizient beeinflusst die Prozesstemperatur deutlich.

Die Simulation der Größenverteilung der Kokspartikel wurde unter Verwendung eines stationären Modells durchgeführt, das chemische Reaktionen beinhaltet. In der aktuellen Forschung wird ein Modell vorgeschlagen, das in der Lage ist, die Partikelgrößenverteilung zu berücksichtigen. Es ist bemerkenswert, dass die im Modell berechnete Partikelgrößenverteilung gut mit Daten aus der industriellen Praxis übereinstimmt.

Das Gleichungssystem beschreibt chemische Reaktionen, Wärme- und Stoffübertragung zwischen gasförmigen und festen Phasen. Das Modell liefert Prognosen bezüglich den Temperaturen von Gas und Koks, des Umwandlungsgrads, des Massendurchflusses, der Gaskonzentrationen und sowie der Geschwindigkeit der Massenumwandlung.

Nomenclatures

A	area	[m2]
c_p	specific heat capacity	[kJ/kg/K]
d	particle diameter	[m]
$\bar{d}$	Sauter diameter	[m]
$\dddot{\bar{d}}$	particle mean diameter	[m]
D	diffusion coefficient	[m2/s]
D_{kiln}	diameter of the kiln	[m]
E	activation energy	[kJ/kmol]
h_C	reaction enthalpy regarding to carbon	[kJ/kg]
h_{CO}	reaction enthalpy regarding to CO2	[kJ/kg]
H	height of kiln	[m]
k	reaction coefficient	[m/s]
L	air demand	[kga/kgf]
$\dot{M}$	mass flow rate	[kg/s]
M	molecular weight	[kg/kmol]
n	number of particles	[-]
O	specific surface area	[m2/m3]
p	partial pressure of gas	[Pa]
P	Total pressure,	[Pa]
q	heat transfer	[W]
$\dot{q}$	heat flux	[W/m2]
$\dot{Q}$	heat flow rate	[W]
R	universal gas constant	[J/mol/K]
t	combustion time	[min]
T	temperature	[oC] or [K]
$\tilde{v}$	volume fraction of the particles	[m3/m3]
V	total volume of the particles	[m3]
w	velocity	[m/s]
X	conversion degree	[-]
Z	length of the kiln	[m]

Greek symbols

α	heat transfer coefficient	[W/m^2/K]
β	mass transfer coefficient	[m/s]
ε	emissivity	[-]
λ	excess air number	[-]
λ	thermal conductivity coefficient	[W/m/K]
ρ	density	[kg/m^3]
σ	Stefan-Boltzmann constant	[W/m^2/K^4]
ν	kinematic viscosity	[m^2/s]
ψ	void fraction	[-]

Subscripts

amb	ambient
bed	packed bed
conv	convection
c	coke
co	co-current flow
CO	carbon monoxide
co_2	carbon dioxide
f	furnace
g	gas
O_2	oxygen
rad	radiation
s	stone
t	total
z	length

Dimensionless number

Nu	Nusselt number
Pr	Prandtl number
Re	Reynolds number
Sc	Schmidt number
Sh	Sherwood number

Table of Contents

COMBUSTION BEHAVIOR OF LUMPY COKE PARTICLE UNDER SHAFT KILN CONDITIONS I

PREFACE II

ACKNOWLEDGEMENT III

ABSTRACT V

ZUSAMMENFASSUNG VII

NOMENCLATURES IX

1 INTRODUCTION 1

1.1 Coke 1

1.2 Shaft kiln: process description and applications 1

1.3 Copula Furnace for melting 2

1.4 Shaft kiln problems 4

1.5 Motivation 5

2 LITERATURE REVIEW 7

2.1 Introduction 7

2.2 Model Formulation 9

2.2.1 Void fraction 9

2.2.2 Pressure drop 10

2.3 Heat transfer of packed bed 11

2.4 Mass transfer of packed bed 13

2.5 Reaction coefficient for the Boudouard 14

3 COKE PARTICLES WITH HYPER STOICHIOMETRIC AIR FLOW 17

3.1 The Reaction model 17

3.2 Reaction Mechanism 18

3.3 Mass transfer 19

3.4 Analytical Solution for the combustion time 21

3.4.1 Basic equation for the combustion time 21

3.4.2 For countercurrent flow 23

3.4.3 For the co-current flow 25

3.5 Particles size distribution inside the shaft kiln 26

3.6 Simulation results of coke particle distribution 29

4 CASE OF COKE COMBUSTION WITH HYPO STOICHIOMETRIC AIR FLOW 40

4.1 Introduction 40

4.2 The model: Case of combustion with excess air number <1 40

4.3 Experimental Method 42

4.3.1 Experimental Setup 42

4.3.2 Experimental Measurements 44

4.4 Experimental Analysis 44

4.4.1 Burning behavior of the coke in carbon dioxide atmosphere and air 44

4.4.2 Conversion of Coke (mass balance and CO measurement) 45

4.4.3 Kinetic model for the coke 46

4.5 Simulations of kinetics model for the coke reaction 49

4.5.1 Change of mass with combustion time 49

4.5.2 Gas Concentration 50
4.5.3 Rate of change of mass 52
4.5.4 Combustion time with Boudouard effects 53

4.6 Summary 54

5 MODELLING OF COKE COMBUSTION INSIDE SHAFT KILN WITH GIVEN STONE TEMPERATURE 55

5.1 Introduction 55

5.2 Energy and mass balances and equations 57
5.2.1 Process description 57
5.2.2 One dimensional approach 57
5.2.3 Determination of heat transfer coefficients for the kiln 58
5.2.4 Energy balance 59

5.3 Mass Balances 61

5.4 Operating parameters 62
5.4.1 Parameter for the model 62
5.4.2 Solving the system 63

5.5 Influence of the excess air number 64

5.6 Influence of the size of coke particles 66

5.7 Influence of the initial stone temperature 68

5.8 The influence of the heat radiation 71

5.9 Case of $\boldsymbol{\lambda} \geqslant 1$ with Boudouard effect 74

5.10 Case of $\lambda < 1$ with Boudouard effect 76

5.11 Influence of initial stone temperature when $\boldsymbol{\lambda} < 1$ 83

5.12 Influence of mass flow rate 86

5.12 Influence of amount of coke 87

5.13 Conclusion 90

6 MODELLING OF COKE COMBUSTION WITH PROCESS TEMPERATURE . 91

6.1 The model 91

6.2 Energy balance on stone particle 91

6.3 Results and discussions 92
6.3.1 Influence of excess air number 92
6.3.2 Initial stone temperature 94
6.3.3 Influence of stone particle size 95

6.4 Summary 99

7 CONCLUSION 100

REFERENCES 102

LIST OF PUBLICATIONS 105

CURRICULUM VITAE 106

1 Introduction

1.1 Coke

Coke is a solid fuel with high carbon content. The composition of coke depends on its origin and generally contains 90-97% carbon and 1% residual volatile, 1% sulfur and 1-8% of ash layer. Coke has been widely used over the centuries as a source of thermal energy as a high-carbon fuel for hard burnt lime, soda and sugar production, melting of cast iron and rock for mineral wool in cupola furnace, pig iron in a blast furnace. In general, coke with the uniform particle size of 20 to 100 mm is suitable for different applications. For example, the large sizes of coke particles are used in melting furnace.

1.2 Shaft kiln: process description and applications

Shaft kiln is probably the first type of kiln that was used for many industries and various fuels have been used. The solid particles move slowly downward through the kiln by the gravitational force. The particles are continuously charged from the top of the kiln, while air is injected from the bottom. Heat is generated by oxidation of fuel coke particles. The process of the shaft kiln is based on countercurrent flow principle between air and fuel. It moves slowly downwards through three zones namely; preheating zone, combustion zone and cooling zone.

The coke particle size decreases during the combustion process. The combustion air is fed into the kiln below the cooling zone. As soon as the air comes in contact with the coke, oxidation begins and the gas temperature rises steeply. Heat for the calcination is generated by oxidation of coke particles in combustion zone in which the coke reacts with oxygen to form carbon monoxide. It reacts in the gas phase with the oxygen to produce carbon dioxide. Towards the top of the kiln, the concentration of carbon dioxide in gas phase rises and oxygen concentration decreases. The carbon dioxide reacts with coke and in turn produces carbon monoxide, which further reacts with oxygen in the gas as long as it is available. Coke lump shape and surface area to volume ratios which would provide additional information on the gasification behavior of coke were considered to impact on coke reactivity. With an excess air number less than one,

a Boudouard-zone is formed between the preheating zone and the combustion zone, where almost no oxygen is available and coke reacts only with carbon dioxide to form carbon monoxide.

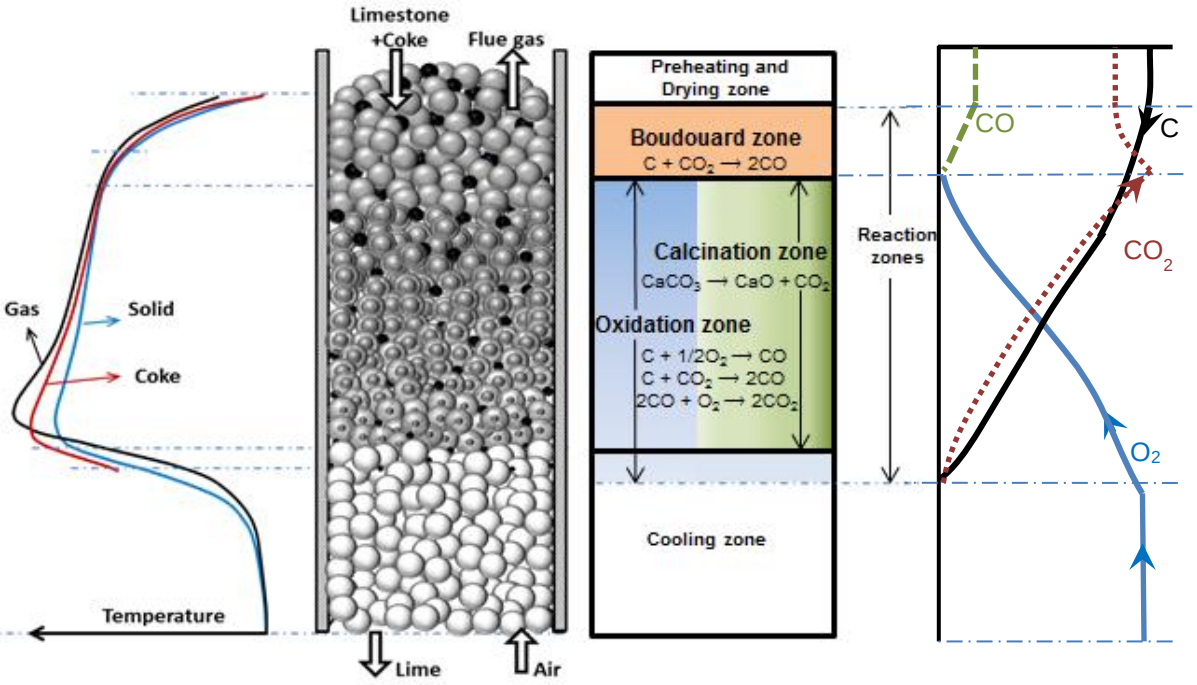

Figure 1.1: Schematic of Mixed feed shaft kiln and mass profile of solid and gas

Mixed feed kilns currently in operation generally use coke or anthracite as the fuel for lime burning. When the coke is used as the fuel, it produces high reactivity lime. Figure 1.1 shows schematically a shaft kiln as an example for the calcination of limestone ($CaCO_3 \rightarrow CaO + CO_2$). Limestone and coke particles are filled from the top of the kiln and then poured into the shaft and slowly downwards through three zones onto the packed bed. The coke starts to burn when the temperature raises about 600 ^{o}C. The coke burn in the reaction zone and limestone is decomposed in the calcination zone when the temperature reaches for calcination in the range of 820 and 900 ^{o}C [1]. The kiln is fed with a feed of stone size in a range of 30 to 150 mm. The operating conditions of soda and sugar production are different from the used of lime production because it is necessary to produce flue gas with the high amount of carbon dioxide.

1.3 Copula Furnace for melting

The coke bed shaft type cupola furnace is a highly effective process for smelting iron in casting production. Coke produced from blends of coking

coals has a wide range of applications and 90% of the coke is used for iron production in the blast furnace [8].

A furnace was the primary method for melting used in iron foundries. The air burns with the coke mainly to CO_2. Then CO_2 reacts with coke to CO according to the Boudouard reaction $C + CO_2 \rightarrow 2CO$. The produced CO prevents the oxidizing of the iron. In the case of the blast furnace, the CO reduces the iron ore according to $FeO + CO \rightarrow Fe + CO_2$. The CO_2 reacts again with the coke to give CO. Initially, a bed of coke is laid in the cupola above the bed and is ignited. The raw materials typically consist of pig iron, scrap or alloy steel and domestic returns which are charged through the opening at the top of the cupola. Air for proper combustion is supplied through the tuyere provided at the bottom. Then the air reacts with the packed coke and with liquid metal as it ascends in the shaft. The air has to be burnt with an excess air number lower than one so that CO is produced to protect the iron from oxidation. The heat generated from coke combustion with gas is the major source of energy for the melting process and is mainly consumed by heating and melting of scrap metal (iron and steel). Schematic of cupola furnace is shown in Figure 1.2 [5]. After melting of scrap, coke, which is the only solid, forms a packed bed in the high temperature region. In the shaft, the scrap melts when the temperature reaches its melting point and forms numerous liquid drops in the coke bed. The mineral charge is heated to the molten state at the temperature of 100 to 1650^{o}C in a coke-fired cupola furnace. Coke combustion in the furnace produces carbon monoxide, carbon dioxide, sulphur oxide and nitrogen oxide emissions.

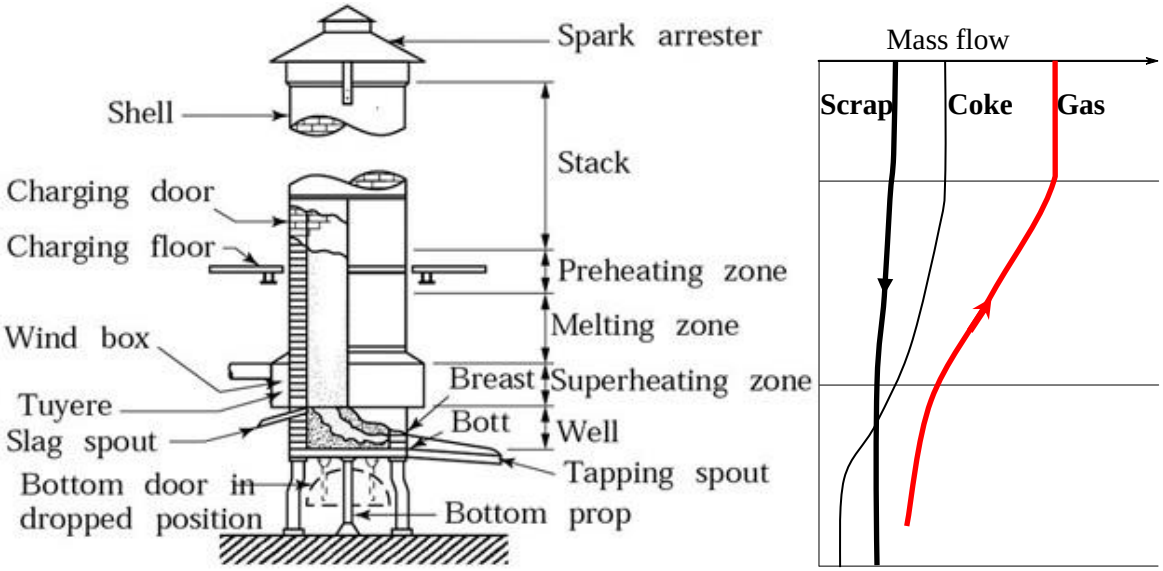

Figure 1.2: Schematic of Cupola furnace and mass flow profile [5]

The reaction between C and CO_2 known as Boudouard reaction ($C+CO_2 \rightarrow 2CO$) has always been a subject of study because of its scientific as well as technological importance. Being highly endothermic and consuming carbon directly from the coke in many metallurgical and industrial processes, this reaction has gained much importance. For example, the blast furnace process to reduce iron ore [10], the cupola furnace process for melting iron scrap, the shaft kiln process to produce lime and dolomite ($CaCO_3 \rightarrow CaO + CO_2$), the production process of manganese and chromium alloy, the production of micro-porous materials of valuable properties from carbonaceous surfaces, etc. Modeling of a process involving the influence of Boudouard reaction can be described mathematically with the knowledge of reaction kinetic parameters and their dependence on the type of coke. Boudouard reaction is an important process inside the kiln, especially on a blast furnace. The reduction of iron oxides is not achieved by carbon directly, as reactions between solids are typically very slow, but by carbon monoxide. Based on a number of studies, it has been found that internal surface area changes with the conversion of the particle.

1.4 Shaft kiln problems

The process in the shaft kiln bases on the countercurrent flow of charged materials and combustion gas. Therefore, it is difficult to predict the combustion time, which becomes one of the major problems. Combustion time depends on the density and diameter of the charged particles. Although shaft kiln has been

used over the centuries, the investigation of the fundamentals which affect its performance is restricted. For the effective operation of a kiln, the size and type of coke should be properly adjusted.

The properties of coke and size can have a significant impact on the performance of kiln and process of materials. With non-uniform coke particle size, the height of zone of the kiln changes, where the small particle of coke burn fast, which leads to the movement of preheating and combustion zones. Therefore, the flue gas exits from the kiln with a high temperature which causes high energy loss. Particle distribution of coke inside the kiln is critical to evaluate a kiln operation. The main problem is that large feed particle which is more difficult to calcine uniformly and it also required longer burning time. Imperfect conversion reactions inside the kiln and incomplete mixing of limestone and coke can also be a problem.

1.5 Motivation

It can be clearly seen that measurements are impossible inside shaft kilns because of high temperature in burning zone and large size of the kiln. From the industrial experience, it is known that every coke of different origin has an individual combustion behavior. Then this study is to research in which way parameters influence the combustion process. The knowledge gap from the literature is the reaction zones are overlapped each other. Moreover, the influences of size distribution have been investigated to understand the physical process and interaction energy lost during discharging or with flue gases. For modelling the process in the kiln, the combustion behavior of coke has to be studied. It depends on the following factors:

- Oxidization reaction
- Boudouard reaction
- Mass transfer
- Heat transfer by convection and radiation
- Size distribution of solid particle
- Ash layer
- Excess air number
- Density of coke (type of coke)

- Process temperature (coke, stone and gas)
- Countercurrent flow of the air and the fuel

To generalize the combustion behavior of coke, all these factors have to be studied. This work has been done by systematically analyzing coke combustion, gasification, and radiation and convection effect during combustion. Much more emphasis has been put on the modeling and understanding of the physical and chemical processes and their interaction which dominate the burning phenomenon. The kinetic coefficient for gasification of coke by CO_2 was estimated by performing experimental investigation. The objective of this work is to provide insight to study and understand the behavior of coke combustion in specific process. By analyzing the influences of the combustion of coke with different operating conditions (excess air number, throughput, the size of particles, reactivity), it is easier to optimize the industrial kiln's efficiency.

The thesis is structured into four main parts: the analytical study of combustion of coke particles with hyper stoichiometric air flow including the size distribution and different individual coke diameter, the coke combustion with the environment of CO_2 (experimental investigation), combustion of coke particles with hypo stoichiometric air flow, modelling of coke particle with constant stone temperature and modelling of coke particle with process temperature.

2 Literature review

2.1 Introduction

Many studies have been carried out to study the combustion in order to a better design of shaft kilns. The main types of shaft kilns are the single shaft countercurrent flow heating kiln and multiple shaft parallel flow heating kiln. In most cases, the studies mainly focused on lime burning. EI-Fakharany [1] studied the modelling of monodisperse coke combustion particle in a lime shaft kiln using unsteady state condition. The length of the combustion zone was given as the initial value. In the model, she showed that the influence of the fuel ratio, excess air number, limestone size and coke size are strong on kiln performance while the influence of limestone reactivity and coke reactivity are weak. And she found that the conversion of limestone and coke depend on size of the particles are the opposite effect. Herz. F [2] studied the combustion behavior of coke and anthracite with oxygen. They showed that the combustion is dominated by mass transfer and that the ash layer has an influence. Similarly, the influence of the excess air number in normal shaft kiln was reported by Herz.F [12], demonstrated the dependence of specific energy consumption on the carbon dioxide concentration in the flue gas based on the experiments he performed. Masoud.P [3] studied the effect of parameters: coke particle size, inlet air velocity and the amount of coke for sintering bed. Verma [4] simulated a mixed-fixed kiln fired with coke, however, at each zone boundary temperature which is obtained from simulated and given as boundary and is observed to be different in his study. The analysis and simulation of combustion of coke in shaft kilns are developed from the mass and energy balances. Ulzama [5] studied the reaction of coke samples in carbon dioxide. He showed that the reaction is dominated by chemical kinetics which is dependent on the origin of the coke. Reaction with CO_2 with an activated carbon at 900^{o}C was tested by Sabri Ergun [6]. They reported the reactivity of carbon was calculated at high pressure for fine particle and the pressure reactivity ration can either increase or decrease with increasing pressure, depending upon the diffusion limitation. Hallak [7] simulated and found that CO formed during the Boudouard reaction strongly influences the energy consumption. According to the demand of the industrial application, researchers have studied the coke

combustion in shaft kilns. Hai Do [8] developed a numerical model for normal lime shaft kiln, which takes into account the heat and mass transfer to calculate dynamically the complete temperature and concentration profiles of the gas and solid. Analysis of the coke as a reducing agent of ore, heat source of blast furnace by two reactions was performed by Yoshoaki Yamazaki [10]. Coke reacts with oxygen at the bottom part of a blast furnace and coke reacts with carbon dioxide at the middle part of the blast furnace. The model was built upon lumpy coke and presented the method to enhance coke solution- loss reactivity was briefly discussed. The fundamental investigations to support both the reactivity and the strength have studied in the blast furnace. However, no studies are available on dealing with coke reactions under shaft kiln conditions including reaction with oxygen and carbon dioxide. The literature review provides very few information on the combustion of coke under shaft kiln conditions including operation parameter and design parameters.

In cupola, liquid metal drops downward in the coke bed and they react with coke and upwards coming gas. The heat transfer and combustion reaction related to melting process in the shaft kiln had been introduced. Much work has been done on the heat transfer, fluid flow and combustion reaction of the melting process, the temperature profiles of the gaseous and solid phases in the shaft. Many studies were focused on the investigation of temperature and gas composition profiles in the shaft on the basis of heat balance and fluid flow in the process. However, those investigations did not address the combustion time with chemical reactions that govern the product metal composition.

The coke has to be burnt out completely before passing it onto the cooling zone in lime shaft kiln. Distribution depends on the type of mixing between stone and coke which would be either uniform mixing or incomplete mixing. The distribution of coke inside the kiln is critical to good kiln operation. The reason for the incomplete combustion of the coke and fuel inside the furnace is due to non-uniform size distribution of coke and limestone in bed. It leads to the rapid reduction of the temperature in the furnace. When the excess air number is larger than one, combustion time depends on mass transfer and is independent of reactivity. Size distribution and density are dominated by hyper stoichiometric air flow. In the case of the excess air number less than one, the fuel can no longer

be completely oxidized, which leads to high concentrations of CO in the flue gas. The reaction with the carbon dioxide, Boudouard reaction is encountered when the excess air number less than one and the process is reacting rate limited. Coke combustion is a complex process involving the combination of different aspects: heat and mass transfer and chemical kinetics. Where coke is used in mixed feed kiln, coke reacts with CO_2 to form CO. At high temperature and without enough oxygen for combustion, the coke has low reactivity according to the reduction of CO_2. The exhaust gases with high CO content are very hazardous for soda and sugar industries.

Shaft kilns are basically packed bed reactors with an upward-flow of hot gases passing counter-current the downward-flow of feed consisting of the solid particles [5]. A packed bed is characterized by the following parameters.

2.2 Model Formulation

2.2.1 Void fraction

The void fraction of the particle bed is normally defined as the free volume fraction of the bed and it can be calculated from the void volume and the total volume of the bed as:

$$\Psi = \frac{V_{void}}{V_{total}} = 1 - \frac{V_{solid}}{V_{total}}. \qquad (2.1)$$

Where $V_{void}, V_{solid}, V_{total}$ are the void volume, solid volume and total volume of the bed respectively. Shaft kilns are basically packed bed reactors with an upward-flow of hot gases passing counter-current the downward-flow of feed consisting of the solid particles. A packed bed is characterized by the void fraction. The void fraction is influenced by the method of charging (random or regular, lose or dense), particle shape (sphere, cylinder, lumpy, etc.) and particle size distribution. If the particles have the same diameter then the packing is called monodispersed and its void fraction is approximately 0.4. If there are only a few fine particles they fill in between the gaps of the big particles. As a result, the free bed volume and therewith the void fraction decreases considerably until the gaps are filled. The minimum value of the void fraction depends on the diameter ratio between the

coarse and the fine particles. The lower this ratio is the higher the value of the minimum void fraction becomes. If the ratio between the largest and the finest particle is lower than two, the decrease of the void fraction is relatively small. For this condition the pressure drop is not significantly increased.

2.2.2 Pressure drop

Pressure drop in a packed bed is important for designing the kiln and also to achieve the maximum efficiency. The gas flow through the packed bed causes a high pressure drop. Therefore, it is necessary to classify the solid to keep the pressure drop as low as possible. The pressure drop is influenced by the reciprocal value of the void fraction with the power of three and by the reciprocal particle size. In a packed bed with particles of different size, the small particles fall into the gap between the large particles and reduce the void fraction. A packed bed with particles of equal size has the lowest pressure drop. As a consequence, the particles have to be sieved and classified before fed into the kiln. The ratio between the diameter of the largest and the smallest particle in a kiln should be lower than two to avoid the high pressure drop.

A number of experimental and theoretical studies have been conducted on the pressure drop in the packed bed. The most widely used correlation is Ergun equation [6]. The Ergun equation is a combination of Kozeny-Carmen and Burke-Plumber equations for energy losses due to flow through a packed bed. When there is no flow through the packed bed, the gravitational force (including buoyancy) acts downward. The Ergun equation for pressure drop through the packed bed is as follows:

$$\frac{\Delta P}{\Delta L} = 150\,\frac{(1-\epsilon_b)^2}{{\epsilon_b}^3}\,\frac{\mu_f U}{(\varphi\overline{d_p})^2} + 1.75\,\frac{1-\epsilon_b}{{\epsilon_b}^3}\,\frac{\rho_f U^2}{\varphi\overline{d_p}}\,. \qquad (2\text{-}2)$$

The pressure drop along the length of the packed bed depends on void fraction(ϵ_b), the properties of fluid (viscosity (μ_f), and density (ρ_f)), velocity of fluid (U) and particle geometry,(φ) the spherical of particles and an equivalent particle diameter ($\overline{d_p}$) have to be calculated.

For the pressure drop in packed bed, consisting of spherical particles, exists the equation put forward by Brauer [9], which is similar to Ergun equation:

$$\frac{\Delta P}{\Delta L} = 160\ \frac{(1-\Psi)^2}{\Psi^3}\ \frac{\eta.w}{\bar{d_p}^2} + 3.1.\frac{(1-\Psi)}{\Psi^3}\ \frac{\eta.w^2}{\bar{d_p}}\ [\frac{\eta.(1-\Psi)}{\rho_f.w.\bar{d_p}}]^{0.1}\ . \qquad (2\text{-}3)$$

Brauer's correlation is based on experimental data and applies to a packed bed, consisting of spherical particles of the same diameter [9]. For the calculation of pressure drop for a bed consisting of spherical particles of different size, appropriate correction functions have to be considered. The first term of the Ergun equation describes the change of pressure by the viscous force and the second term describes inertia force. The constants are based on experimental data for many shapes of particles, but the equation is most accurate for spherical particles. The design of packed bed is based on the mechanism of heat and mass transfer, the flow and pressure drop of gas through the bed.

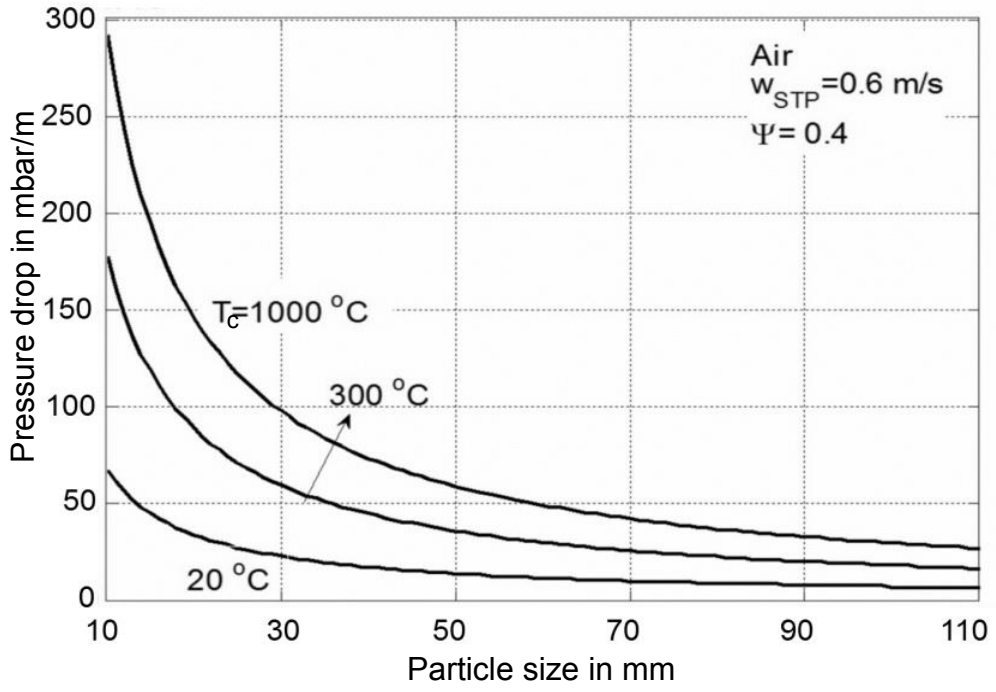

Figure 2.1: Influence of particle size on pressure drop [11]

2.3 Heat transfer in packed bed

The heat transfer from the gas to solid particles is dominated by convection in the model. The convective hear transfer is modeled based on Nusselt correlations for

single particles as described in detail in heat transfer in packed bed. The heat transfer coefficient is calculated from the correlation:

$$\alpha = \frac{Nu_b \cdot \lambda_g}{d_c} \quad . \tag{2-4}$$

Where d_c the size of the particle, λg, the gas thermal conductivity, Nu_b , the Nusselt number for the kiln and for the packed bed [11] is

$$Nu_b = 2 + 1.12 \cdot \mathrm{Re}^{\frac{1}{2}} \cdot \mathrm{Pr}^{\frac{1}{3}} \cdot \left(\frac{1-\Psi}{\Psi}\right)^{\frac{1}{2}} + 0.005 \cdot \mathrm{Re} \; . \tag{2-5}$$

The Reynolds number Re in Eq. (2-5) is defined as:

$$\mathrm{Re} = \frac{w.d}{\nu \cdot \psi}, \tag{2-6}$$

where w is the gas velocity if no packing was present (superficial velocity) , ν is the gas kinematic viscosity and d is the spherical characteristic diameter of particle. The Prandtl number is defined as:

$$\mathrm{Pr} = \frac{\nu \cdot \rho_G \cdot c_{pG}}{\lambda_G}, \tag{2-7}$$

where ρ_G is the density and c_{pG} is the specific heat capacity of the gas.

The convective heat transfer from gas phase to coke is calculated using

$$q_{gc} = \alpha_{gc} \cdot A_c (T_g - T_C) \quad . \tag{2-8}$$

Where A_C is the surface area of the coke per unit volume of the kiln. The calculation of A_C is described in later sections.

The convective heat transfer is slightly superposed by radiation. This is emitted mainly by the CO_2 from the decomposition and the fuel combustion, to use a heat transfer coefficient by radiation, which is defined as

$$q_{rad} = \varepsilon \cdot \sigma \cdot A_C (T_C^4 - T_S^4) \; . \tag{2-9}$$

Where ε is the emissivity, σ is the Stephan-Boltzmann constant (5.67_x10^{-8} W/m^2K^4). In the model, it is assumed that the coke particles have a uniform temperature. Since the temperature gradient in the coke particle in the combustion zone is at a minimum when the reaction rate is controlled by mass transfer.

2.4 Mass transfer in packed bed

The mass transfer coefficient of a single particles surface to the surrounding as is calculated by the Sherwood function. The Sherwood function for a single sphere particle in a laminar flow is given as:

$$Sh = 0.664.Re^{0.5}.Sc^{0.33} \quad . \tag{2-10}$$

And the convective mass transfer in a packed bed can be calculated from the Sherwood function, which is analogized to the Nusselt function [11] as:

$$Sh = 2 + 1.12.Re^{0.5}.Sc^{0.33}\frac{(1-\Psi)^{1/2}}{\Psi} + 0.05Re \quad . \tag{2-11}$$

Then the mass transfer coefficient of particles is calculated from:

$$\beta = \frac{D \cdot Sh}{d_{c,z}} \quad . \tag{2-12}$$

The Schmidt number is defined as:

$$\mathrm{Sc} = \frac{\nu}{\mathrm{D}} \ . \tag{2-13}$$

The influence of the mass transfer on diameter and temperature at different velocity is shown in figure 2.2 and 2.3. It can be observed that the larger diameter of coke, the lower value of mass transfer coefficient is. At high temperature, the mass transfer coefficient is higher compared to that of the lower temperature. Mass transfer coefficient varies in the range of velocity.

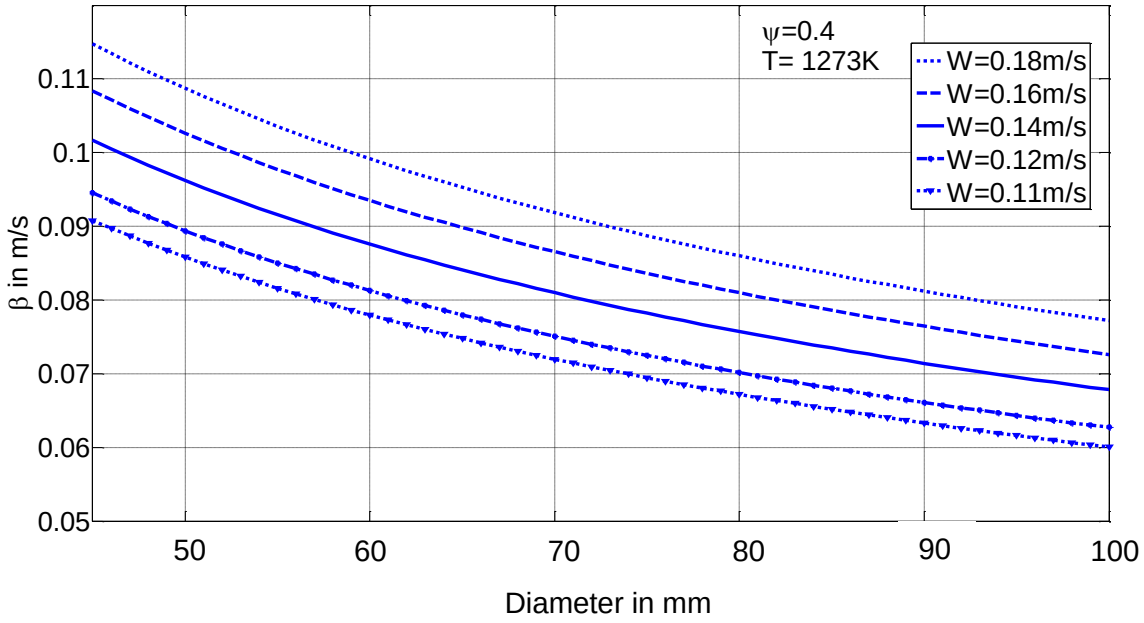

Figure 2.2: Influence of particle size on mass transfer coefficient

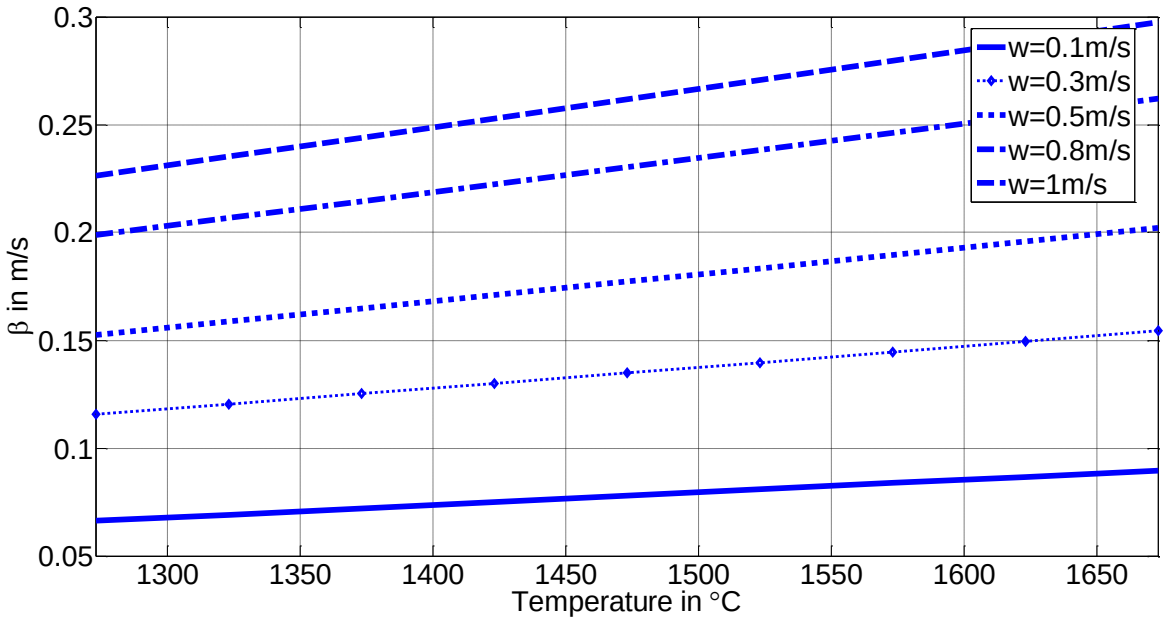

Figure 2.3: Influence of temperature on mass transfer coefficient

2.5 Reaction coefficient for the Boudouard

Figure 2.5 illustrates a comparison of mass-related reaction coefficient found by different investigators. It can be seen that the values of reaction coefficient differ from one another according to the origin of coke. Most of the previous

investigations were based on the powdered sample because of its suitability to determine the activation energy and the effect of gas composition on the conversion and, therefore, also the governing reaction mechanism. Furthermore, the reactivity of different types of the coke can also be compared.

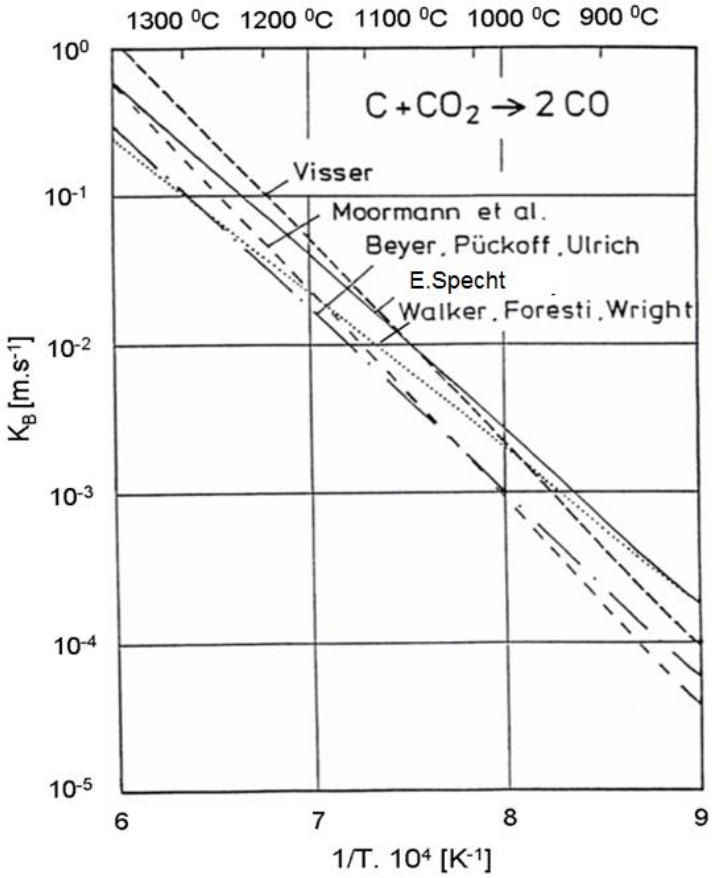

Figure 2.4 Comparison of various area-related reaction coefficients apparent of Boudouard reaction for graphite [5]

Table 2.1 is the experimental result from Ulzama and he explained a summary of apparent and true values of activation energies. (The activation energy of complex reactions is a combination of the activation energies of the elements, the concept of apparent activation energy is used in addition to the true activation energies, determined from the Arrhenius equation.) He described the dependence of Boudouard reaction on different types of coke. During the gasification process, the internal surface area changes and the value of internal surface area along the progress of the reaction he mentioned.

From the period study of Ulzama [5], the values of the pre-exponential factor and activation energy of reaction were found to be $5.42x10^6$ and 222 $kJ.mol^{-1}$ respectively using graphite. The values of activation energy of coke given in the literature cover a range from 113 to 414 $kJ.mol^{-1}$ and most of them have a value between 220 and 260 $kJ.mol^{-1}$.

Table 2.1: Apparent (Poland and Czech coke) and true activation energy (Graphite) of Boudouard reaction [5]

$C+CO_2 \rightarrow 2CO$	
Coal Type	**Activation Energy ($kJ.mol^{-1}$)**
Graphite	226
Poland coke	166
Czech coke	141

3 Coke particles with hyper stoichiometric air flow

3.1 The reaction model

The model includes some assumptions including reaction kinetics. For the model, assumptions are necessary to allow for the complex chemical and physical nature of the solid particles fed to the kiln. The model assumptions are:

- coke particles are spherical
- there is no ash layer at the surface of the particles
- the density of the particles remain constant during the combustion process.

Particle size is reduced as the initial mass is decreased slowly from the particle surface. If the reaction rate is very fast, all the oxygen is consumed as it reaches the particle surface. For large coke particles, particle diameter continuously shrinks because of heterogeneous reactions such as carbon with oxygen and carbon with carbon dioxide. Figure 3.1 shows the possible reaction mechanism of single coke particle and the direction of the gases flow.

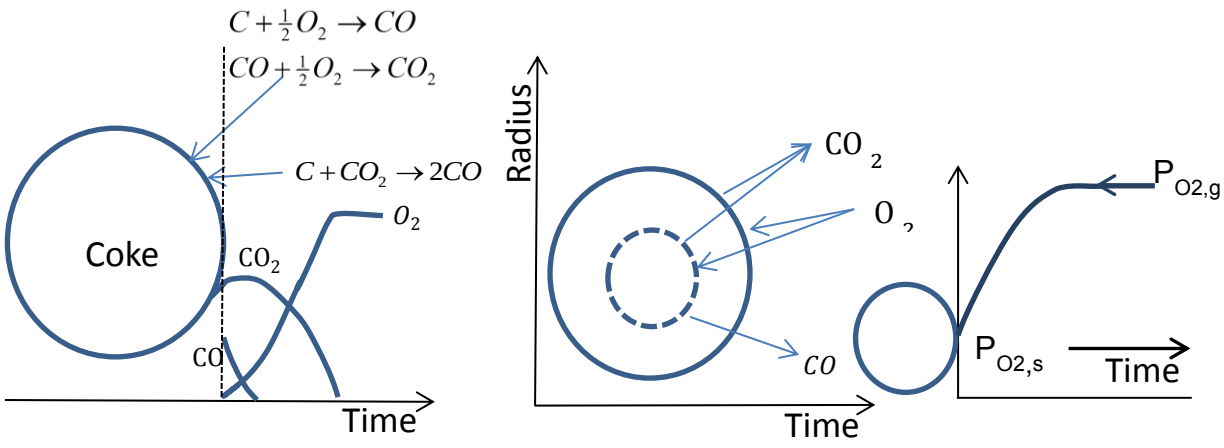

Figure 3.1 Basic scheme of profile in combustion process for single coke particle

The oxygen from air diffuses to the surface of the coke particle and reacts with carbon to form carbon dioxide and carbon monoxide. The carbon dioxide produced diffuses back to the surface of the particle and reacts with carbon to

form carbon monoxide. Oxygen concentration keeps on decreasing due to combustion and it is counterbalanced by the production of carbon dioxide. In high conversion of coke, the particle is exposed to a high concentration of CO_2 and this might be the only possible reason that there is always 100% conversion of particles even for a non-existential concentration of oxygen at the end of the process [5]. The kinetics of coke combustion was investigated using the multiple reactions model and the process is developed. To simulate a process occurring inside a kiln, the details of mechanisms of the bed are studied. On this basis, the combustion time, particle distribution of coke and heat transfer (temperature effect) inside the kiln can be estimated.

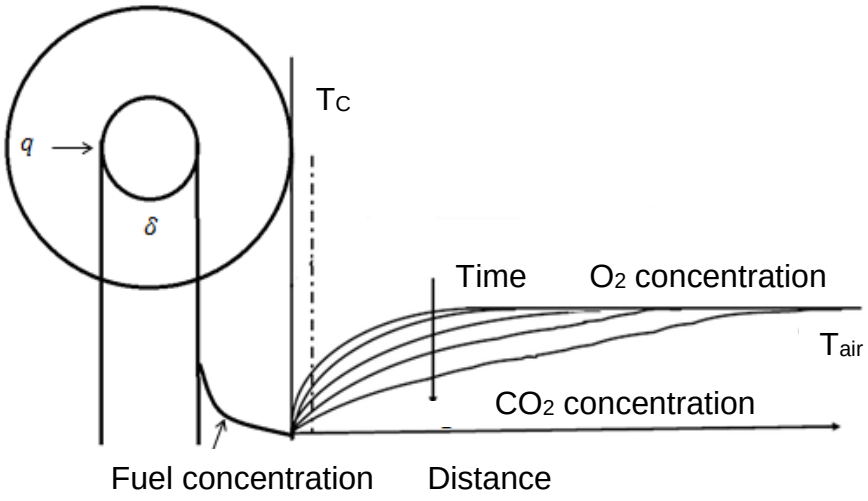

Figure 3.2: Schematic diagram of coke combustion

3.2 Reaction mechanism

The mechanism involved in the combustion process includes exothermic and endothermic reactions with complicated reaction mechanisms. The combustion process of a coke particle can be described by the following reaction.

$$O_{2,\text{gas}} = O_{2\,\text{ad}} \qquad \text{(a)}$$

$$O_2 = O + O\ . \qquad \text{(b)}$$

The second step is a surface reaction between the adsorbed reactant and carbon to produce adsorbed carbon mono-oxide.

$C + O = CO$. (c)

The homogeneous reaction, CO oxidation results in a high temperature.

$CO + 1/2O_2 = CO_2$. (d)

The reaction takes place at surface of particles due to the fact that the particle surface temperature is always less than the gas temperature near the surface and coke reacts with oxygen to produce carbon monoxide. The endothermic reaction between carbon and carbon dioxide to produce CO is called the Boudouard reaction and it can be described as:

$C + CO_2 = 2CO.$ (e)

We assume that the Boudouard reaction is much slower than oxidation, therefore we considered the global reaction to be

$C + O_2 = CO_2.$ (f)

The reaction coefficient between carbon and oxygen is given in the following equation and the reaction depends on the temperature of the coke particle. The reaction rate constant and activation energy can be derived from the experimental results and these can vary depending on the origin of the particle and chemical kinetics.

$$k_i = k_o . e^{-E/RT_c} \quad . \qquad (3\text{-}1)$$

The experimental investigation found that the value k_o ranges from 7000 to 7500 and the activation energy, E, from 75000 to 10000 KJ/mol for coke with oxygen reaction. Details of the different experimental methods are discussed in the next chapter.

3.3 Mass transfer

The change of mass flow of the coke from solid to gas is directly proportional to the change of oxygen from gas to solid and is given by:

$$d\dot{M}_C = \frac{\tilde{M}_C}{\tilde{M}_{O_2}} . d\dot{M}_{O_{2,z}} \quad . \qquad (3\text{-}2)$$

where $\tilde{M}_C$ and $\tilde{M}_{O_2}$ are the molecular masses of the carbon and oxygen respectively. The oxygen transported to the coke surface for combustion is given by

$$\dot{M}_{O_{2,1}} = \beta A_c \frac{(P_{O_{2,g}} - P_{O_{2,s}})}{R_{O_2} T_g} \text{ , kg/s .} \quad (3\text{-}3)$$

Where β is the mass transfer coefficient, $P_{O_{2,s}}$is the partial pressure of oxygen at the surface, $P_{O_{2,g}}$ is the partial pressure of oxygen in the gas, A_c is the area of the coke particle, and R is the universal gas constant.

The reaction rate is described as:

$$\dot{M}_{O_{2,2}} = k_{O_2} A_c \frac{P_{O_{2,s}}}{R_{O_2} T_g} \text{ , kg/s.} \quad (3\text{-}4)$$

From equation 3.3 and 3.4, by eliminating $P_{O_{2,s}}$, the mass flow rate of oxygen is given as follows:

$$\dot{M}_{O_2} = \frac{1}{1/\beta + 1/K_{O_2}} A_c \frac{P_{O_{2,g}}}{R_{O_2} T_g} \quad . \quad (3\text{-}5)$$

The change of mass flow rate of the coke is equal to the reaction rate per unit area for a single particle:

$$\frac{dM_C}{dt} = \frac{1}{1/\beta + 1/k_{O_2}} \cdot A_C \frac{P_{O_2,g}}{R_{O_2} T_g} \frac{\tilde{M}_C}{\tilde{M}_{O_2}} . \quad (3\text{-}6)$$

The mass transfer is obtained from the Sherwood number:

$$\beta = \frac{D \cdot Sh}{d_{c,z}} \text{ ,} \quad (3\text{-}7)$$

where D stands for the diffusivity (m^2/s), $d_{c,z}$ is the size of the particle and Sh is the Sherwood function for the packed beds which is given as ,

$$Sh \approx 1.12 . Re^{0.5} . Sc^{0.33} \frac{(1-\Psi)^{1/2}}{\Psi} . \quad (3\text{-}8)$$

However in the current study, the constant number 2 in the original equation is omitted because its influence is small.

Figure 3.1 shows the variation of mass transfer on velocity and reaction coefficients with a coke diameter of 60 mm with the respect to the temperature. The mass transfer increases with an increase of temperature and velocity. The value of the reaction rate coefficient on oxygen is observed to be very high above 900 ^{o}C compared to mass transfer. The reaction rate coefficient with carbon dioxide was found to be much higher above 1300 ^{o}C. From this analysis, it can be see that the reaction coefficient is important for the low temperature process.

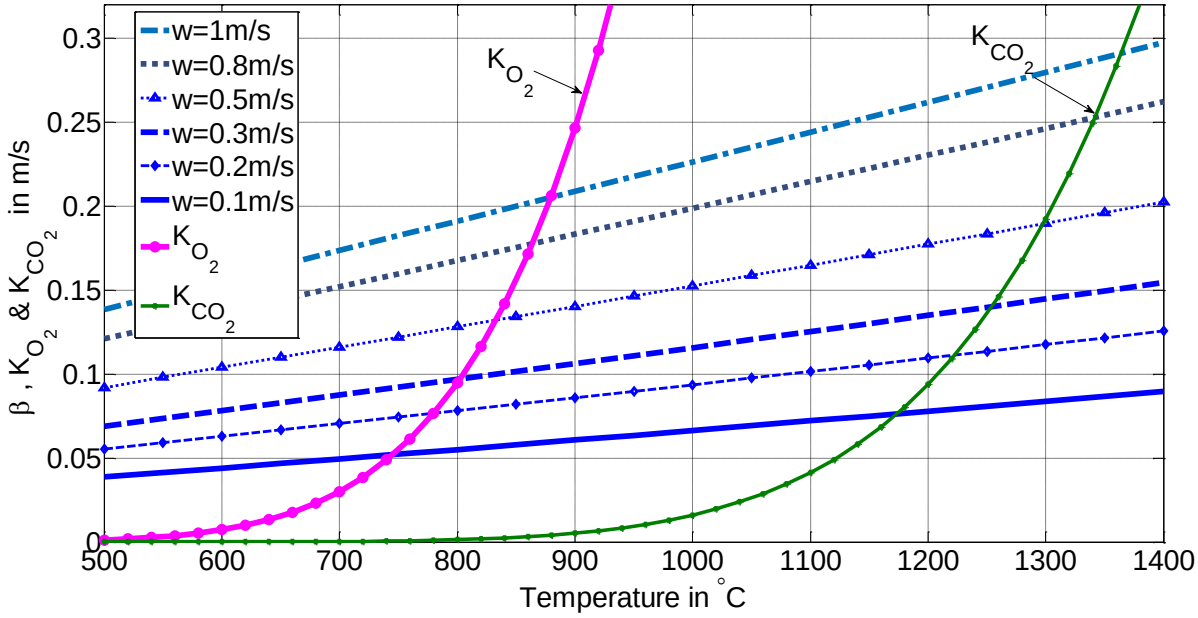

Figure 3.3: The influence of the temperature and the velocity upon the mass transfer and reaction rate

3.4 Analytical Solution for the combustion time

3.4.1 Basic equation for the combustion time

As seen in Figure 3.3, we assumed that the initial temperature is high which leads to a higher reaction coefficient rate. Hence, the influence of reaction rate on combustion time is negligible for high temperature processes. The change of mass flow of the coke can be defined from the equation 3.3

$$\frac{dM_C}{dt} = \frac{\beta(t)}{R_{O2} \cdot T} \cdot p_{O2(t)} \cdot A_{\delta(t)} \cdot \frac{\tilde{M}_C}{\tilde{M}_{O_2}} \ . \quad (3\text{-}9)$$

The mass is expressed by the diameter δ and

$$M_C = \rho_c \frac{\pi}{6} \delta^3 \ . \quad (3\text{-}10)$$

The area can be expressed as:

$$A_\delta = \pi \cdot \delta^2 \ . \quad (3\text{-}11)$$

From equation 3-11, the mass change rate is quantified by:

$$\frac{dM_C}{dt} = \rho_C \frac{\pi}{2} \delta^2 \frac{d\delta}{dt} \ . \quad (3\text{-}12)$$

Finally, equations 3-9 and 3-12 are connected to give the diameter change:

$$\frac{d\delta}{dt} = \frac{2.24 \cdot \tilde{M}_C \cdot}{R_{O2} \cdot T_g \cdot \rho_C \cdot \tilde{M}_{O2}} \cdot \frac{D_{O_2} \cdot Sc^{0,33} \cdot w^{0.5} (\frac{1-\Psi}{\Psi})^{0.5} P_{O2,t}}{\delta^{0.5} \cdot \nu^{0.5} \cdot \Psi^{0.5}} \ . \quad (3\text{-}13)$$

According to the above equation, the change in diffusion of air on the coke surface, viscosity and velocity of air with respect to temperature are given respectively in the following equation from Specht [11]:

$$\frac{D}{D_0} = \frac{T_g}{T_0}^{1.75} \ , \quad (3\text{-}14)$$

$$\frac{\nu}{\nu_0} = \frac{T_g}{T_0}^{1.75} \ , \quad (3\text{-}15)$$

$$\frac{w}{w_0} = \frac{T_g}{T_0} \ . \quad (3\text{-}16)$$

By substitution from the above equation for temperature ratio, the combustion time is as follows:

$$\frac{d\delta}{dt} = \frac{2.24 \cdot \tilde{M}_C \cdot}{R_{O2} \cdot T_0 \cdot \rho_C \cdot \tilde{M}_{O2}} \cdot \frac{D_{0,O_2} \cdot Sc^{0,33} \cdot {w_0}^{0.5} (\frac{1-\Psi}{\Psi})^{0.5} P_{O2,t}}{\delta^{0.5} \cdot {\nu_0}^{0.5} \cdot \Psi^{0.5} \cdot \left(\frac{T_0}{T_g}\right)^{0.375}} \quad . \tag{3-17}$$

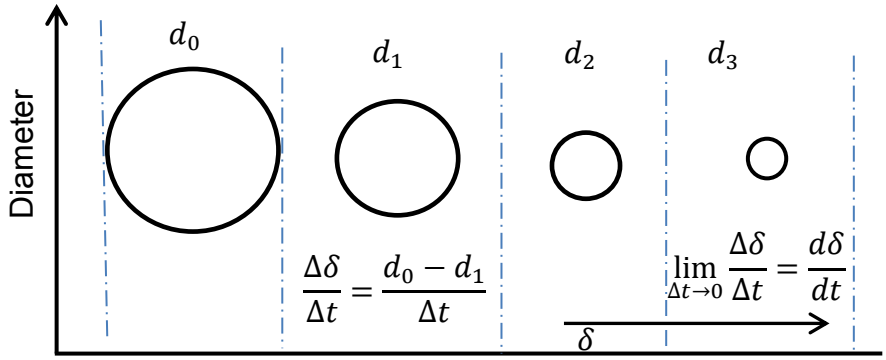

Figure 3.4: The schematic of the change of diameter by time on mass change

3.4.2 For countercurrent flow

The change of oxygen partial pressure depends on whether the air flow is counter flow or co-current flow. Partial pressure is related to the initial diameter, d_0 and change of diameter, δ. As soon as the particle contacts the oxygen, combustion started, however, the coke particle and the oxygen had opposite flow directions. This means that when the particle is completely burnt out, the partial pressure of oxygen reaches its initial value, $P_{O2,0}$. At the top of the kiln, the higher excess air number has a higher residual concentration of oxygen. The oxygen's partial pressure in the ambient gas changes according to the combustion of the particles at the particles surface as follows:

$$P_{O2(t)} = P_{O2,0}\left(1 - \frac{\delta^3}{\lambda . {d_0}^3}\right) . \tag{3-18}$$

Substituting equation 3-14 into 3-13 and assuming that the initial condition is $t = 0$, $\delta = d_0$ and similar to the final condition at $t = t_c$, $\delta = 0$.

$$\int_0^t dt = \frac{R_{O2} \cdot T_0 \cdot \rho_C \cdot \tilde{M}_{O2}}{2 \cdot \tilde{M}_C \cdot P_{O2,0}} \cdot \frac{{\nu_0}^{0.5} \Psi^{0.5}}{1.12 \cdot D_{0,O_2} Sc^{0,33} \cdot {w_0}^{0.5} \left(\frac{1-\Psi}{\Psi}\right)^{0.5}} \left(\frac{T_0}{T_g}\right)^{0.375} \int_0^{d0} \frac{\delta^{0,5}}{\left(1 - \frac{\delta^3}{\lambda . {d_0}^3}\right)} d\delta \, . \tag{3-19}$$

From this integration, the combustion time of coke particles is calculated for countercurrent flow as:

$$t_c = \frac{0.446.\tilde{M}_{O2}.T_0}{\tilde{M}_C \cdot P_{O2,0}} \cdot \frac{\Psi}{(1-\Psi)^{0.5}} \frac{R_{o2} \cdot Sc^{0.17}}{{D_{0,O_2}}^{0.5}} \cdot \left(\frac{T_0}{T_g}\right)^{0.375} \frac{\rho_C . d_0^{1.5}}{{w_0}^{0.5}} \cdot \sqrt{\lambda} \operatorname{arctanh}\left(\frac{1}{\sqrt{\lambda}}\right) \quad . \tag{3-20}$$

The analytical solution for the combustion time is shown in Figure 3.5 and Figure 3.6. The influence of the temperature on the combustion time is shown and the combustion time decreases with increasing temperature and the influence of temperature is not much higher, as seen in Figure 3.5. The influence of size of coke particle on combustion time is expressed in Figure 3.6.

It can be seen that combustion time depends on the type of coke (density), ρ_C, the size of coke (size distribution power of 1.5), d_0, the throughput of the kiln (the velocity from the injected air), w_0 and the excess air number λ. The influence of the temperature is with the power of 0.375 relatively slow.

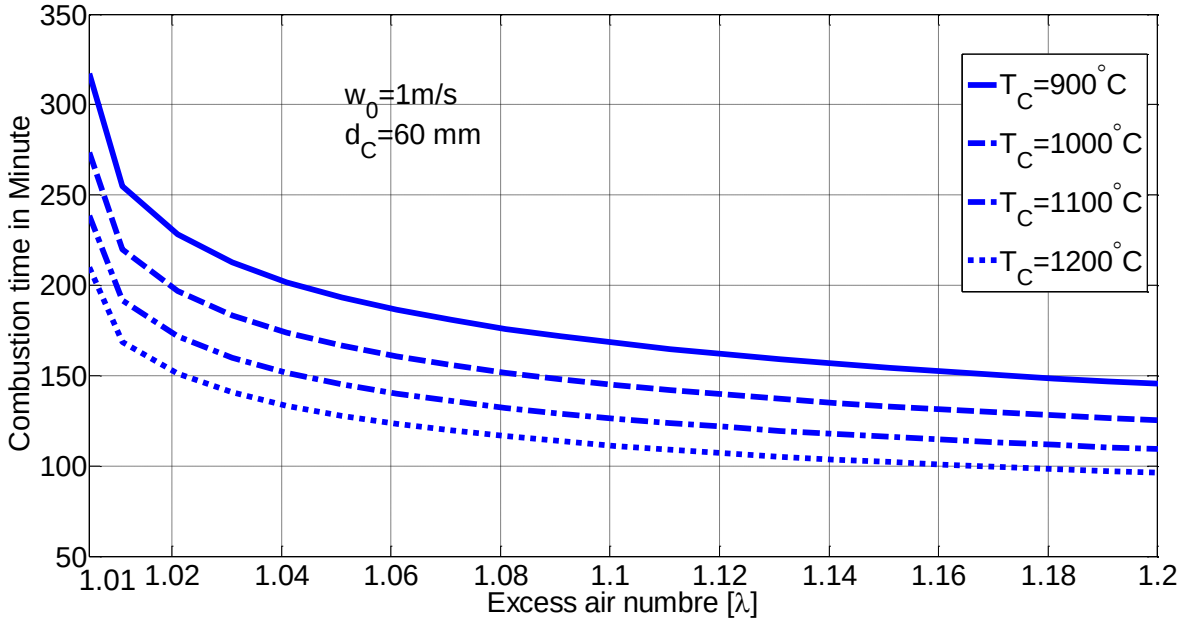

Figure 3.5: Combustion time of coke for different temperature versus excess air number for countercurrent flow

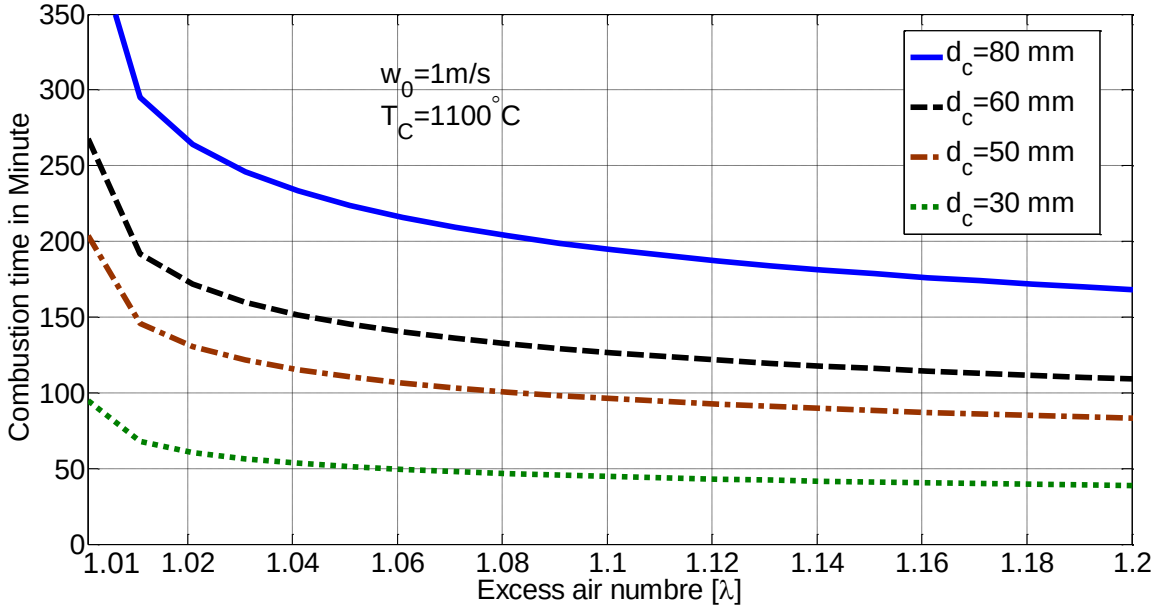

Figure 3.6: Combustion time of coke with different size

3.4.3 For the co-current flow

In a boiler vessel, coal or coke is burnt co-current to air. In co-current flow, the partial pressure of oxygen burnt with coke in the same direction, the concentration of oxygen is calculated with respect to excess air number using the following equation:

$$P_{O_{2(t)}} = P_{O_{2,0}} - \frac{P_{O_{2,0}}}{\lambda}\left(1 - \frac{\delta^3}{{d_0}^3}\right) \quad . \tag{3-21}$$

Inserting this in equation 3.17, gives

$$\frac{d\delta}{d\,t_{co}} = \frac{2.24\cdot\widetilde{M}_C\cdot}{R_{O2}\cdot T_0\cdot\rho_C\cdot\widetilde{M}_{O2}} \cdot \frac{D_{0,O_2}\cdot Sc^{0,33}\cdot {w_0}^{0.5}\left(\frac{1-\Psi}{\Psi}\right)^{0.5}}{\delta^{0.5}\cdot {\nu_0}^{0.5}\cdot\Psi^{0.5}\cdot\left(\frac{T_0}{T_g}\right)^{0.375}} \frac{P_{O_{2,0}}\left(1-{}^1\!/_\lambda+{}^1\!/_\lambda\left({}^\delta\!/_{d_0}\right)^3\right)}{\delta^{1/2}}. \tag{3-22}$$

$$\int_{d_0}^{0} \frac{\delta^{1/2}}{P_{O_{2,0}}\left(1-{}^1\!/_\lambda+{}^1\!/_\lambda\left({}^\delta\!/_{d_0}\right)^3\right)}\, d\delta = \frac{2.24 D_{0,O2}.Sc^{0,33}.\left(\frac{1-\Psi}{\Psi}\right)^{0.5}.{w_0}^{0.5}}{R_{O2}T_0\rho_c{\nu_0}^{0.5}\Psi^{0.5}} \frac{\widetilde{M}_C}{\widetilde{M}_{O2}} \int_0^t d\,t_{co} \quad . \tag{3-23}$$

The initial condition for the integration is $t = 0$ while $\delta = d_0$ and similarly the final condition at $t = t$ and $\delta = 0$.

$$t_{co} = 0.75 \frac{R_{o2} T_g . \tilde{M}_{O2}}{D_{0,O2} P_{O_{2,0}} \tilde{M}_C Sc^{0.33} {w_0}^{0.5} (\lambda-1)^{0.5}} \frac{{\nu_0}^{0.5} \rho_c d_0^{1.5} \lambda}{(1-\Psi)^{0.5}} \operatorname{arctanh}\left(\frac{1}{(\lambda-1)^{0.5}}\right) . \quad (3\text{-}24)$$

From the above equations, the ratio of the countercurrent and co-current flow for the combustion time is written as the following equation:

$$\frac{t_{co}}{t_{count}} = \frac{1.3.\lambda^{0.5}}{(\lambda-1)^{0.5}} . \frac{\operatorname{arctanh}\left(\frac{1}{\sqrt{\lambda}}\right)}{\operatorname{arctanh}\left(\frac{1}{(\lambda-1)^{0.5}}\right)} . \quad (3\text{-}25)$$

In this equation only the excess air number has influence. This ratio is shown in Figure 3.7. For the countercurrent flow, combustion time is faster than the co-current flow. When the excess air number is one, the ratio of the combustion time $\frac{t_{co}}{t_{count}}$ goes to infinity, when excess air number goes to infinity, $\frac{t_{co}}{t_{count}}$ is one.

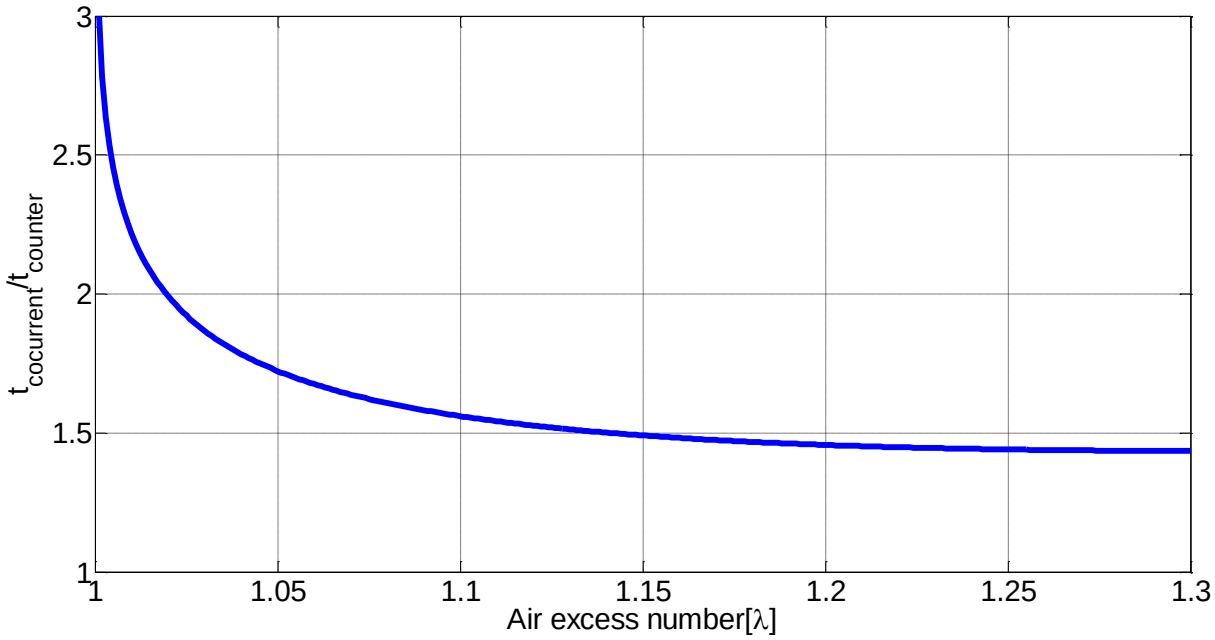

Figure 3.7: Combustion time ratio for co-current and countercurrent flow with the influence of excess air number

3.5 Particles size distribution inside the shaft kiln

The combustion of coke particles is influenced by the physical and chemical properties of solids such as size distribution of the coke particles, solid charged, reaction, mass transfer and so on. Among these factors, the coke size is the most practical parameter to be manipulated. In a shaft kiln, smaller particles burn

faster and energy is lost with flue gases. Larger particles require a longer time for combustion and also energy is lost during discharging, it can be seen in Figure 3.8. A good understanding of size distribution will provide the influential parameters on the kiln operation. Particle size distribution (PSD) and material type are of vital importance in the design of industrial equipment including fixed- and fluidized-bed reactors, blast furnaces and fixed-bed gasifiers [19]. Literature review provided only for the fine powder particles mostly for fluidized bed.

The mathematical model including particle size distribution is developed in this section. The temperature inside the kiln is considered as a constant 1100^{o}C in this model. The rate of total mass changed is determined by the summation of the change of mass of each coke particles. If the temperature of every individual particle is required, the individual heat transfer has to be calculated, for which the Nusselt and Reynolds numbers have to be determined with the specific diameter. However, this model neglected the temperature effect. The mass change of particles of coke is from equation 3.13:

$$\frac{d\delta_i}{dt} = \frac{2.24 \cdot \tilde{M}_C \cdot}{R_{O2} \cdot T_0 \cdot \rho_C . \tilde{M}_{O2}} \cdot \frac{D_{0,O_2} \cdot Sc^{0,33} \cdot {w_0}^{0.5} (1-\Psi)^{0.5} P_{O_2,t}}{{\delta_i}^{0.5} \cdot {\nu_0}^{0.5} . \Psi} \left(\frac{T_0}{T_g}\right)^{0.375} \quad . \tag{3-26}$$

The change of oxygen partial pressure depends on the total change of mass of the coke. At the beginning, $P_{O_2,0}$, the air comes from the bottom of the kiln, the change of the partial pressure is directly proportional to the ratio of initial mass and actual mass.

$$P_{O_2,t} = P_{O_2,0}\left(1 - \frac{1}{\lambda}\frac{M_{C,t}}{M_{C,0}}\right) \quad . \tag{3-27}$$

From equation 3-26, the actual mass of particle i and initial mass of particle can be expressed by the diameter δ_i and $d_{0,i}$ with the mass fraction. The mass fraction can be calculated using from the ratio of actual mass and initial mass of the particle.

$$x_i = \frac{M_{i,0}}{M_0} \quad . \tag{3-28}$$

From equation 3-27, the actual mass of particle i and initial mass of particle can be expressed by the diameter δ_i and $d_{0,i}$ with the mass fraction.

$$P_{O_{2,t}} = P_{O_{2},0}\left(1 - \frac{1}{\lambda}\frac{\sum_{i=1}^{n} {\delta_i}^3 x_i}{\sum_{i=1}^{n} {d_{0,i}}^3 x_i}\right) . \quad (3\text{-}29)$$

From equation 3-10 and 3-12 , the change of mass of coke

$$M_{C,i} = \frac{\pi}{6}{\delta_i}^3 \quad , \quad \frac{dM_{C,i}}{dt} = \rho_C \frac{\pi}{2}{\delta_i}^2 \frac{d\delta_i}{dt} \quad . \quad (3\text{-}30)$$

Then the total mass change of coke can be defined

$$\frac{dM_{c,t}}{dt} = \sum \frac{dM_{C,i}}{dt} \quad . \quad (3\text{-}31)$$

For the total mass change of the coke particles from equation 3-26 and 3-31 is as follows

$$\frac{dM_{c,t}}{dt} = \frac{3.52 \cdot \widetilde{M}_C \cdot}{R_{O2} \cdot T_0 . \widetilde{M}_{O2}} \cdot \frac{D_{0,O_2} \cdot Sc^{0,33} \cdot {w_0}^{0.5} (1-\Psi)^{0.5} P_{O_2,t}}{{\nu_0}^{0.5} . \Psi} \left(\frac{T_0}{T_g}\right)^{0.375} \sum_{n=1}^{i} {\delta_i}^{1.5} \quad . \quad (3\text{-}32)$$

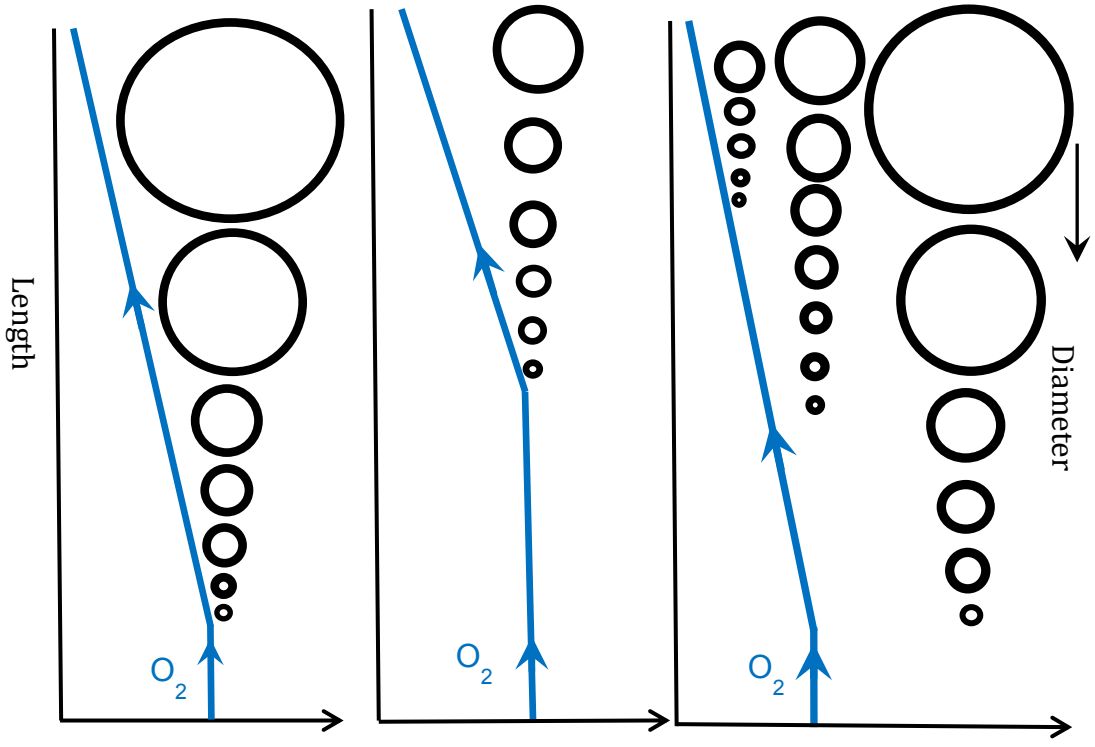

Figure 3.8: Change of mass according to the oxygen concentration

The Sauter diameter is generally determined from particle size distribution, which is mainly used as an index to describe the combustion time of coke. The Sauter diameter is under predicted to find the combustion time for particle size distribution. Therefore the model underestimates combustion time for particle distribution. The mean diameter of the particles $\bar{d}_{Sauter}$ is described by the Sauter diameter with diameter base, area base and volume base as:

$$\bar{d}_{Sauter} = \left[\sum_{i=1}^{n} \left(\frac{V_{c,i}}{V_{c,t}} \cdot \frac{1}{d_{c,i}} \right) \right]^{-1}, \quad \text{(3-33-a)}$$

$$\bar{d}_{Sauter} = \left[\sum_{i=1}^{n} \left(\frac{V_{c,i}}{V_{c,t}} \cdot \frac{1}{d_{c,i}^{\,2}} \right) \right]^{-1/2}, \quad \text{(3-33-b)}$$

$$\bar{d}_{Sauter} = \left[\sum_{i=1}^{n} \left(\frac{V_{c,i}}{V_{c,t}} \cdot \frac{1}{d_{c,i}^{\,3}} \right) \right]^{-1/3}, \quad \text{(3-33-c)}$$

where $V_{c,t}$ represents the total volume of the particles, and $V_{c,i}$ is the volume of the particle i. Sauter diameter is estimated from equation 3-33-a. The conversion degree of coke particles is calculated by

$$X_c = 1 - \frac{m_c}{m_{c,i}} = 1 - \left(\frac{\delta}{d_0}\right)^3. \quad \text{(3-34)}$$

3.6 Simulation results of coke particle distribution

For the simplest case, the particles size distribution inside the kiln is approximated as five different coke sizes. The particles are moving down from the top of the kiln and the air is injected from the bottom of the kiln. It is assumed that all the particles of coke inside the kiln fall within five different ranges of diameter: 30 mm, 42 mm, 55 mm, 67 mm and 80 mm respectively. Different distributions are defined and case distributions are shown in table 3.1.

Table 3.1: The particle coke distribution percentage for the simulation

Diameter (mm)	% of disribution (Volume based)			
	Case 1	Case 2	Case 3	Case 4
30	6%	90%	20%	16%
42	34%	4%	20%	20%
55	34%	2%	20%	20%
67	13%	2%	20%	24%
80	13%	2%	20%	20%
Sauter diameter	50	31	48	50

For each case distribution, the oxygen concentration represents the total change in the distribution of particles. The effect of particle distribution inside the kiln on combustion time is shown in Figure 3.9, 3.10, 3.11, 3.12. For each class of distribution, oxygen represents the total change of coke mass. The maximum combustion time is when there is the same distribution inside the kiln. The smallest coke particle and the biggest particle significantly influence the combustion time. The model is capable of involving the particle distribution by using equation 3.32.

The smallest particle, with a diameter of 30 mm took nearly 90 minutes when it had the total amount of 6%. The biggest particle with a diameter of 80 mm, is completely burnt out after 180 minutes when it has the total amount of 13%, as shown in Figure 3.9. At the beginning, the burning of coke starts immediately and the conversion of coke is faster at the beginning and at the end. Since the excess air number of 1.1 is used in the model, the concentration of oxygen remains 2% when it leaves the top of the kiln.

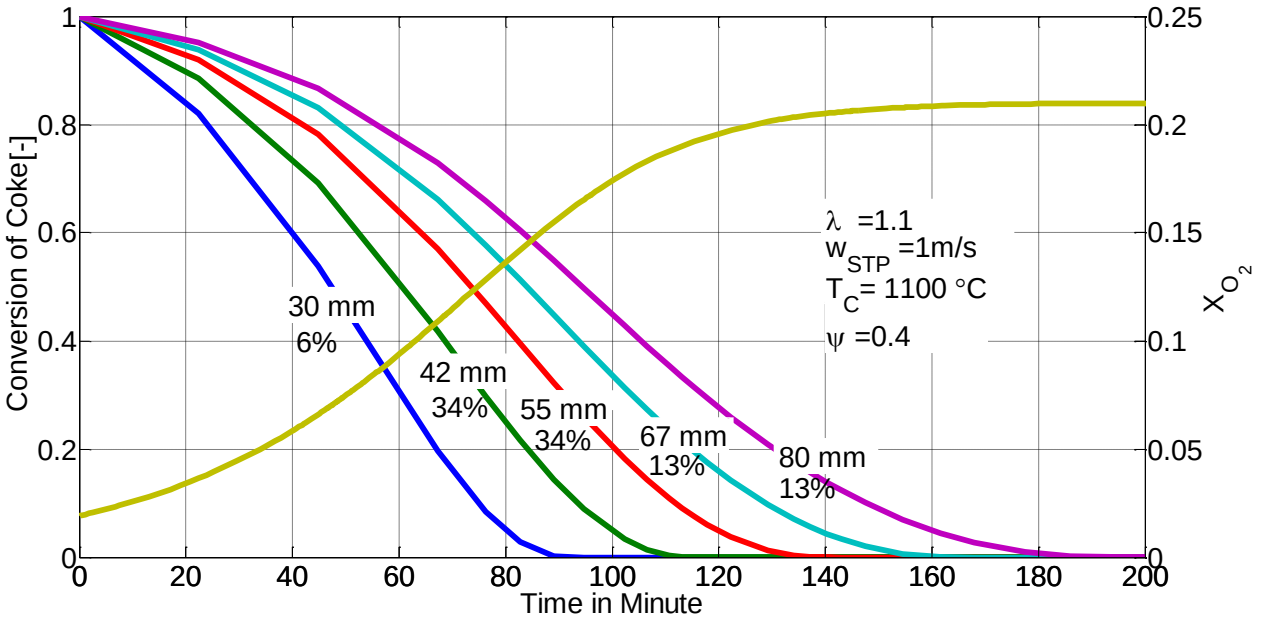

Figure 3.9: Conversion of coke particle distribution: case 1

When the smallest particle dominates inside the kiln, the combustion time is significantly decreased, as shown in Figure 3.10. It can be seen that the smallest particles (30 mm) take around 60 minutes while the amount of smallest diameter is 90% that because of the oxygen concentration is higher when the smallest particles started the combustion.

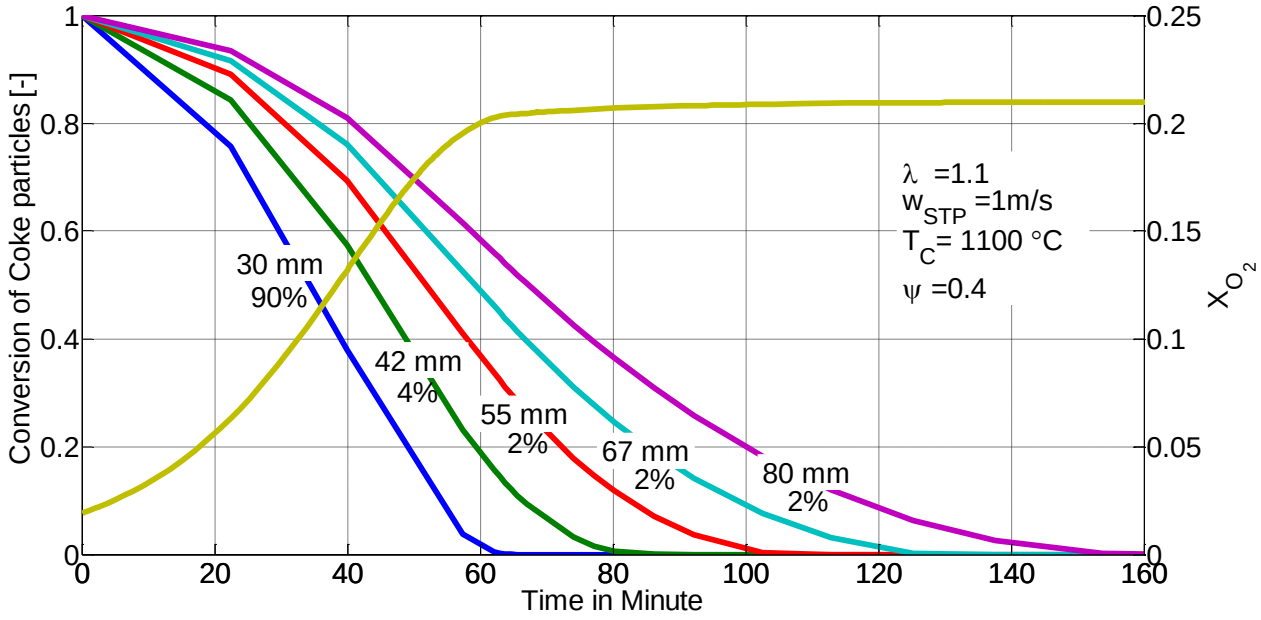

Figure 3.10: Conversion of coke particle distribution: case 2

Figure 3.11 and 3.12 show how the conversion degree of coke is affected by the particle size. It is assumed that the percentage for each particle size is the same, 20% (case 3). The smallest coke particle with a diameter of 30 mm has the shortest combustion time about 85 minutes and particles with a diameter of 80 mm burnt out completely after 180 minutes in case 3 distribution. The same combustion time can apply in case 4 distribution.

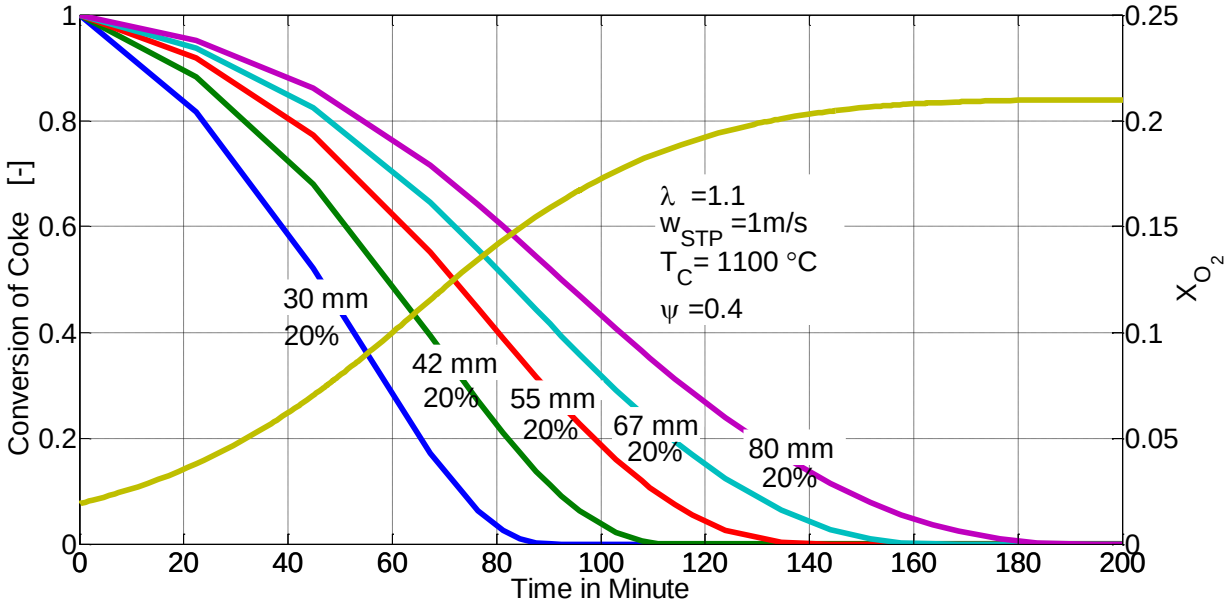

Figure 3.11: Conversion of coke particle distribution: case 3

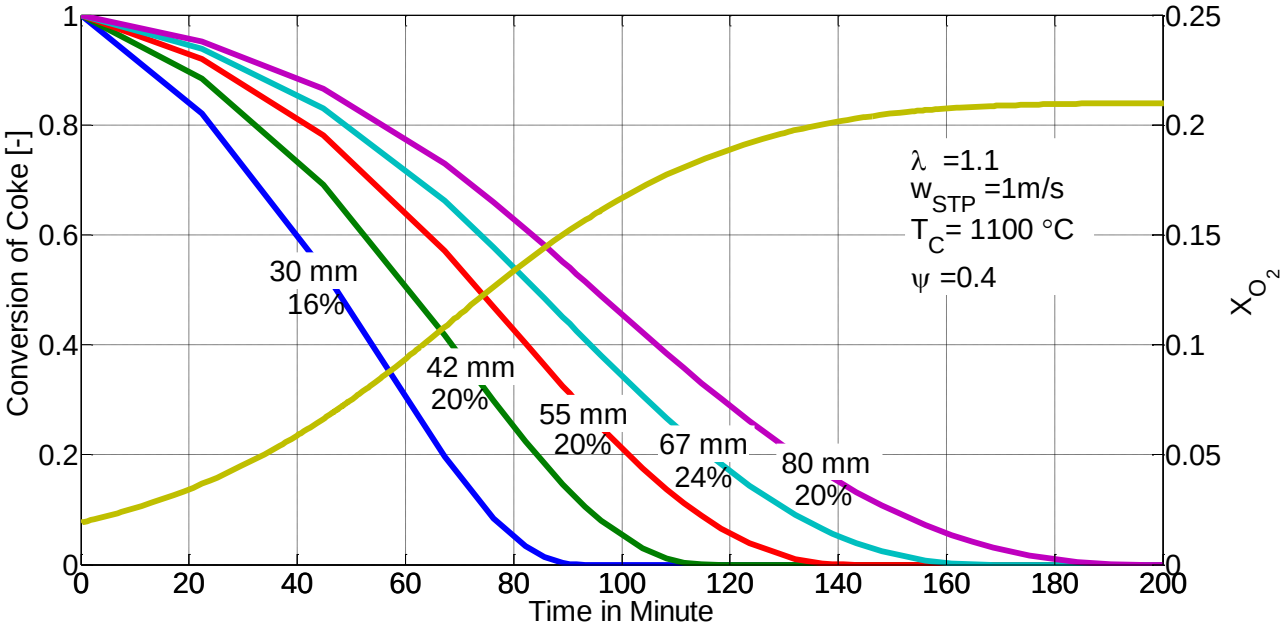

Figure 3.12: Conversion of coke particle distribution: case 4

According to the Figures, one can see that a large increase in the proportion of the smallest particles, with a diameter of 30 mm has a major influence on combustion time. By increasing the percentage of the smaller particles, combustion time could be decreased. The influence of the particle distribution on the kiln is investigated by changing the particle size distribution while the particle size remains the same.

Consequently, the diameter of the smallest and largest particles depends on the kind of internal distribution at the beginning and end of combustion. Now the question arises how the total mass changes, because this affects the energy yield. The change of total mass is simulated for all case distribution.

Figure 3.13 represents the comparison between the total change of mass of coke particles (case 1 distribution) and the Sauter diameter. The two different simulation results with Sauter and total change of mass indicated the same conversion at the beginning of the combustion: however, Sauter is much faster than the total mass case 1 distribution after 30 minutes of combustion time and at the end. Combustion time is much faster than the case distribution. So it is difficult to describe the combustion time with the Sauter diameter.

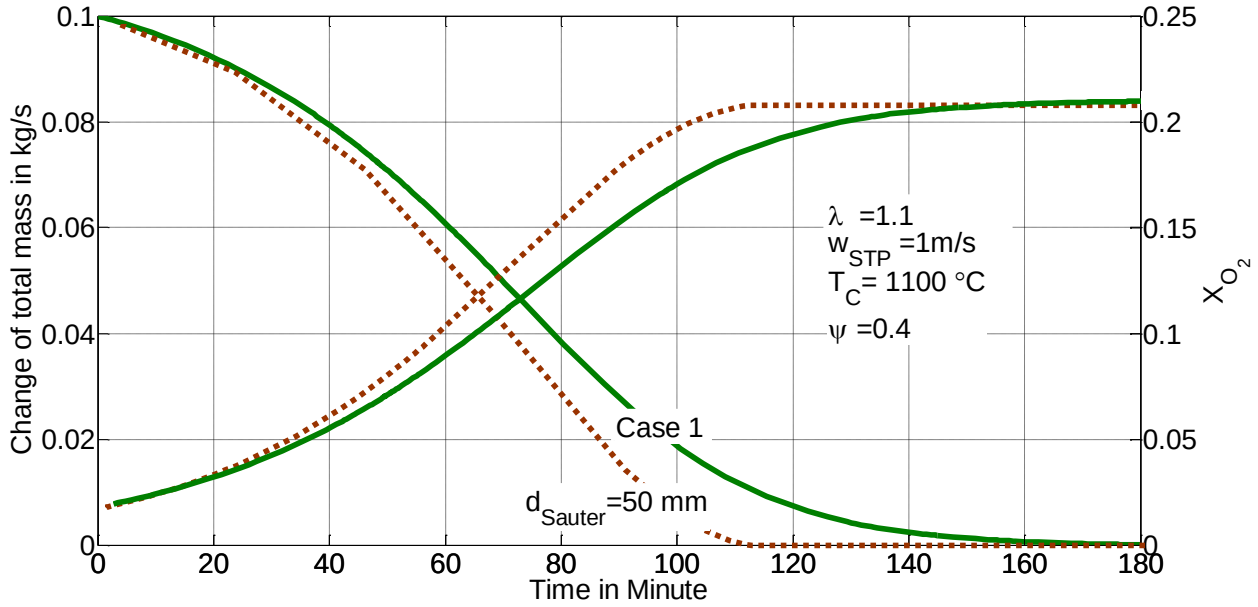

Figure 3.13: Comparison between corresponding Sauter diameter and case 1 distribution

According to the combustion time with the curvature of Sauter diameter is far from total change of mass case distribution, the mean diameter of the particles $\bar{d}_C$ is described by mean of all particles including volume fraction of the each particles. The mean diameter is expressed to obtain the distribution by diameter base, area base and volume base as:

$$\bar{\bar{\bar{d}}}_C = \sum_{i=1}^{n}\left(\frac{V_{c,i}}{V_{c,t}}\cdot d_{c,i}\right), \qquad \text{(3-35-a)}$$

$$\bar{\bar{\bar{d}}}_{C_{II}} = \left[\sum_{i=1}^{n}\left(\frac{V_{c,i}}{V_{c,t}}\cdot d_{c,i}^{\,2}\right)\right]^{1/2}, \qquad \text{(3-35-b)}$$

$$\bar{\bar{\bar{d}}}_{C\,III} = \left[\sum_{i=1}^{n}\left(\frac{V_{c,i}}{V_{c,t}}\cdot d_{c,i}^{\,3}\right)\right]^{1/3}, \qquad \text{(3-35-c)}$$

Table 3.2: The mean diameter of the particle coke case distribution

Diameter (mm)	Case 1	Case 2	Case 3	Case 4
Mean diameter	54	32.7	54.8	56

Figures 3.14, 3.15 and 3.16 and 3.17 show the comparison between three simulations. They are

1. total mass change of different case distribution in table 3.1
2. mean diameter corresponding to each case in table 3.2
3. single size coke particle simulation which has the same combustion time with case distribution.

The issues arise if the profile of the total can be described with only one characteristic diameter. The comparison of the simulation between the mean diameter and total mass change of case distribution is shown.

Figure 3.14 represents the combustion time with the results of three simulations which are mentioned in Figure 3.13. The one size coke particles is the same ending of combustion time with case 1 distribution, coke diameter of 62 mm is found, however, the curve is not the match at the beginning of the combustion. It is found that the calculated combustion time based on the model is closed to mean diameter, however, both Sauter and mean diameter have a shorter combustion time compared to the case distribution.

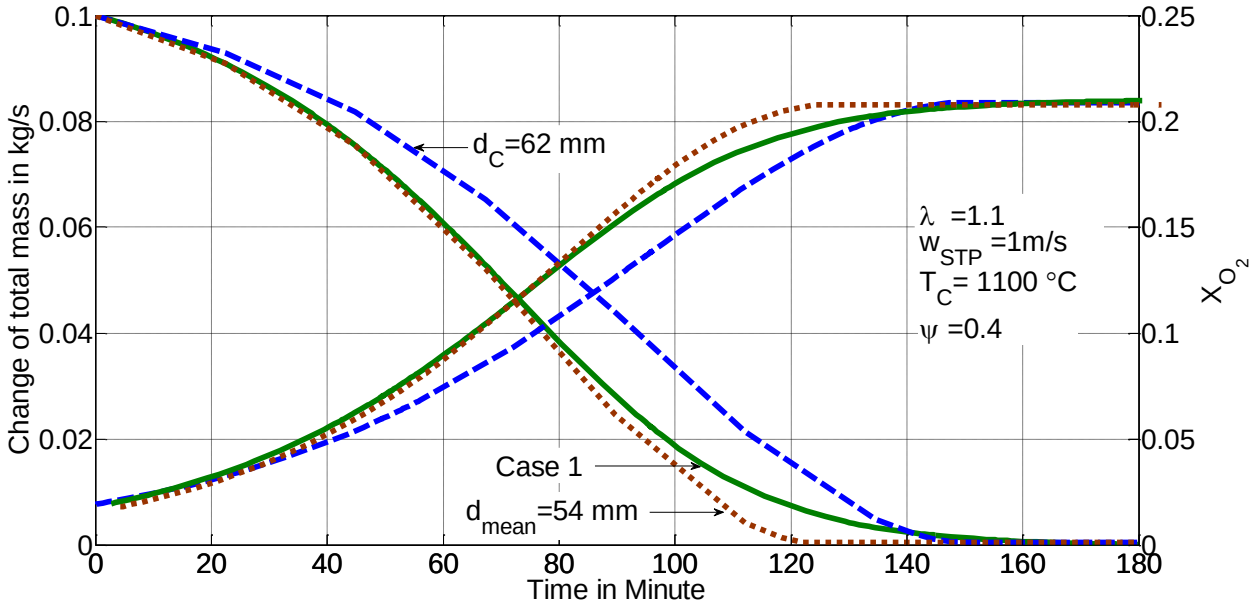

Figure 3.14: Comparison between one particle, corresponding mean diameter and case 1 distribution

As seen from Figure 3.15, the total mass in case 2 distribution (90% of small particles) and mean diameter indicates the same combustion time at the beginning and the middle. However, mean diameter is faster than the total change of mass case 2 distributions at the end. One size particle diameter of 40 mm has the same combustion time with case 2 distribution.

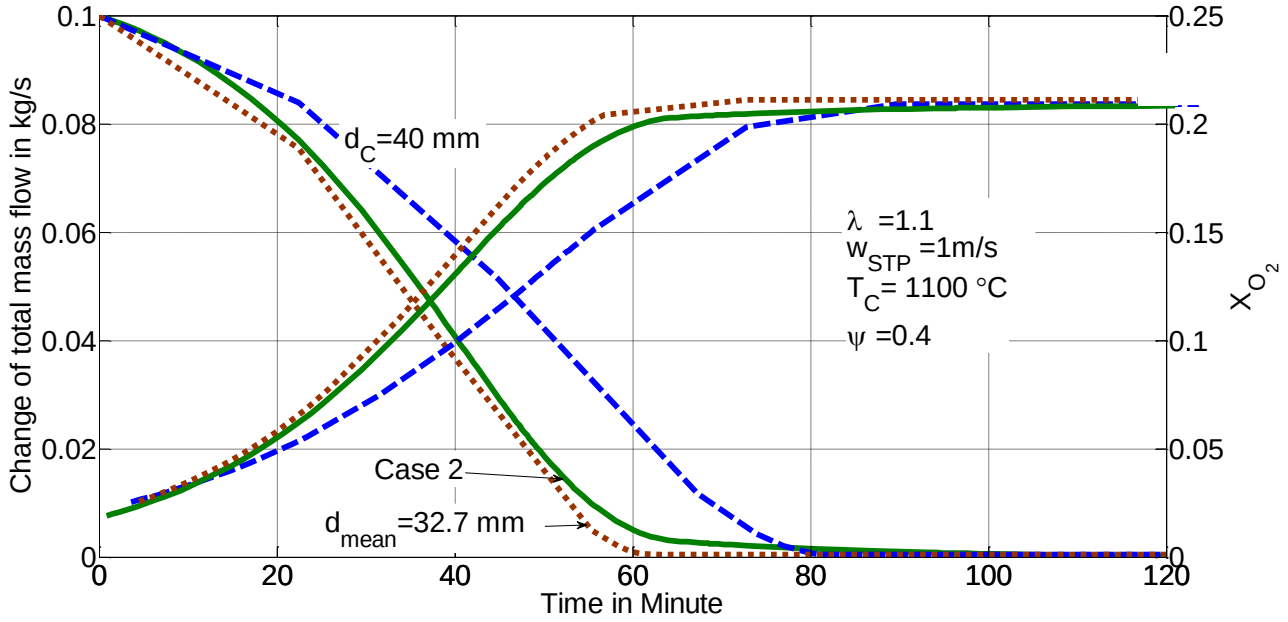

Figure 3.14: Comparison between one particle, corresponding mean diameter and case 2 distributions

Figures 3.16 and 3.17 describe the change of total mass and mean diameter as a function of combustion time under the same conditions for case 3 and case 4 distribution. It can be observed that the profiles of total distribution and mean diameter are similar at the beginning of combustion, however, the combustion time for the total and mean diameter profile is quite different: nearly 40 minutes. To get the same combustion time with the total distribution, the one size particle 64 mm and 65 mm are calculated for case 3 and case 4 distribution.

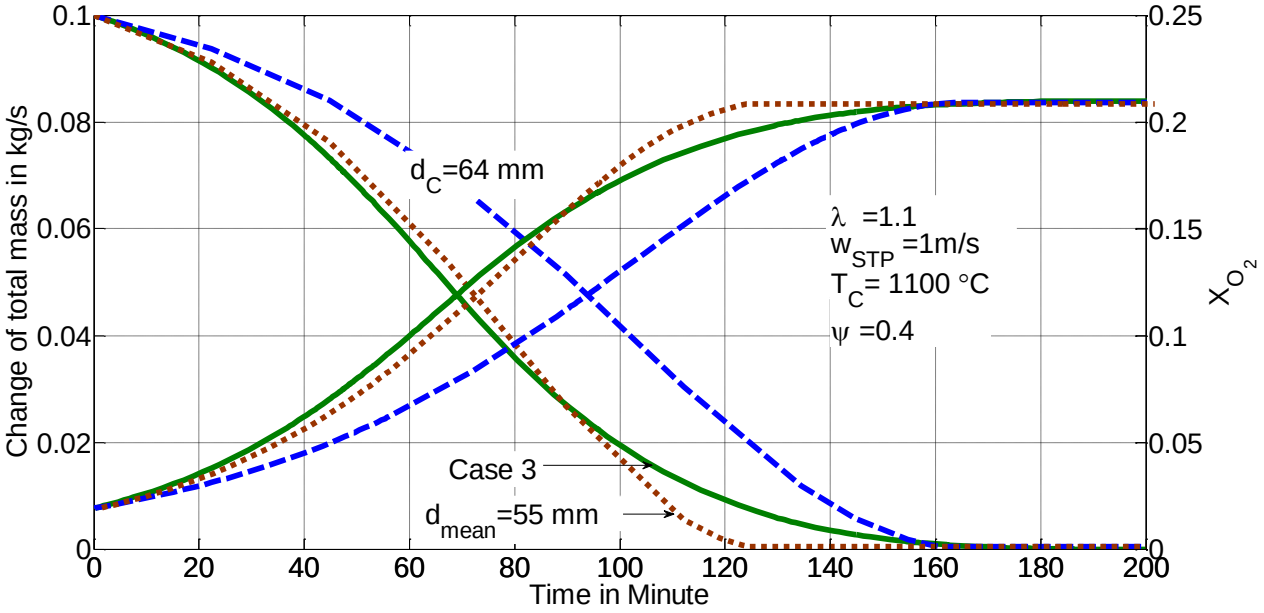

Figure 3.15: Comparison between one particle, corresponding mean diameter and case 3 distributions

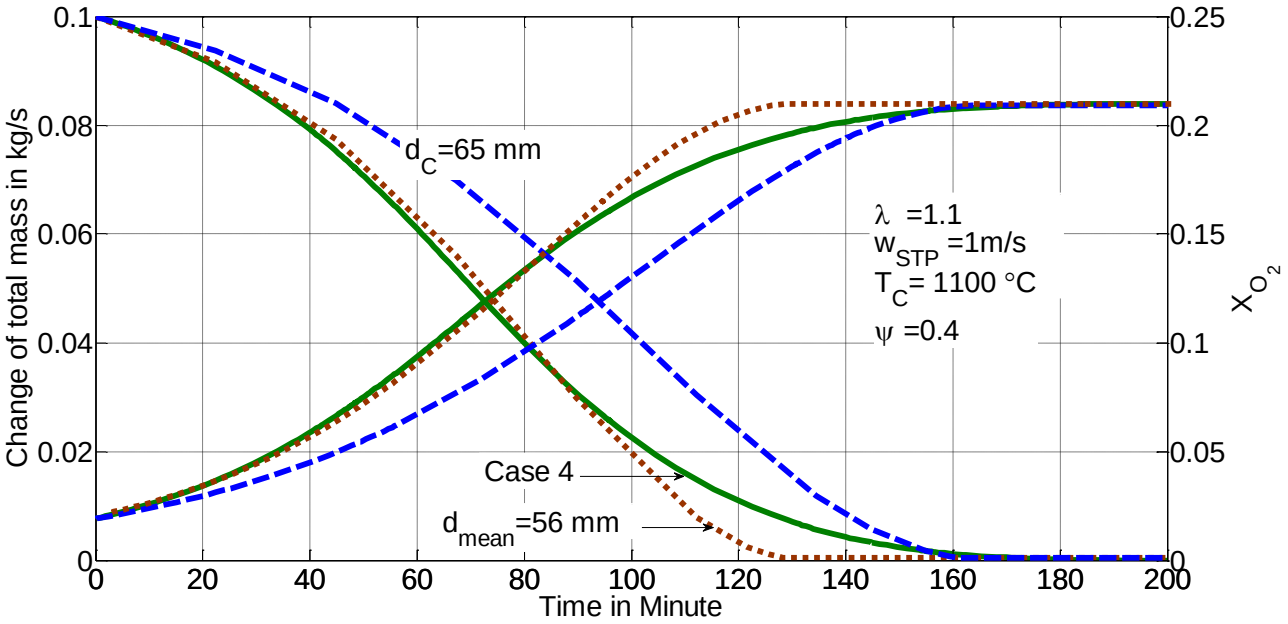

Figure 3.16: Comparison between one particle, corresponding mean diameter and case 4 distributions

In Figure 3.17, showing the combustion time for all particles, it can be seen that the biggest particles needed the longest combustion time, and that this also depends on the size distribution. Combustion takes around 63 minutes when the coke particles had the amount of 90% on same size 30 mm, however, the

combustion time takes around 82 minutes when it has 20% inside the kiln and 85 minutes when 13% inside the kiln. So the particle distribution inside the kiln also played an important parameter and the model is able to calculate for case distribution.

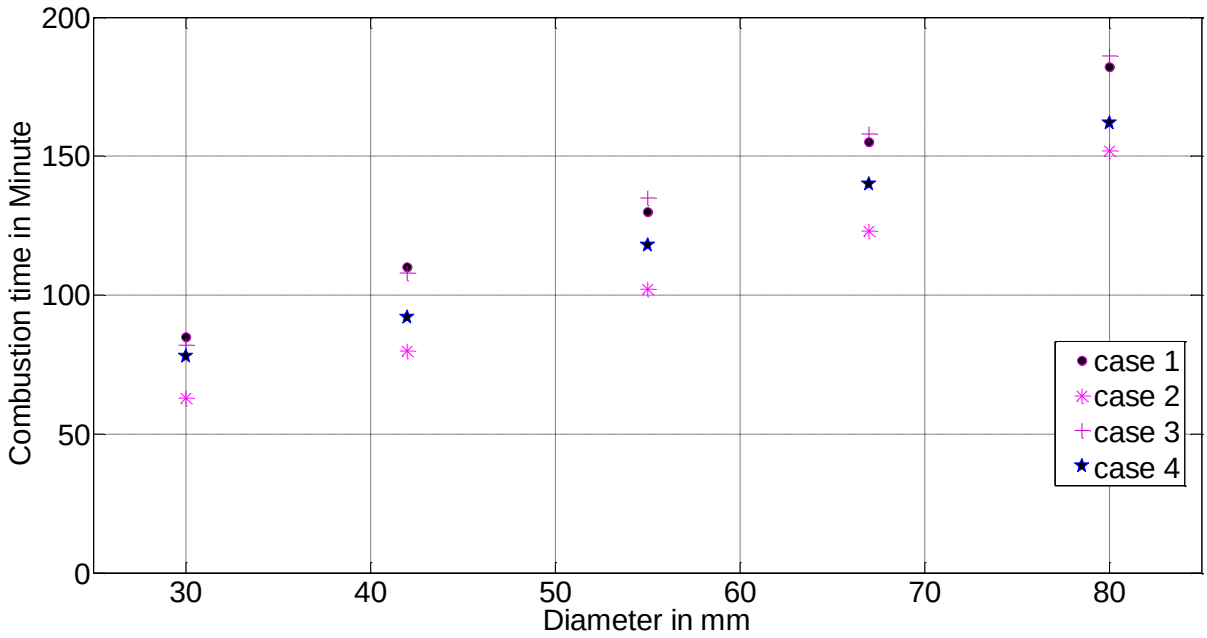

Figure 3.17: Comparison of case 1, case 2, case 3 and case 4 on combustion time

The comparison of combustion time between mean diameter and case distribution did not show significant difference at the beginning and middle of the combustion time, however, they have strong effect on combustion length at the end. With the number of large particles, the combustion time is increased. However, when an amount of the small particle size decrease and surface area increases, as a result the five particle size distribution in different ratios has much more effects on combustion time, especially the burning time on the smallest and largest particles. It is found that five different sizes of coke also have a major influence on the combustion length when there is a different percentage. The greater the proportion of smaller coke particles, the more obvious the combustion time effect is. The profile of total depends on the distributions and considering on distribution is closed to reality.

Table 3.3: Combustion time on coke particles distribution (polydisprese)

Diameter [mm]	Combustion time [Minute]			
	Case 1	Case 2	Case 3	Case 4
30	85	63	82	78
42	110	80	108	92
55	130	102	135	118
67	155	123	158	140
80	182	152	186	162

Table 3.4: Combustion time on coke particles distribution (monodisprese)

Diameter [mm]	Combustion time [Minute]
30	48
50	92
60	120
80	172

In Table 33 and 3.4, it can be seen that the combustion time for polydisperse and monodisperse particles. With the amount of large particles, the combustion time is increased (see Table 3.3 and 3.4). However, the amount of small particle decreases and surface area increases, as a result the five particle size distribution on different ratio is much more effects on combustion time. We also found that five different size of coke also give a big influence on the combustion length when there is different percentage can be seen in Table 3.3. The more the smaller coke particles ratio are, the more obvious the combustion time effect is. So the particle distribution inside the kiln also played an important parameter.

4 Case of coke combustion with hypo stoichiometric air flow

4.1 Introduction

Being highly endothermic and consuming carbon directly from the coke, Boudouard reaction is very important to investigate. Energy is generated by oxidation of coke particles in combustion zone. The coke reacts with oxygen to produce carbon dioxide. Towards the kiln top, the concentration of carbon dioxide rises and oxygen concentration decreases. When oxygen is completely burnt out, the carbon reacts with CO_2. Therefore, the Boudouard reaction has to be included. The Boudouard reaction has lower reaction rate and takes place when the temperature is high. However, the effect of Boudouard reaction on the process cannot be omitted from modeling when the excess air number is less than one. When the oxygen completely burnt out, the Boudouard reaction is dominated.

In a mixed feed lime shaft kiln, the length and the position of combustion and Boudouard zone decisively depend on the excess air number and the lump size of the solid fuel. Therefore, it is important to study the reaction behavior of coke in the combustion zone and in the Boudouard zone.

4.2 The model: Case of combustion with excess air number <1

In this section, a mathematical model for combustion of coke particles is presented for the case of excess air number less than one. The model considers the effect of both carbon direct oxidation and Boudouard reaction. During these processes, O_2 concentration keeps decreasing and it is counterbalanced by the production of CO_2. At a higher conversion, the particle is exposed to the high concentration of CO_2 and then CO_2 reacts with carbon to give again higher rate for the Boudouard reaction. Effective values of process parameters i.e. reaction

coefficient of Boudouard reaction and carbon oxidation reaction are determined from the experimental work. The model describes the kinetics of the conversion process in shaft kiln with the influence of both direct oxidation and Boudouard reaction. The change of the total mass flow of the coke depends on both reactions as the following equation:

$$\frac{dM_C}{dt} = \frac{dM_{C,Bou}}{dt} + \frac{dM_{C,ox}}{dt} . \tag{4-1}$$

The change in mass flow of the coke in Boudouard zone and oxidation zone is calculated with the following equation:

$$\frac{dM_{C,Bou}}{dt} = \frac{1}{1/\beta_{CO_2} + 1/k_{CO_2}} \cdot \frac{P_{CO_2,g}}{R_{CO_2} \cdot T} \cdot \frac{\tilde{M}_C}{\tilde{M}_{CO_2}} \cdot A_C \ . \tag{4-2}$$

$$\frac{dM_{C,ox}}{dt} = \frac{1}{1/\beta_{O_2} + 1/k_{O_2}} \cdot \frac{P_{O_2,g}}{R_{O_2} \cdot T} \cdot \frac{\tilde{M}_C}{\tilde{M}_{O_2}} \cdot A_C . \tag{4-3}$$

In the equation 4-2 and 4-3, P is partial pressure along the kiln length, R is specific gas constant and $\tilde{M}$ is molar mass. In this reaction, for oxidation is $k_{O_2} >> \beta_{O_2}$ and for the Boudouard is $k_{CO_2} << \beta_{CO_2}$. If the temperature is greater than above 900 ^{o}C, the reaction coefficient is influence on coke combustion.

The partial pressure of oxygen and carbon dioxide in the kiln changes according to the reaction due to the countercurrent flow, they are depicted in equation 4.4 and 4.5 respectively.

$$P_{O_2,g} = P_{O_2,0} \cdot (\ 1 - \frac{d_{ox}^3}{\lambda \cdot d_o^3}) . \tag{4-4}$$

$$P_{CO_2,g} = P_{O_2,0} \cdot \frac{\delta^3}{\lambda \cdot d_{ox}^3} . \tag{4-5}$$

$P_{O_2,0}$ and $P_{CO_2,0}$ are the initial partial pressure of oxygen and carbon dioxide in the gas.

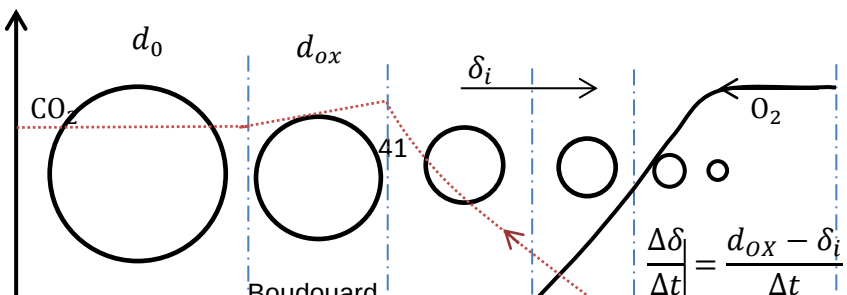

Figure 4.1: The schematic diagram of change of diameter d_{ox} and δ

At the Boudouard zone, the diameter of the coke which reacts with carbon dioxide is determined as an empirical relation (see in Figure 4.1) from the mass and will be present as a function of the excess air number:

$$M_{ox} = \lambda \cdot M_0, \rho V_{ox} = \lambda \rho \mathrm{V}_0 \quad . \tag{4-6}$$

As density is same, volume is expressed by the diameter,

$$d_{ox} = \sqrt[3]{\lambda} \cdot d_0 \quad \text{when } \lambda<1. \tag{4-7}$$

In the equation, λ is excess air number, d_{ox} is the coke diameter after changing by oxidation in empirical form and d_0 is initial diameter.

4.3 Experimental Method

4.3.1 Experimental Setup

In order to investigate the reaction coefficient, the experimental measurements were carried out in a tube furnace. The experimental setup is as shown in Figure 4.2. The laboratory furnace has a length of 1200 mm and an inner diameter of 80 mm. The tube was heated by the electric furnace. The coke sample was hanged from the mass balance to the center of the tube with a stainless steel wire (see Figure 4.2). A required gas or air is introduced from the bottom of the furnace with a known volumetric flow rate. The probe gas analyzer was mounted at the

top of the kiln. During the experiment, the contents of gases in flue gas and temperature of flue gas were simultaneously recorded. Moreover, the furnace temperature and bed temperature also measured. A variety of cokes with different density and size were taken for the experiments.

The coke particles used here have fixed geometry as a sphere. A coke sample sphere around a diameter of 30mm is used. A hole of 1 mm in diameter is drilled at the center of the particle to insert a thermocouple (see Figure 4.3) and core temperature was also recorded. A packed bed of inert materials at the bottom was placed to realize a homogeneous distribution of this gas stream inside the kiln.

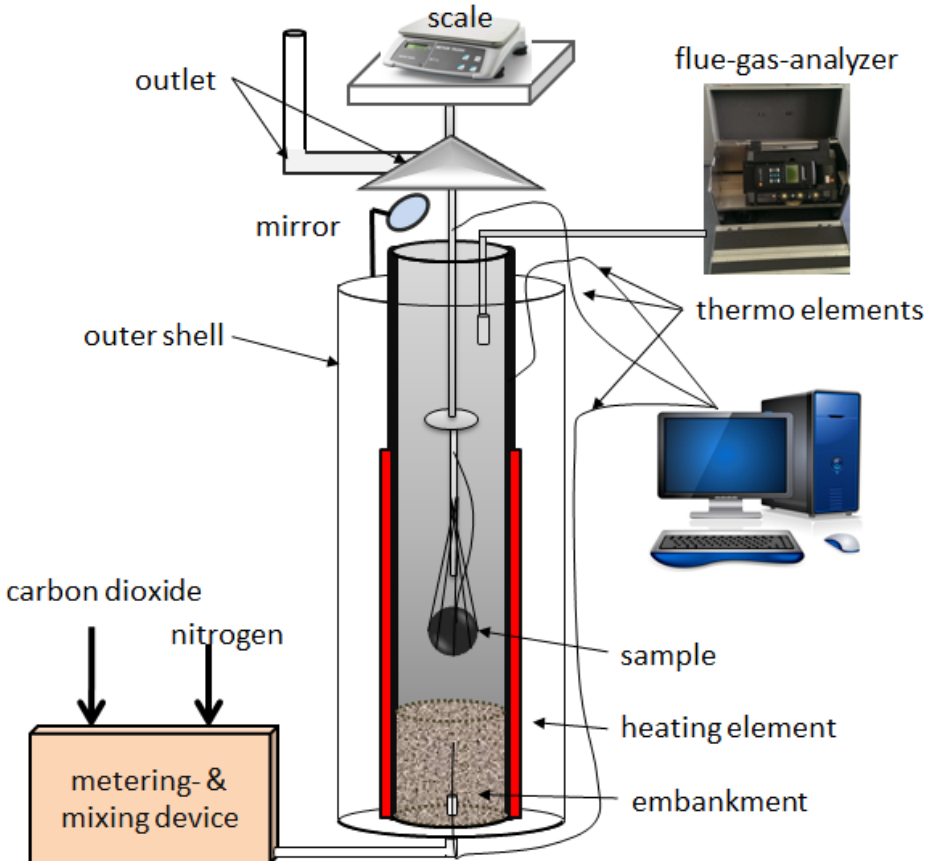

Figure 4.2: The schematic diagram of experimental apparatus

Before combustion After combustion

Figure 4.3: The sample coke before and after combustion with carbon dioxide (sample 1)

4.3.2 Experimental Measurements

During the experiment, core temperature, the weight loss and flue gas are measured simultaneously. A gas (nitrogen, carbon dioxide or mixed) enters the kiln at the bottom. Weight loss because of the gasification reaction was measured by mass balance. The experiments also covered the measurements of gases concentration of oxygen, carbon dioxide, carbon monoxide using gas analyzer.

The maximum temperature of the furnace is at 1200^{o}C. A gas (nitrogen) enters the kiln at the bottom firstly and heated up a specific temperature. At the same time, no combustion takes place. When the temperature reached up to 700^{o}C, carbon dioxide enters from the bottom of the kiln and combustion started.

4.4 Experimental Analysis

4.4.1 Burning behavior of the coke in carbon dioxide atmosphere and air

Figure 4.4-a shows the measured temperatures and the mass loss of the sample in one of the CO_2 experiment series, and Figure 4.4-b with air. The furnace is first heated to about 800°C, while supplying nitrogen, and then this temperature is kept constant for about 10 minutes. The sample reaches a temperature which is approximately 750°C. Afterwards carbon dioxide is fed into the furnace instead of nitrogen and the Boudouard reaction begins.

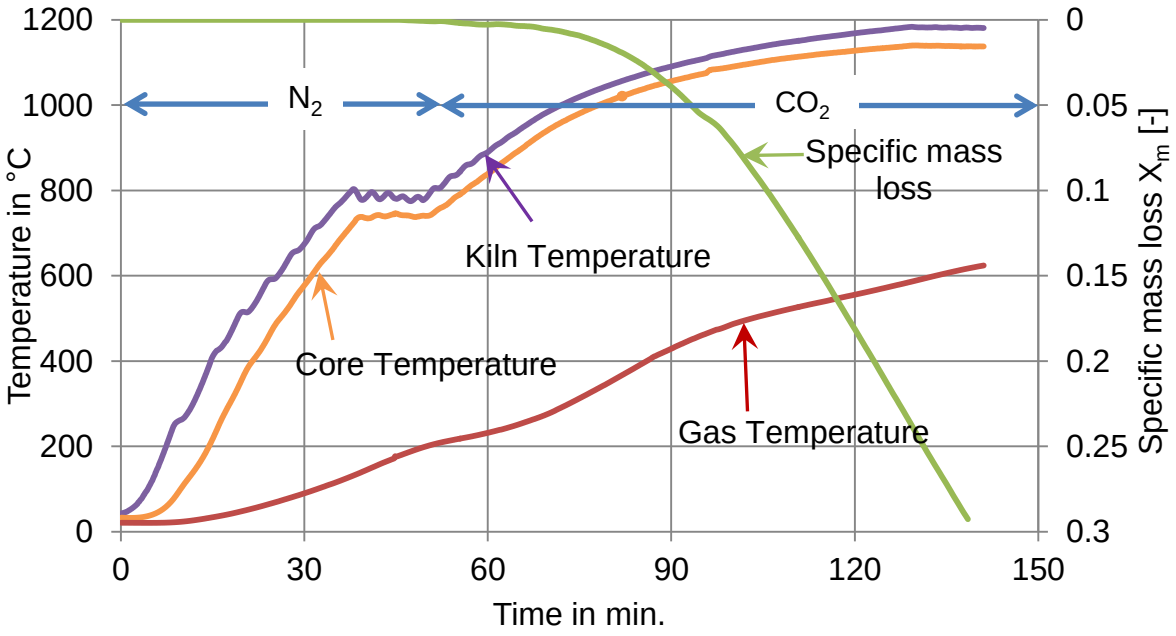

Figure 4.4-a: Measurement of the temperature and mass loss (with CO_2)

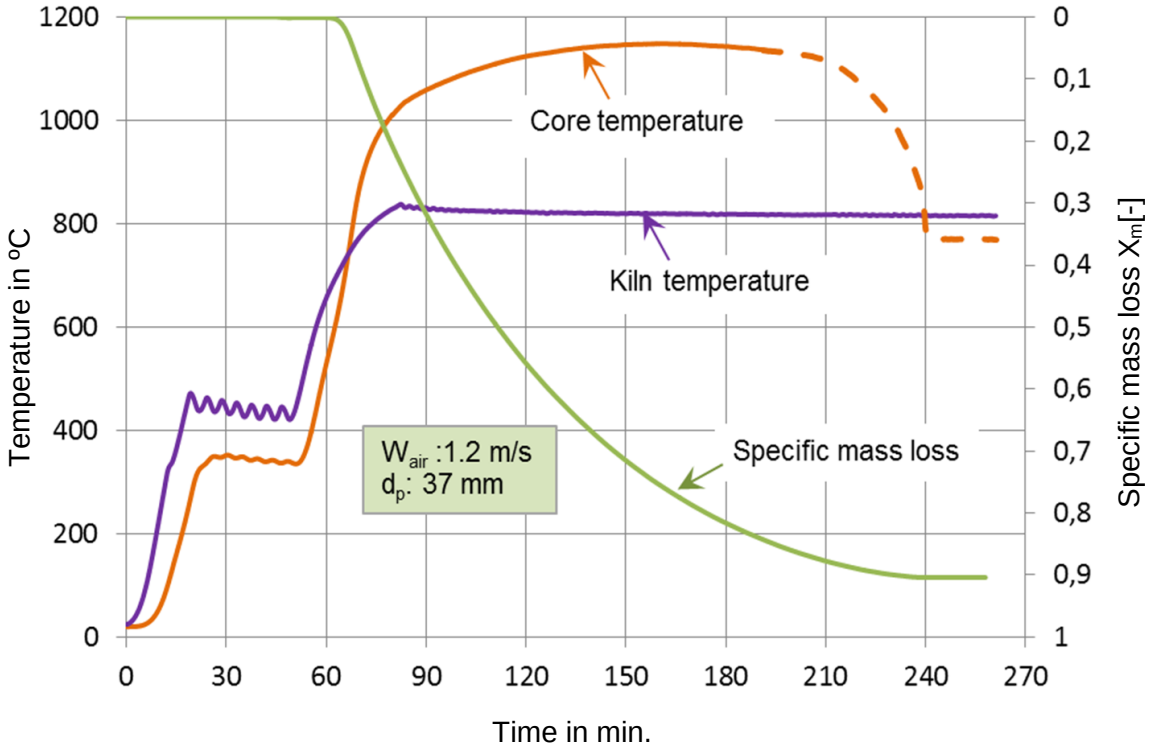

Figure 4.4-b: Measurement of the temperature and mass loss (with air)

4.4.2 Conversion of Coke (mass balance and CO measurement)

The furnace is heated up to 1180 °C. The core temperature increases and remains below the furnace temperature during the entire experiment time, since

the Boudouard-reaction is an endothermic reaction. The addition of CO_2 gas starts the reactions, which can be recognized by the mass loss. However, this reaction is initially very slow, but it quickly accelerates with increasing core temperature.

Figure 4.5 shows the conversion of carbon in grams per unit time as a function of the core temperature. The conversion is the derivative of mass loss curve in Figure 4.5. The CO-measurement is derived from continuous measurement of the CO concentration in the exhaust gas. Both curves look almost identical.

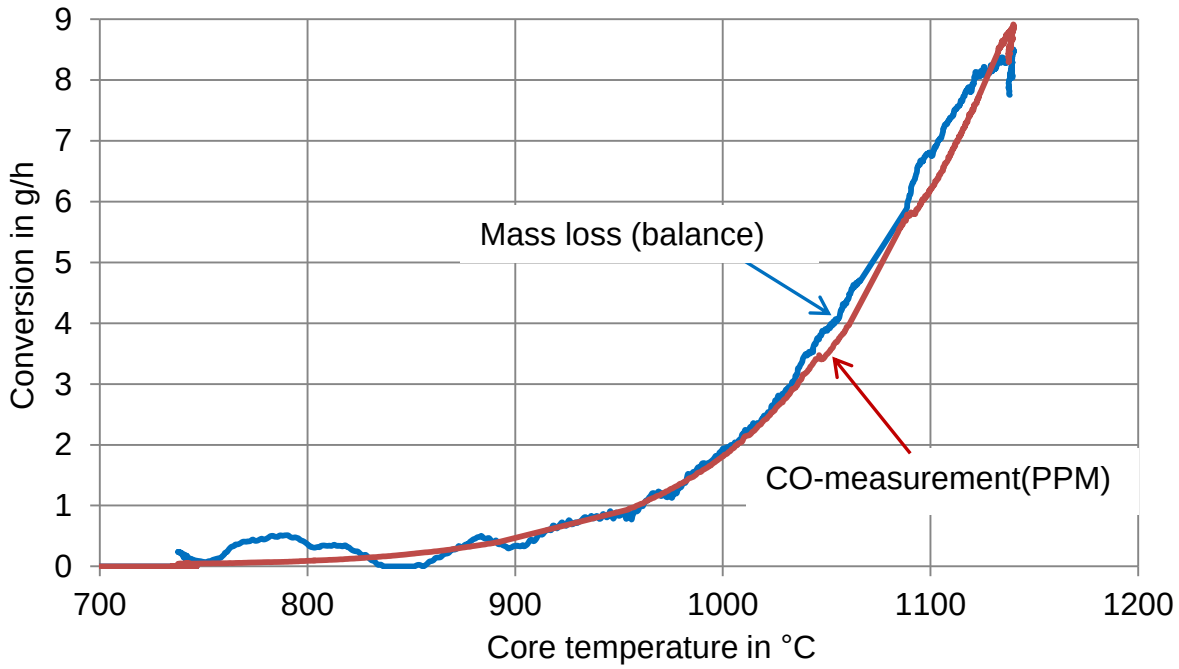

Figure 4.5: Conversion of coke by the experimental measurement (with CO_2)

4.4.3 Kinetic model for the coke

The carbon dioxide is transferred to the surface by convection. It is assumed that the reaction takes place on a small zone at the surface. The reaction in the pore is not considered. The reaction coefficient is therefore an apparent coefficient related to the outer surface. The reaction coefficient of O_2 and CO_2 can be calculated with the following equation

$$k_{CO2} = \frac{1}{\frac{p_{CO2,g}}{R_{CO2} \cdot T_g \cdot q_C} \cdot \frac{\tilde{M}_C}{\tilde{M}_{CO2}} - \frac{1}{\beta}} . \qquad (4\text{-}8)$$

$$k_{O2} = \frac{1}{\frac{p_{O2,g}}{R_{O2} \cdot T_g \cdot q_C} \cdot \frac{\tilde{M}_C}{\tilde{M}_{O2}} - \frac{1}{\beta}} \quad . \tag{4-9}$$

Here $P_{CO_{2,g}}$ and $P_{O_{2,g}}$ arethe partial pressure of carbon dioxide and oxygen in the inlet gas, R_{CO2} and R_{O2} are specific gas constant, T_g is gas temperature, $\tilde{M}_C$ is molar mass of carbon, $\tilde{M}_{CO2}$is molar mass of CO_2, $\tilde{M}_{O_2}$is molar mass of O_2, β mass transfer coefficient which is calculated on the basis of the analogy of heat and mass transfer from known inflow conditions. q_C, the rate of change of the carbon per area, which is from the experimental results and is shown in Figure 4.5

$$q_C = \frac{dM/dt}{A_C} \quad . \tag{4-10}$$

From the conversion, the apparent reaction coefficient k_{CO2} is calculated by means of equation 4.8. Figure 4.6 summarizes the list of one group samples with similar diameter. All conditions are given the same and coke reacted with carbon dioxide. Coke particle are used nearly the same size range: 36-38 mm and density ranging from 920 to 1079 kg/m^3. From this figure, it can be noticed that each of coke of same type give different ranges but the same trends. The reaction coefficients may vary dependence on size and density.

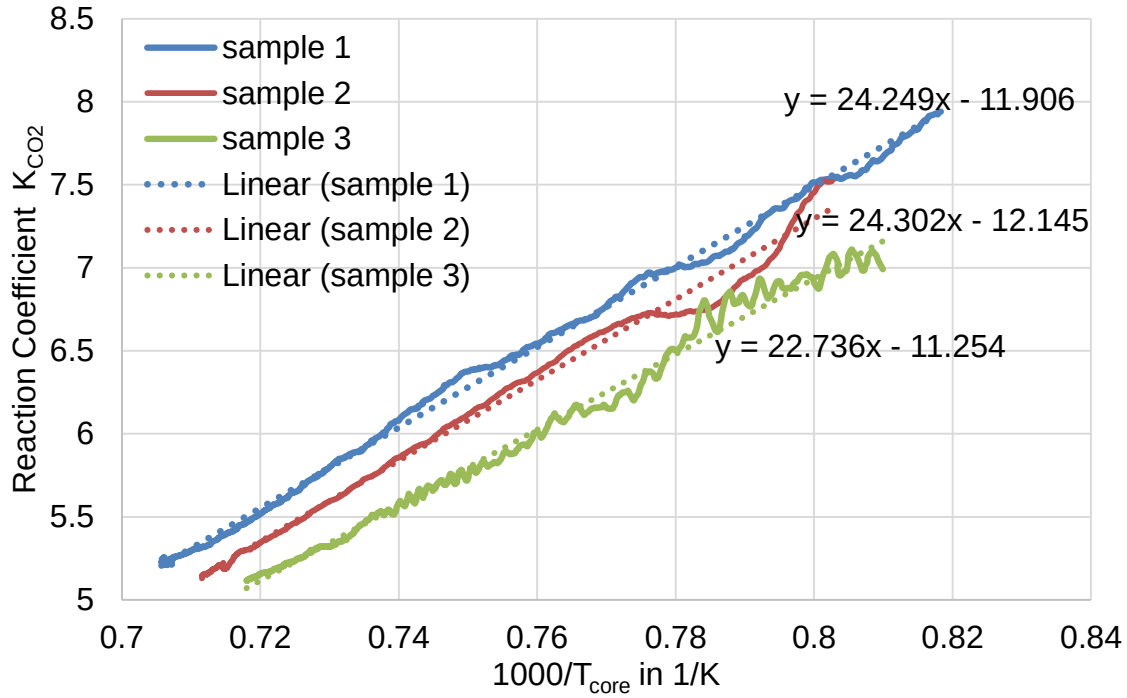

Figure 4.6: Comparison of experiments with samples of different size and density

The results are shown in Figure 4.7 for coke particles under different condition. The reaction coefficient is described by the Arrhenius correlation. The logarithmic plot of k_{CO2} over the reciprocal of absolute temperature T_{Core} allows the determination of the activation energy E_A from the slope of the curves.

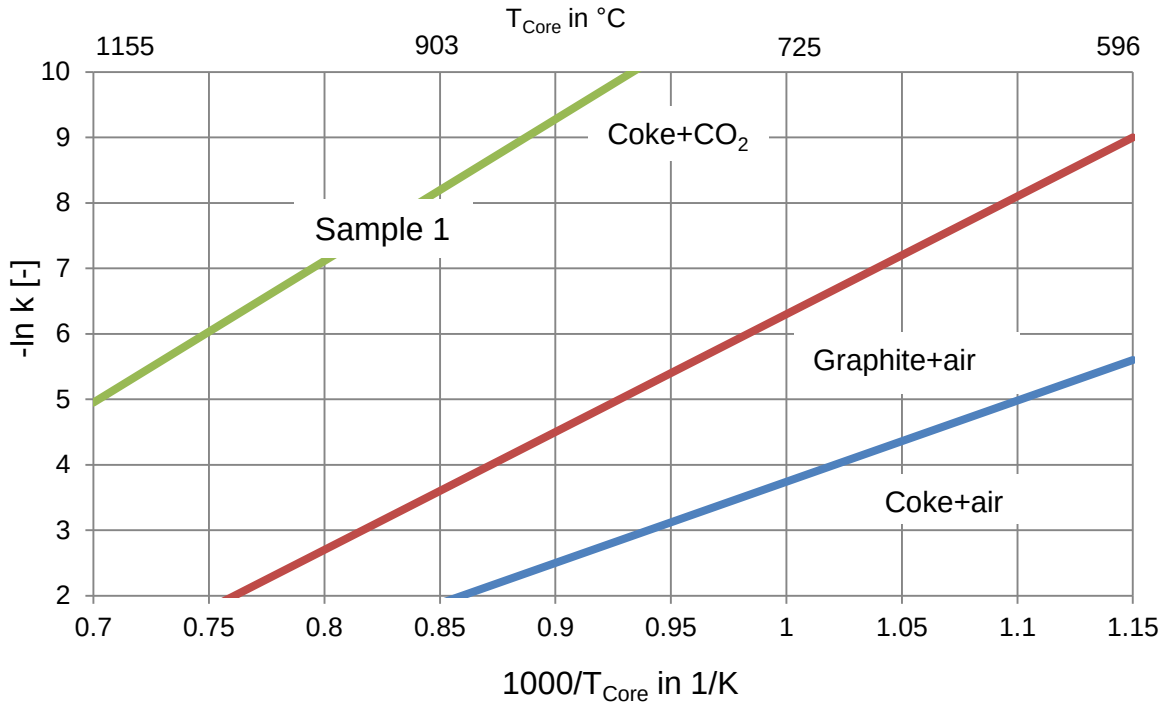

Figure 4.7: Reaction coefficient of coke and graphite under different condition

Based on experimental investigation, the influence of CO_2 partial pressure over the process can be better described by linear approximation. Experimental investigations implicate that Langmuir-Hinshelwood formulation rewritten with modification of exponent partials pressure. Furthermore, the good compatibility of results for surface related reaction coefficients has been observed for a broad range of parameter values. The new set of values of reaction coefficients for coke in an environment of CO_2 is obtained on the basis of experimental study. The value of reaction coefficient for the Boudouard reaction was used in the further modeling of the combustion of coke particles. The kinetic analysis provides the values of activation energies and pre exponential factors which are compared to a variety of data available in the literature.

From the experimental, the Arrhenius equation can be rewritten as follows:

$$k_{CO_2} = k_0.e^{-E_A/RT_c}$$

$$k_0 = 30\times10^3 m/s$$

$$E_A = 202[KJ/mol]$$

$$k_{CO_2} = 30\times10^3.e^{-E_A/RT_c}$$

$$k_{O_2} = k_0.e^{-E_A/RT_c}$$

$$k_0 = 6.3\times10^3 m/s$$

$$E_A = 100[KJ/mol]$$

$$k_{O_2} = 6.3\times10^3.e^{-E_A/RT_c}$$

Table 4.2 : The different type of coke and experimental with CO_2

C+CO₂→2CO	
Coal Type	**Activation Energy (kJ.mol^{-1})**
sample 1	202.23
sample 2	202.67
sample 3	189.62

4.5 Simulations of kinetics model for the coke reaction

4.5.1 Change of mass with combustion time

Coke is charged from left to right and oxygen from opposite direction. The mass change is related to the initial mass of the particle. After the start of the oxidation,

the more increases the conversion rate in the direction of the gas flow, the higher temperature is. Figure 4.8 shows the comparison of the conversion of coke with different excess air number as a function of time. After 180 minutes, coke is burnt out completely for **λ**=0.8, at 160 minutes for **λ**=0.85 and 150 minutes for λ=0.9 respectively as seen in Figure 4.8.

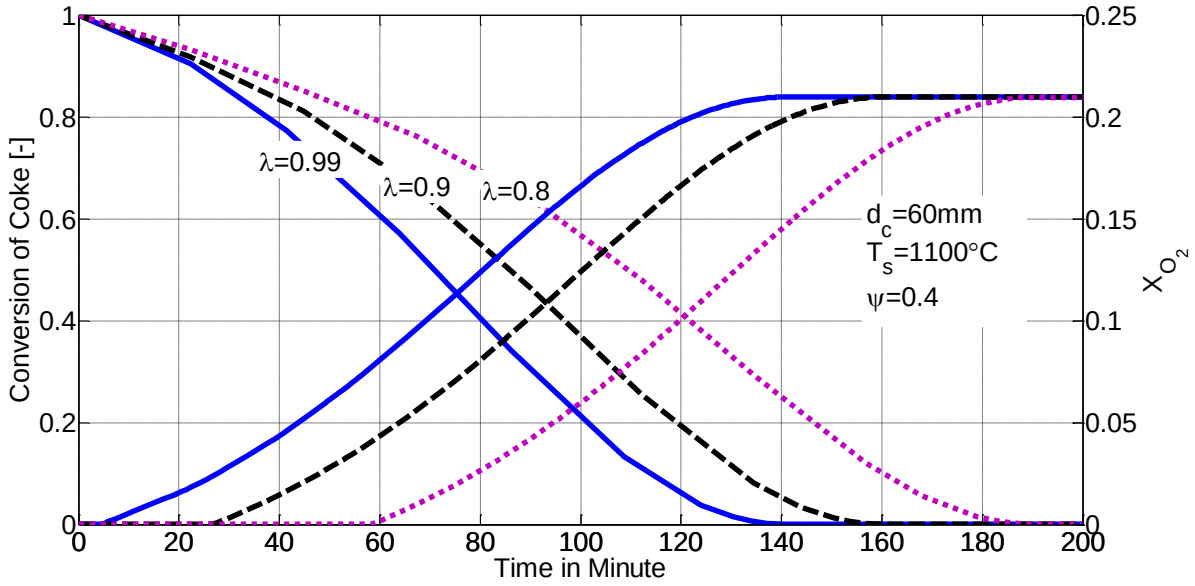

Figure 4.8: Mass change of the coke particles with excess air number

4.5.2 Gas Concentration

The concentration of gas components (O_2, CO_2 and CO) are predicted by the model. The oxygen concentration in gases decreases due to its consumption by the combustion reaction. When the oxygen decreased along the length, the concentration of carbon dioxide increased as seen in Figure 4.9 and 4.10. The produced carbon monoxide by the Boudouard reaction immediately burns with oxygen to produce carbon dioxide. When oxygen is burnt out completely, carbon dioxide reacts with carbon to form carbon monoxide. The concentration of carbon dioxide reaches a maximum when concentration of oxygen is zero. After that carbon dioxide decrease as no more oxygen to burn with carbon and produced carbon dioxide. Consequently, the concentration of CO is started increase because no more oxygen to react with carbon.

For **λ**=0.9 the concentration of oxygen decreased after 140 minutes and **λ**=0.9 is after 130 minutes. At this position the concentration of CO_2 is started to

produce due to the combustion as can be seen in Figure 4.9. The same condition apply for **λ**=0.85 and **λ**=0.8 in Figure 4.10. It can be seen that the combustion time is higher with decreasing excess air number.

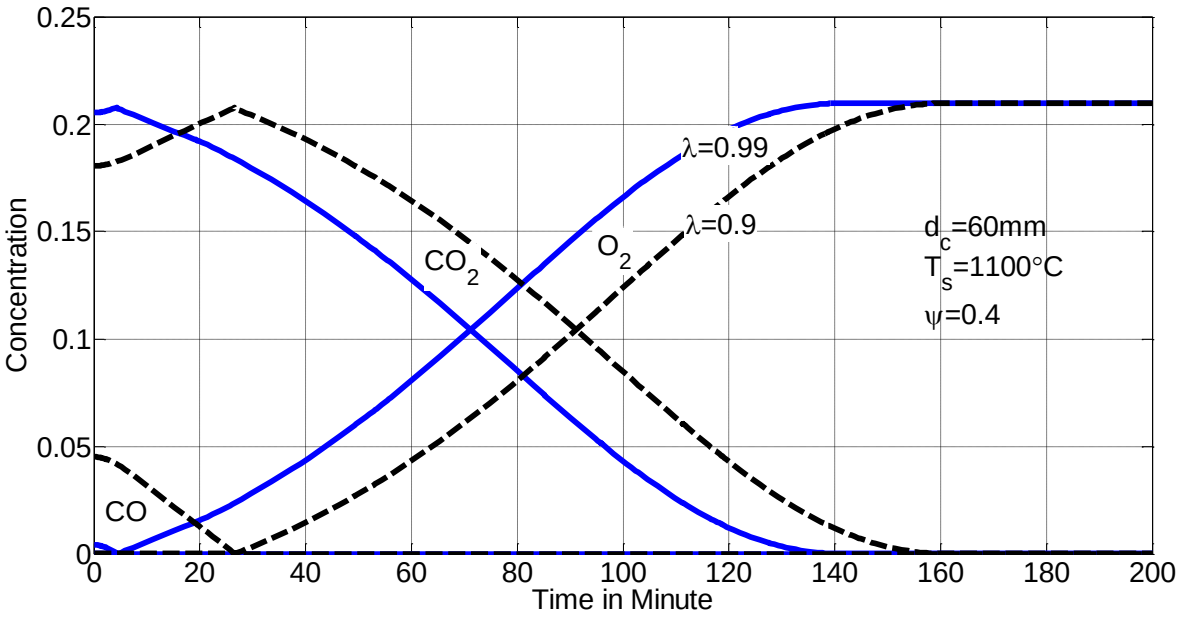

Figure 4.9: Concentration of gases with λ= 0.99 and λ= 0.9

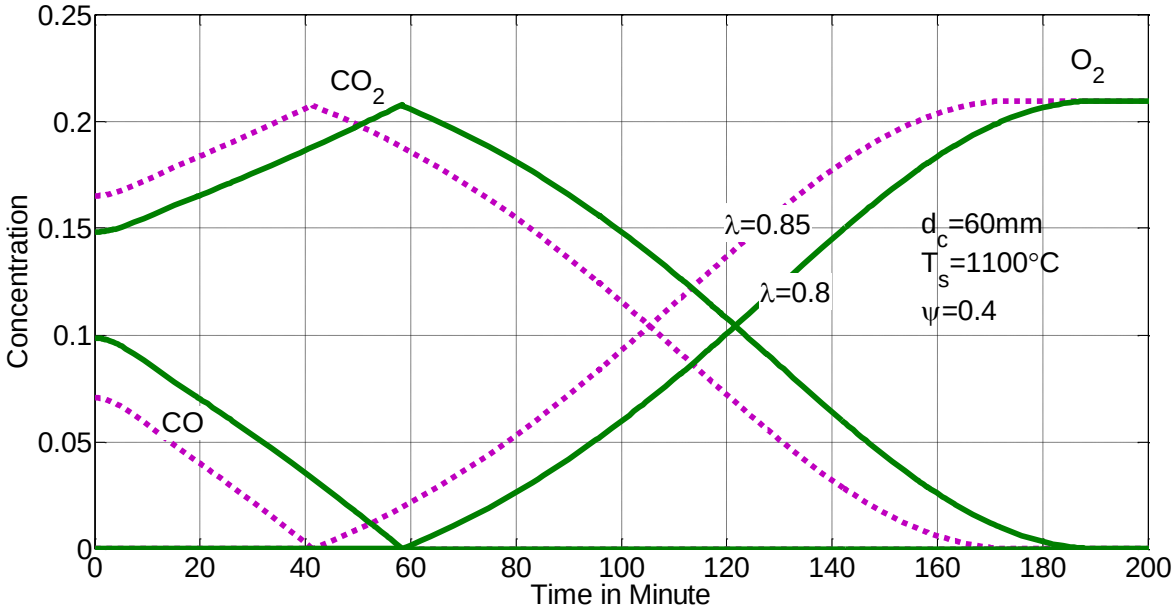

Figure 4.10: Concentration of gases with λ= 0.85 and λ= 0.8

4.5.3 Rate of change of mass

Figure 4.11 and 4.12 shows rate of change of mass flow to direct oxidation and the Boudouard reaction. After the start of the oxidation, the conversion rate increases in the direction of the gas flow. The reason is that the area of the coke increases. However, the partial pressure of oxygen decreases. Therefore, a maximum occurs. After this maximum the conversion rate of the oxidation decreases, because the decrease of the partial pressure has a stronger effect as the increase of the coke area. Until the maximum of the oxidation, the conversion due to the Boudouard reaction is negligible.

For λ=0.8 the conversion rate of oxidation and Boudouard becomes equal at 85 minutes when particle diameter is 60 mm. At this position the concentration of oxygen is 2% and the concentration of carbon dioxide is 18%, as can be seen in Figure 4.10. The concentration of carbon dioxide must be about 10 times higher than that of oxygen so that both conversion rates are equal. This shows that the Boudouard reaction is much slower than the oxidation reaction. The same concentration values apply for λ=0.85, λ=0.9 and λ=0.99.

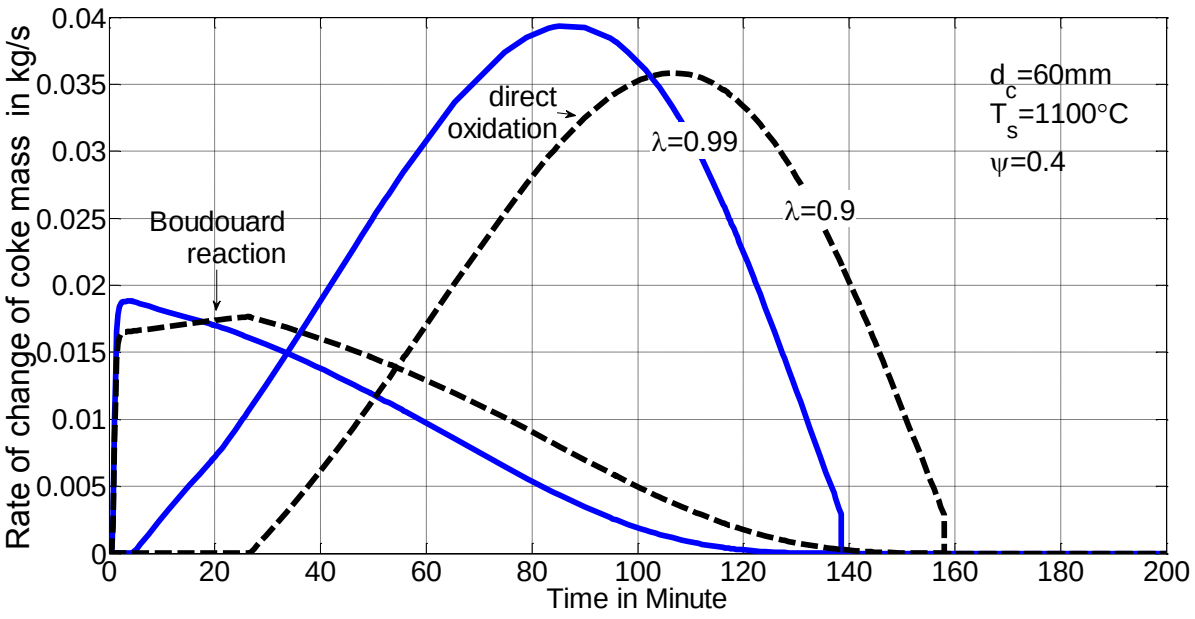

Figure 4.11: Rate of change of mass of the coke particles with direct oxidation and Boudouard reaction

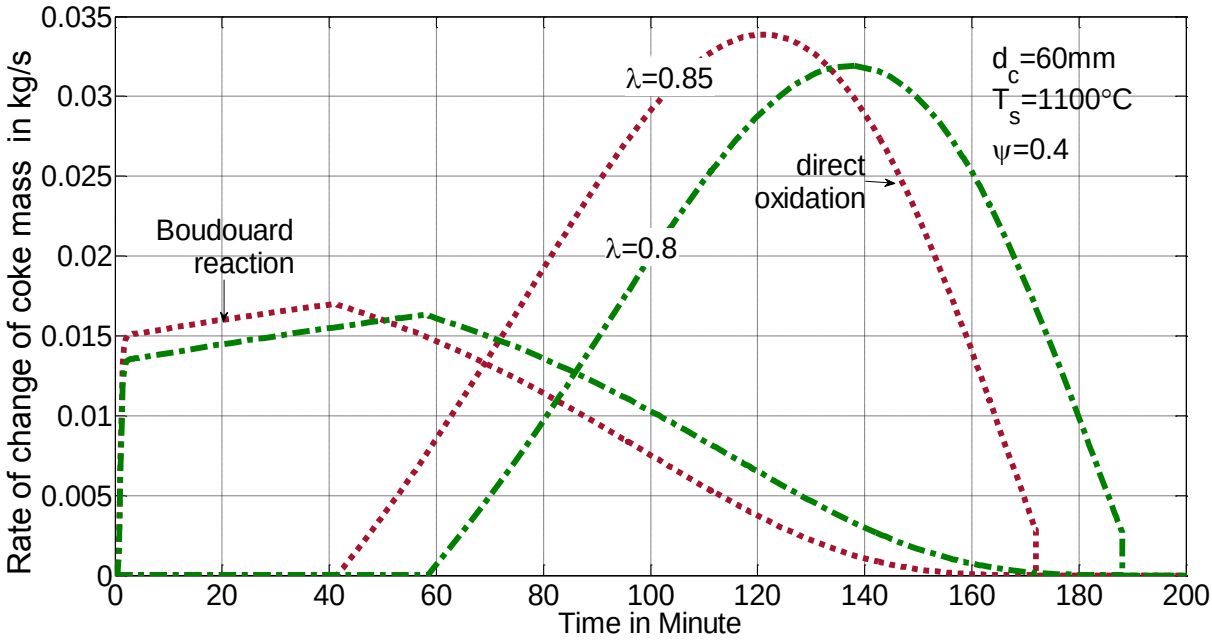

Figure 4.12: Rate of change of mass of the coke particles with direct oxidation and Boudouard reaction

4.5.4 Combustion time with Boudouard effects

Figure 4.13 presents the conversion time of coke particles for different excess air numbers and temperatures. The lower the excess air number, the higher the conversion time and the longer conversion length become. When the temperature is higher, the conversion time is lower. When the temperature is lower than 1000 ºC, the slope of the combustion time sharply increases, especially if the excess air number is less than one. At the lower temperature, the combustion time for different excess air number on combustion time is much higher. There is not much influence for excess air number on the combustion time when the temperature is more than 1200 ºC because the reaction constant for Boudouard is not influence for high temperature.

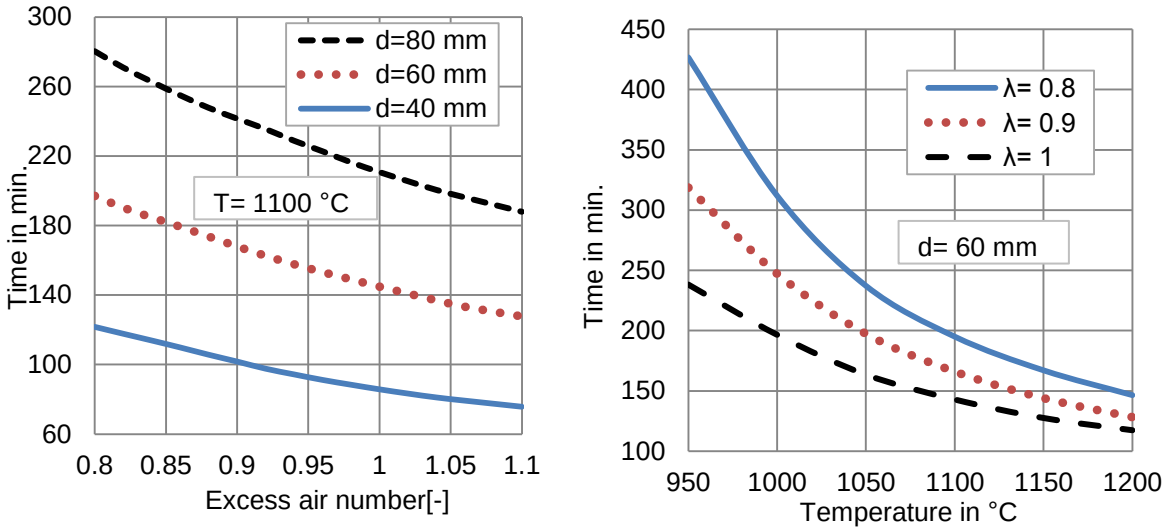

Figure 4.13: Combustion time of coke including Boudouard reaction

4.6 Summary

This work aimed at improving the reaction mechanism of coke particles combustion of the shaft kiln. The mathematical model of the kiln has been developed and supported of coke particles combustion. The rate of change of mass for both Boudouard reaction and direct oxidation, the concentration of carbon dioxide and carbon monoxide in the flue gas of the kiln are calculated for several cases of excess air number. The current approach would provide a good understanding of combustion of coke particles with kinetics reaction. The model is based on a detailed description of the process inside the kiln and the concentration profiles and conversions profiles predicted by the model are compared for validating the model.

This model serves as basic to model the limestone calcination in mixed feed kilns. The heat of the oxidation must be coupled with the endothermic calcination. Then the real profile of the coke and limestone can be calculated. The real temperature of the coke particles additionally influences the length of the Boudouard zone. This indicates that the assumptions made are reasonable for the model to describe the most important phenomena in the kiln.

5 Modelling of coke combustion inside shaft kiln with given stone temperature

5.1 Introduction

The combustion behavior of coke particles inside the kiln is usually an uncertain behavior which has strong influences on the combustion process inside the kiln, creating difficulties for design optimization and regulation. A mathematical model for coke combustion inside a shaft kiln has been used to study the effects of important operating parameters on the kiln operation. However, coke combustion is a highly complex process, involving the combination of different processes like chemical kinetics, heat and mass transfer. The combustion takes place when coke particles come in contact with air. It is also known from previous studies that the lengths of the three zones: preheating zone, combustion zone and cooling zone are different depending on the mass flow rate of solid particles. In this chapter, the influence of process parameters on coke combustion in the combustion zone has been analyzed. The shaft kiln is assumed to be a packed bed of spherical particles with bed porosity of 0.4, for the determination of the heat and mass transfer process. The reaction considered in the shaft kiln is: $C + O_2 = CO_2$ as a global reaction. The following assumptions are made for developing this model:

1. coke particles and stone particles are spherical in shape
2. the packed bed has constant void fraction
3. the conditions at each cross section along the kiln axis are homogeneous
4. the density of the particle stays constant while the particle size changes
5. no ash left on the particle surface during oxidation
6. stone particle size remains constant during the combustion process.

The mathematical model is used to predict the effects of the operating conditions and the performance of the kiln such as combustion length, the temperature of the gas and coke and the change in mass of the coke. The energy

and the mass balance are calculated independently; however, all the equations are coupled.

5.2 Energy and mass balances and equations

5.2.1 Process description

al temperature profile of a normal shaft kiln is shown in Figure 5.1. Coke and stone particles are charged from the top and combustion air enters from the bottom of the kiln. Process parameters of the kiln such as throughput and gas flow are determined by the industrial data. The preheated air enters from the bottom of the kiln and the stone temperature, T_s is considered as a given temperature. The combustion of coke is strongly dependent on size of coke, density of coke and process temperature. To calculate the combustion length, the reaction zone has to be considered and the preheating zone has to be separated. During the combustion of coke particles, the mass fraction decreases continuously until the burnout period.

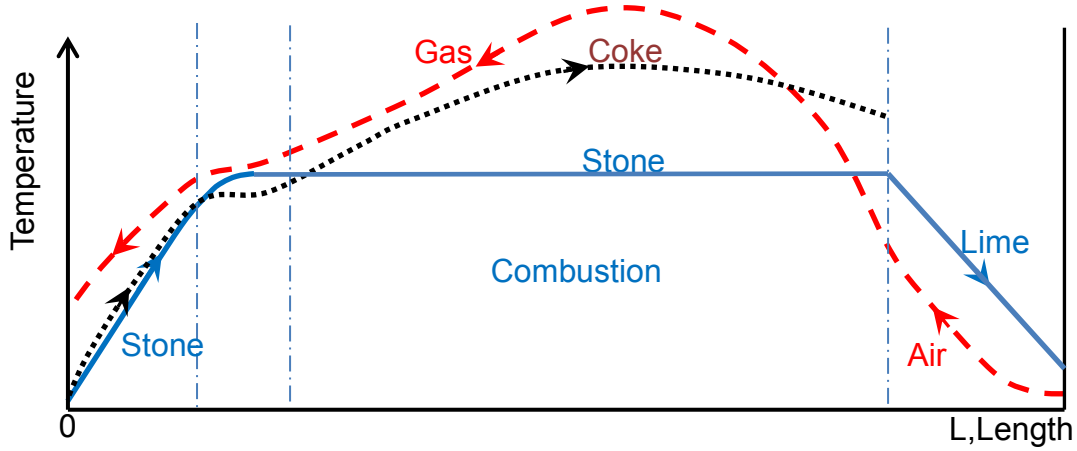

Figure 5.1 Principal of the temperature profile and flow direction of solid and gas

5.2.2 One dimensional approach

A mathematical model has been developed which describes the combustion process simulation of particles with high temperature process inside the shaft kiln. One dimensional energy equation has been solved numerically, with a variable energy source term. 1-D model can be applied where the heat transfer takes place as the heat transfer in the axial direction is negligible compared to the heat transfer in radial direction.

5.2.3 Determination of heat transfer coefficients for the kiln

The heat transfer in a shaft kiln (packed bed) is dominated by convection. One approach to estimate the convective heat transfer coefficient ($\boldsymbol{\alpha}$) in a packed bed is proposed [11] in which a packed bed can be described. The Nusselt correlation in the packed bed is given as:

$$\mathbf{Nu_{bed}} = \mathbf{2} + \mathbf{1.12}.\mathbf{Re}^{\mathbf{0.5}}.\mathbf{Pr}^{\mathbf{0.33}}\frac{(\mathbf{1}-\boldsymbol{\Psi})^{\mathbf{1}/\mathbf{2}}}{\boldsymbol{\Psi}}. \tag{5-1}$$

where ψ is the void fraction of the packed bed.

The Nusselt number is defined as:

$$\mathrm{Nu_{bed}} = \frac{\alpha.\mathrm{d}}{\lambda_g}, \tag{5-2}$$

where d is the diameter of the particle and λ_g is the thermal conductivity of air. The Reynolds number is given by:

$$\mathrm{Re} = \frac{\mathrm{w.d}}{\nu.\psi}, \tag{5-3}$$

where v is gas kinematic viscosity and w is the empty tube velocity that is also known as superficial velocity, if no packing were present in the bed. This velocity is determined by:

$$\mathrm{w} = \mathrm{w_{STP}}.\frac{\rho_{STP}}{\rho}. \tag{5-4}$$

Where w_{STP} is the velocity at STP (standard temperature and pressure) condition, ρ and ρ_{STP} is the density at temperature T and at STP. The velocity w_{STP} is given as:

$$w_{STP} = \frac{\dot{V}_{STP}}{A_f}. \tag{5-5}$$

Here $\dot{V}_{STP}$ is the volume flow of gas at STP and A_f is the cross-section area of the kiln.

5.2.4 Energy balance

The energy balance is established for the gas and the solid fuel (coke particles) in a section of kiln length dz. With a set of energy equation, the diameter of the coke and excess air number are taken into consideration as variable. Energy is supplied in the kiln with the combustion of solid fuel. The heat input for the kilns is from the mass of fuel multiplied by its net calorific value, $M_c h_u$. The energy balance equations are described as following and it depends on the length of the kiln, z:

For the gas,

$$d\left[\dot{\mathrm{M}}_{\mathrm{g}}.\,\mathrm{c}_{\mathrm{p,g}}.\,\mathrm{T}_{\mathrm{g}}\right] = d\dot{\mathrm{M}}_{\mathrm{co}}.\,h_{u,co} - \propto_{\mathrm{s}}.\,\mathrm{dA}_{\mathrm{s}}.\left(\mathrm{T}_{\mathrm{g}} - \mathrm{T}_{\mathrm{s}}\right) - \propto_{\mathrm{c}}.\,\mathrm{dA}_{c}.\left(\mathrm{T}_{\mathrm{g}} - \mathrm{T}_{\mathrm{c}}\right). \qquad (5\text{-}6)$$

The change of enthalpy of gas is equal to the heat generated by the combustion of the coke minus the convective heat transfer between the gas and stone and convective heat transfer between gas and coke. The gas radiation of the CO_2 can be neglected compared to the convective heat transfer because of the small gap between the particles. Here $\dot{\mathrm{M}}_{\mathrm{g}}$ is the mass flow rate of the gas, $\mathrm{c}_{\mathrm{p,g}}$ is the gas specific heat capacity, T_{g} is the gas temperature, T_c is the temperature of the coke, $\dot{\mathrm{M}}_{\mathrm{co}}$ is the mass flow of the coke decomposed CO, $h_{u,co}$ is the fuel calorific heating value with respect to CO, $\propto$ is the heat transfer coefficient, A_{s} is the surface area of the stone, A_{c} is the surface area of the coke particles inside the furnace and it is changing with the length.

For the coke

$$d\left[\dot{M}_c.\,c_{p,c}.\,T_c\right] = d\dot{M}_c.\,h_{u,c} - \propto_c.\,\mathrm{dA}_c.\left(T_c - T_g\right) - \varepsilon_{\boldsymbol{c}}.\,\sigma.\left(\mathrm{T_c}^4 - \mathrm{T_s}^4\right).\,\mathrm{dA}_c. \qquad (5\text{-}7)$$

The change in enthalpy of solid flow is equal to the local heat produced by the combustion of coke subtracted from heat transferred between the coke and the gas plus the radiation heat transfer between coke and stone particles. Here $\dot{M}_c$ represents the mass flow of the coke, $c_{p,c}$ is the coke specific heat capacity, $\boldsymbol{\varepsilon}$ is the emissivity and σ is the Stephan-Boltzmann constant (5.67×10^{-8} W/m^2K^4).

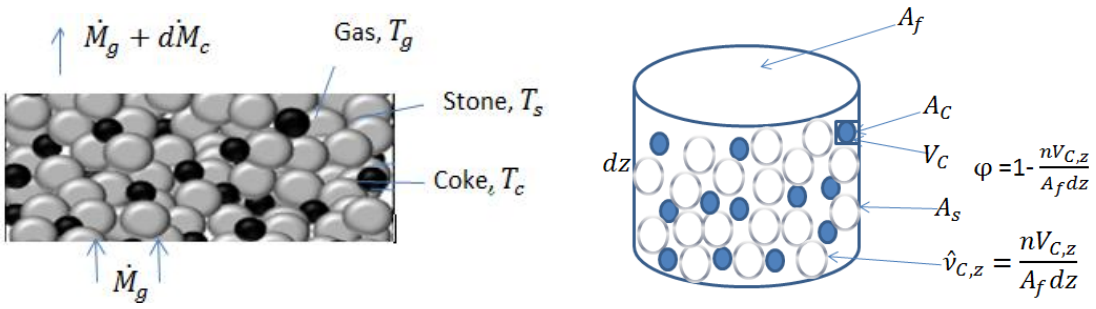

Figure 5.2 Change of coke area along the kiln length

The number of particles, n is constant throughout the combustion chamber, $\frac{dn}{dz} = 0$. The specific area of coke particles is increased, but the total area and the volume fraction is decreased along the length.

$$dA_C = A_f . dz . O_{C,z} . \hat{v}_{C,z} . (1 - \psi). \quad (5\text{-}8)$$

$$dA_s = A_f . dz . O_s . \left(1 - \hat{v}_{C,z}\right) . (1 - \psi). \quad (5\text{-}9)$$

Where, $\mathrm{dA_C}$ is the elemental surface area per unit length of the coke particles inside the shaft kiln, A_f is the cross sectional area of the furnace, $O_{C,z}$ is the specific surface area of the cokes and stones in m^2/m^3, $\hat{v}_{C,z}$ is the volume fraction of the coke particles (the mass fraction is converted into volume fractions using density) the entire particles inside the kiln and the elemental area of the coke in mass reaction, Ψ stands for the void fraction of the bed, $\mathrm{dA_s}$ is the elemental surface area per unit length of the stone particle.

The expression for specific surface area of the coke and stone particles is defined,

$$\mathrm{O_{C,z}} = \frac{A_{C,z}}{V_{C,z}} = \frac{6}{d_{C,z}} \quad , \; O_s = \frac{A_s}{V_s} = \frac{6}{d_s} \quad . \quad (5\text{-}10)$$

The volume of a single particle in the bed is

$$V_{C,z} = \frac{\pi}{6} {d_{C,z}}^3 \; . \quad (5\text{-}11)$$

Where $d_{C,z}$ is the actual diameter of coke particle at specific length, z and $V_{C,z}$ is the actual volume of the particle at specific length, z.

$$\hat{v}_{C,z} = \frac{V_{C,z}}{V_{C,z}+V_{s,z}} \quad . \tag{5-12}$$

$\hat{v}_{C,z}$ is the volume fraction from the ratio of the mass flow rate and density.

$$\hat{v}_{C,z} = \frac{\dot{M}_{C,z}/\rho_C}{\dot{M}_{C,z}/\rho_C + \dot{M}_s/\rho_s} \quad . \tag{5-13}$$

The specific area of coke particle is increased, but the total area and the volume fraction is decreased along the length. To solve the equation 5-6 and 5-7, it is necessary to know the value of the boundary temperature from the entering side. The larger the heat transfer and the higher the kiln, the smaller is the difference in temperature between gas and solid.

5.3 Mass Balances

The mass flow rate of the gas, $\dot{M}_g$ is composed of the mass flow of the coke along the kiln and the mass flow rate of air.

$$\dot{M}_g = \dot{M}_{C,z} + \dot{M}_{a,l} \; . \tag{5-14}$$

The mass flow of air is a function of air demand L, which depends on kind of fuel, and excess air number. The relationship is as follows:

$$\dot{M}_{a,l} = \lambda \mathrm{L} \dot{M}_{C,0} \quad . \tag{5-15}$$

The change of mass carbon from solid to gas is directly proportional to the change of mass flow of oxygen from gas to solid and is given by

$$d\dot{M}_C = \frac{\tilde{M}_C}{\tilde{M}_{O_2}} . d\dot{M}_{O_{2,z}} \quad . \tag{5-16}$$

The change of mass of the coke is equal to the reaction rate per unit volume of the kiln and can be given as:

$$d\dot{M}_C = \frac{1}{1/\beta + 1/k_{O_2}} \cdot dA_C \frac{P_{O_2,g}}{R_{O_2} T_g} \frac{\tilde{M}_C}{\tilde{M}_{O_2}} \quad . \tag{5-17}$$

The experimental investigation of the reaction rate constant K_0, for several types of cokes found out that the value K_o ranges from 7000 to 7500 and the activation

energy (E) from 75000 to 10000 KJ/mol. The mass transfer from the diffusion coefficient and Sherwood number is as follows:

$$\beta = \frac{D \cdot Sh}{d_{c,z}} \ , \tag{5-18}$$

where D is the diffusivity (m^2/s) and Sh is the Sherwood function and it is determined by experiments as,

$$Sh = 1.12.Re^{0.5}.Sc^{0.33}\frac{(1-\Psi)}{\Psi}^{1/2}. \tag{5-19}$$

The change of diameter is related to the change of mass and is dependent on the initial condition of mass flow of the coke particle.

$$d_{c,z} = (\frac{6M_{c,z}}{\pi\rho_c})^{1/3} \quad . \tag{5-20}$$

5.4 Operating parameters

5.4.1 Parameter for the model

Table 5.1 represents the operating parameters that are used in this model. The developed model predicts the gas and coke temperature profiles, change of mass of coke with oxygen concentration, and the gas concentration inside the kiln. The length of the kiln and energy usage depends on each other. On the other hand, the size of the coke particles, excess air number, and mass flow of the coke can be adjusted. The stone particles do not give any energy and reaction

Table 5.1: Input data for the model

1	Shaft diameter, D_{kiln}	D_{kiln}	2	m
2	Mass flow of stone	M_s	55	ton/day/m^2
3	Density of coke	ρ_c	1000	kg/m^3
4	Density of stone	ρ_s	2700	kg/m^3
5	Diameter of coke, d_c	d_c	50-100	mm
6	Specific capacity of coke	$C_{p,c}$	1200	kJ/kg.K
7	Thermal conductivity of coke	λ_c	0.7	W/m.K
8	Calorific heating value coke give	$h_{u,c}$	19000	J/kg
9	Calorific heating value to gas	$h_{u,co}$	10000	J/kg
10	Height of kiln	H	6	m
11	Specific capacity of air	$C_{p,air}$	1005	J/kg.K
12	Air demand	L	11.6	kg-air/kg-c
13	Void fraction	Ψ	0.4	-
13	Excess air number	**λ**	1.05-1.2	-
14	Input temperature of coke	T_c	20	^oC
15	Input temperature of air	T_a	800	^oC

5.4.2 Solving the system

The model consists of mass and heat balance, along with the boundary conditions. The model is solved with an ordinary differential equation solver (ode45) and to deal with a complex coupling of equations and boundary conditions, the boundary value solver (bvp4c) is used to solve the system.

Solid particles (i.e. coke and stone) are charged from the kiln top and oxygen from the bottom of the kiln. An initial condition, the coke temperature at 20ºC ($T_{C(z=0)}$ =20^{o}C) and the preheated air was injected from the bottom of the kiln at 800ºC ($T_{g(z=L)}$ =800^{o}C). The stone particles are preheated to 1200ºC, (T_s=1200^{o}C). The initial mass of coke is 5% of total mass of stone. It is assumed that the size of stone particles remain constant along the kiln length. Due to combustion, the change of mass of coke depends on coke diameter and density. The combustion of coke started nearly at the top of the kiln when coke temperature rises to 700ºC. Since the reaction rate is faster than diffusion, the

carbon is consumed first at the surface. It is assumed that the reaction coefficient for carbon dioxide does not influence the combustion of coke and heat transfer from radiation is neglected.

5.5 Influence of the excess air number

As an example, the change in the mass of coke according to oxygen concentration at various excess air numbers as a function of kiln length is simulated. The mass flow of the stone is defined 55 ton/day/m^2 in this simulation. The coke particles are assumed to be 5% of total solid particles inside the kiln. The influences of excess air number on the combustion process as a function of kiln length is represented in Figure 5.3-a and 5.3-b. When the excess air number is 1.05, the conversion of coke slowly changes before 1 m. The combustion length is approximately 5.5 m for λ= 1.05 and around 4.5 m for λ= 1.1, when the constant stone temperature is 1200^{o}C.

When the constant stone temperature is 1100^{o}C, the combustion length is changed from about 5.8 m for λ= 1.05 and 4.8 m for λ= 1.1 as seen in Figure 5.3-b. The higher the excess air number, the shorter is the combustion length and the higher is the residual of oxygen concentration. With the increasing of constant stone temperature, the combustion length decreases.

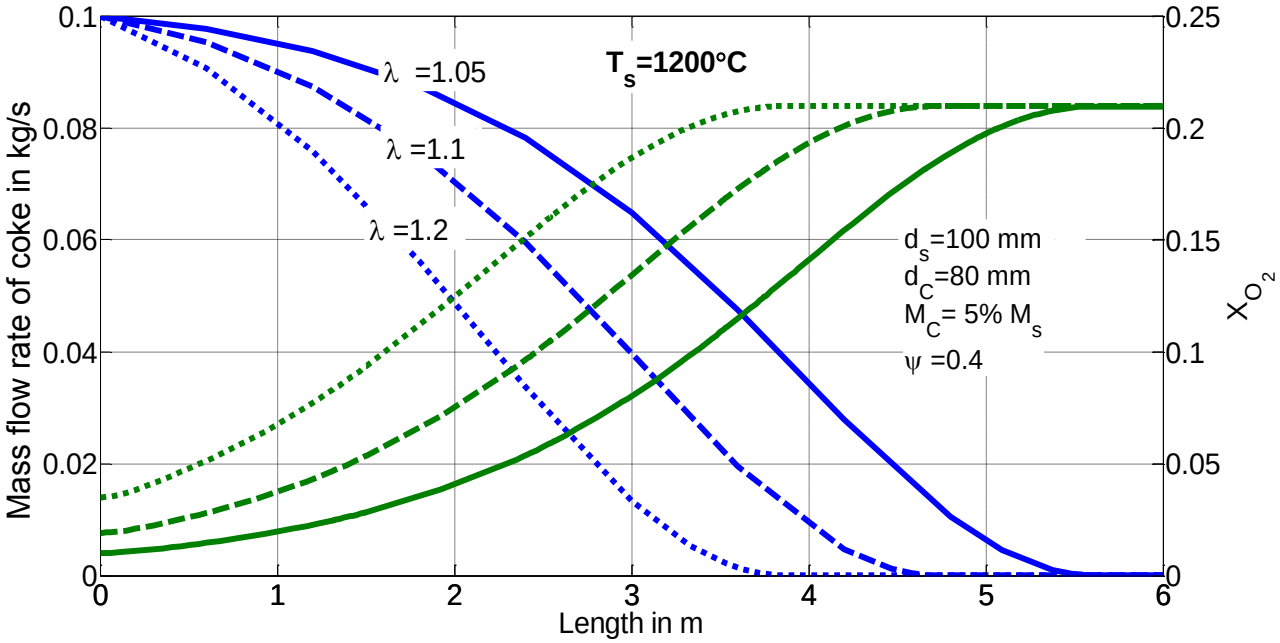

Figure 5.3-a: Mass flow rate of coke and concentration of oxygen along kiln length for T_s=1200^{o}C

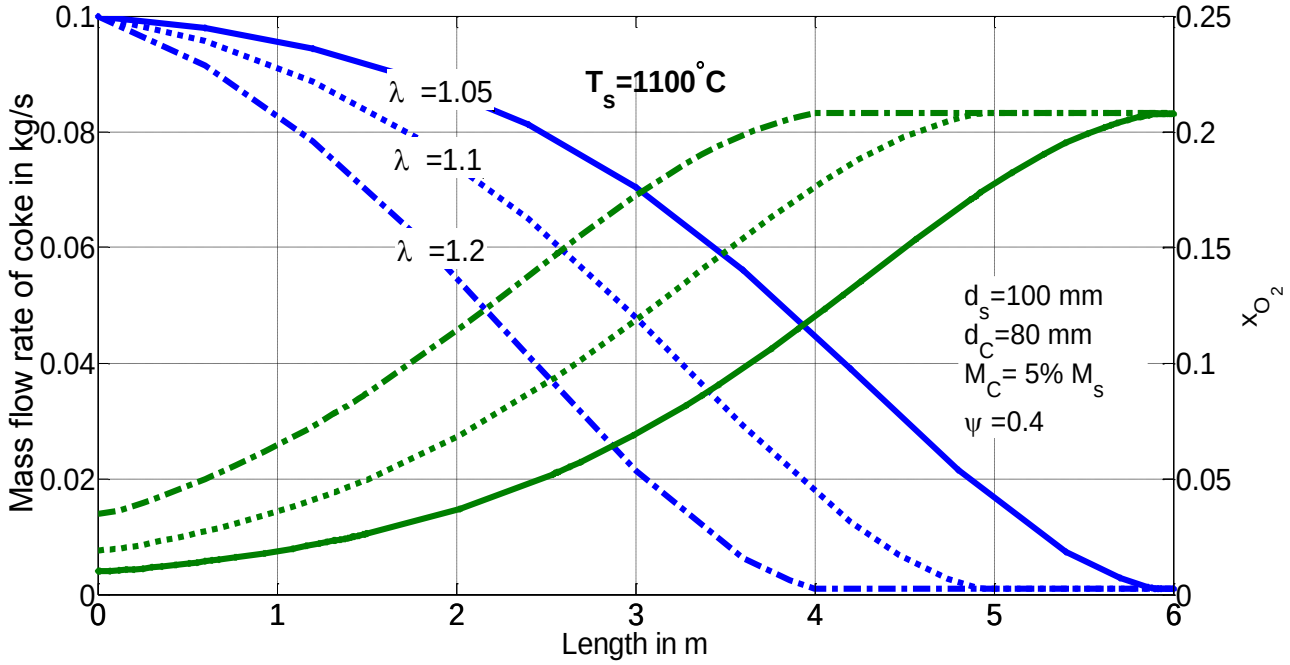

Figure 5.3-b: Mass flow rate of coke and concentration of oxygen along kiln length for T_s=1100°C

Figure 5.4 shows the temperature profile of the gas and coke predicted by the model with different excess air number while stone temperature is considered as a constant at 1100 °C. Therefore the temperature of the particles reaches a maximum before the coke particles are completely burnt out. In the combustion zone, the combustion rate of coke increases and the temperature rise to the maximum of 2100 °C for coke and 1500 °C for gas. Due to the excess air number used in the model, the maximum temperature changes with length.

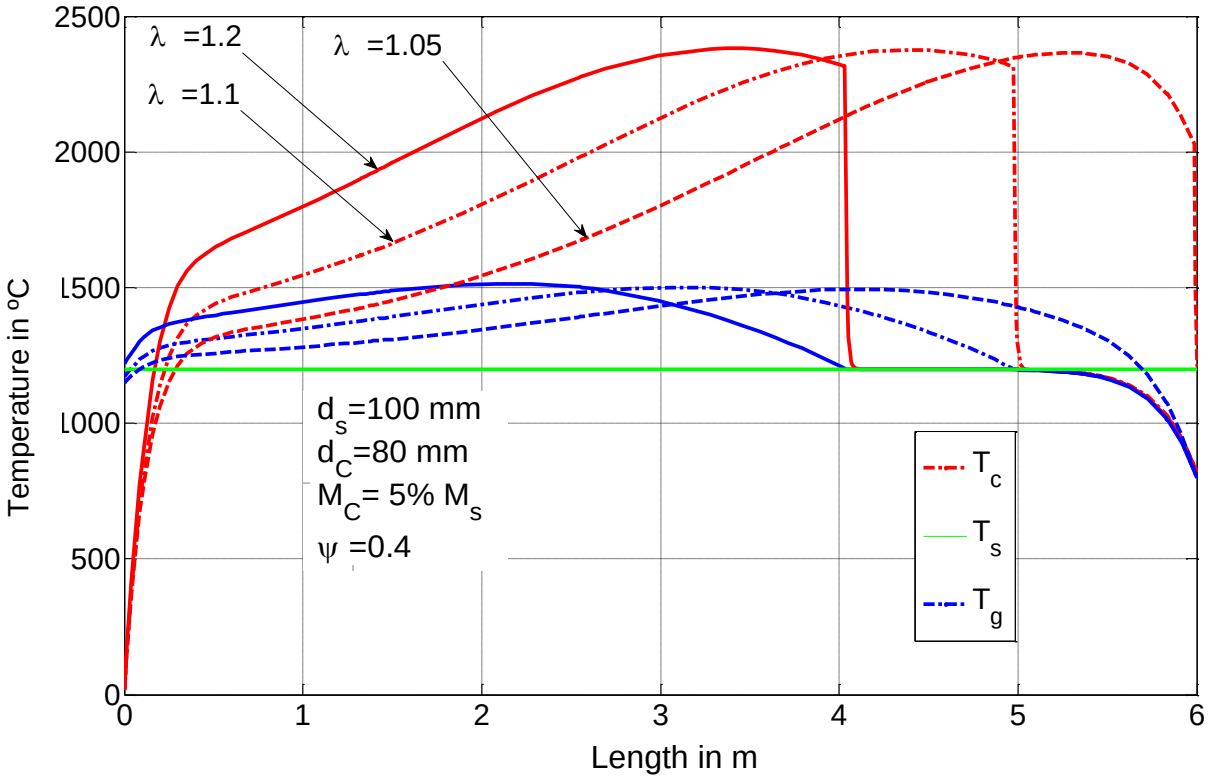

Figure 5.4: Temperature distribution profile along kiln length without radiation

5.6 Influence of the size of coke particles

Figure 5.5 illustrates the change of mass as a function of the kiln length for the different diameter of the coke particles at the given stone temperature 1200°C at **λ**=1.1. The coke particles with diameter of 40mm, 60 mm and 100 mm are considered and the simulation is conducted independently. According to the results, the combustion length for 40mm particle is 1.8 m. When the coke particle size is doubled, the combustion length increases to 4.6 m. So it can be observed that the diameter of the coke particles is proportional to 1.5 power of the combustion length $\frac{d_1}{d_2} \approx (\frac{L_1}{L_2})^{1.5}$.

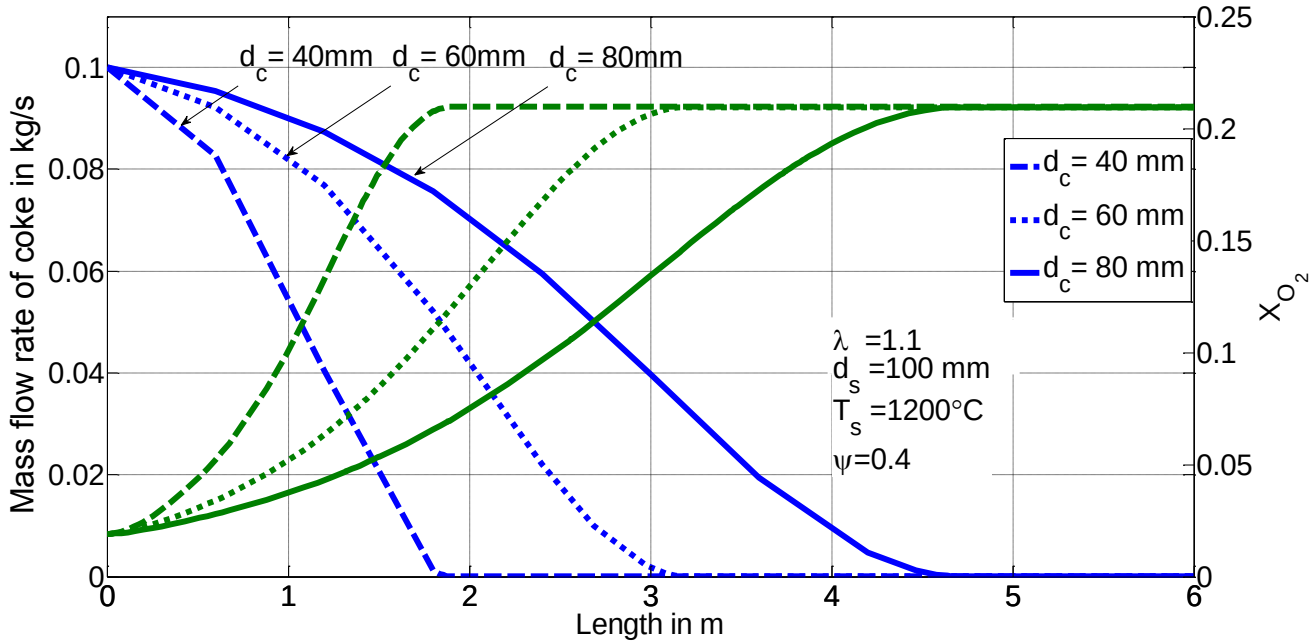

Figure 5.5: Mass flow rate of coke and concentration of oxygen at different coke diameter

Figure 5.6 shows the predicted temperature profile for coke and gas as a function of kiln length at λ=1.1 with different coke sizes. The peak of temperature profiles moves towards to the bottom of the kiln with the increased size of coke particles. The maximum temperature increases with an increase in the size of coke particles since the large coke particles have a smaller surface area per unit mass. The gas temperature reaches a maximum of about 1500^{o}C for d_c= 80 mm and 1300^{o}C for d_c= 40 mm, at that condition the oxygen concentration is about 11%. The gas temperature begins to decrease again after reaching the maximum and it is less than stone temperature when leaving to the kiln top.

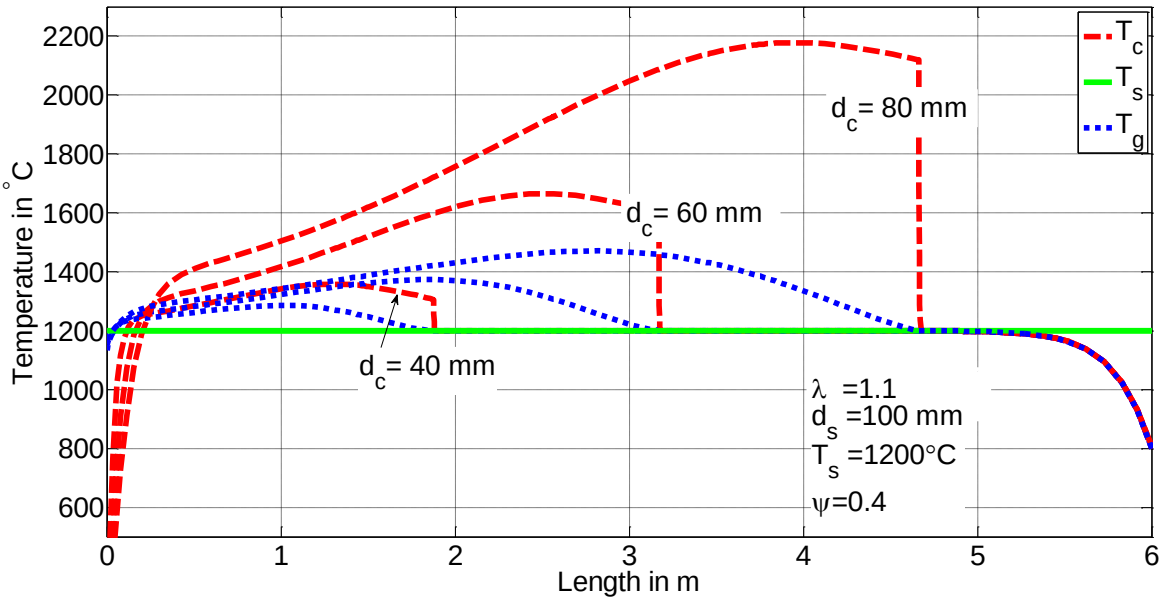

Figure 5.6: Temperature distribution profile along kiln length without radiation

5.7 Influence of the initial stone temperature

Figure 5.7 shows the influence of excess air number as a function of kiln length. All the solid particles enter from the kiln top at the ambient temperature ($T_{c(z=0)}$ =20°C and $T_{s(z=0)}$ =20°C) . When the coke particle temperature rises up to 600°C at the length of 1.8 m, the coke conversion starts slowly. The coke particles burnout completely after kiln length of 5.2 m for λ= 1.2 and 5.8 m for λ= 1.1.

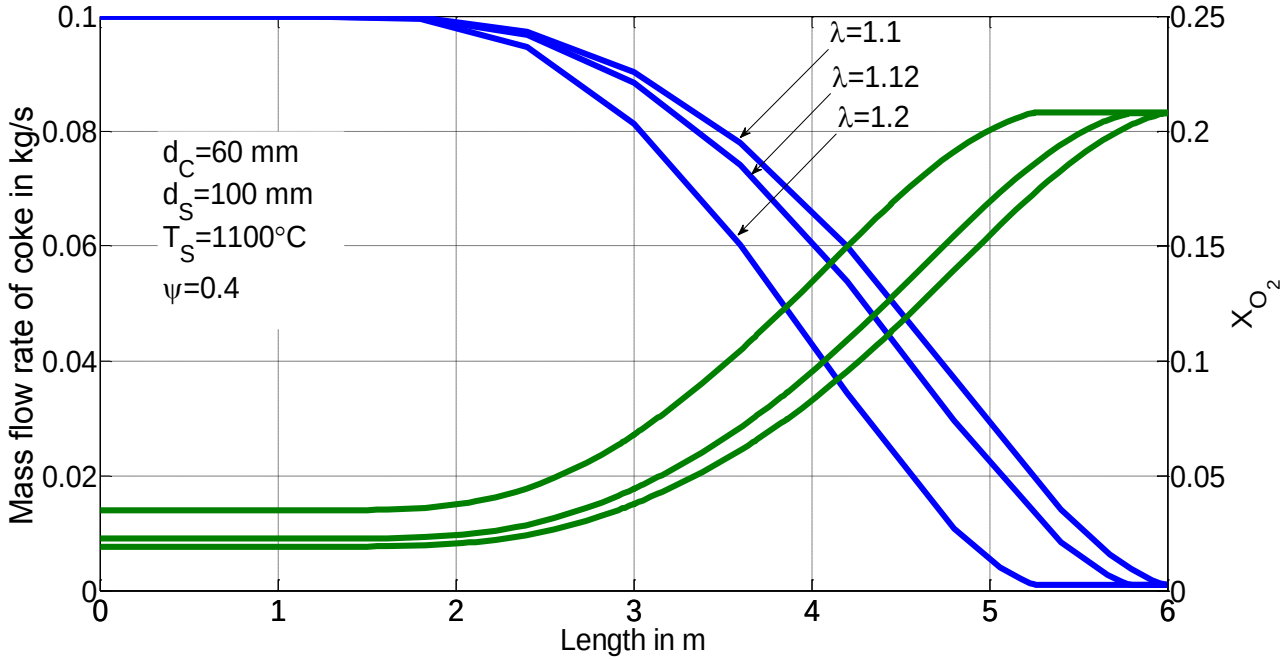

Figure 5.7: Mass flow rate of coke ow along kiln length from top to bottom

Figure 5.8-a shows the predicted temperature profile for coke and gas with λ=1.2. The coke and stone temperature starts from 20^{o}C from the top of the kiln $T_{c(z=0)}$ =20 ^{o}C. At the bottom of the kiln (z=L), the preheated air enters at 800^{o}C. The coke and stone temperature increases linearly along the length of kiln. When the reaction starts, the coke temperature decreases a little but then increases again because of the reaction taking place. The gas temperature is higher than the coke and stone temperature when the specific surface area of coke is small.

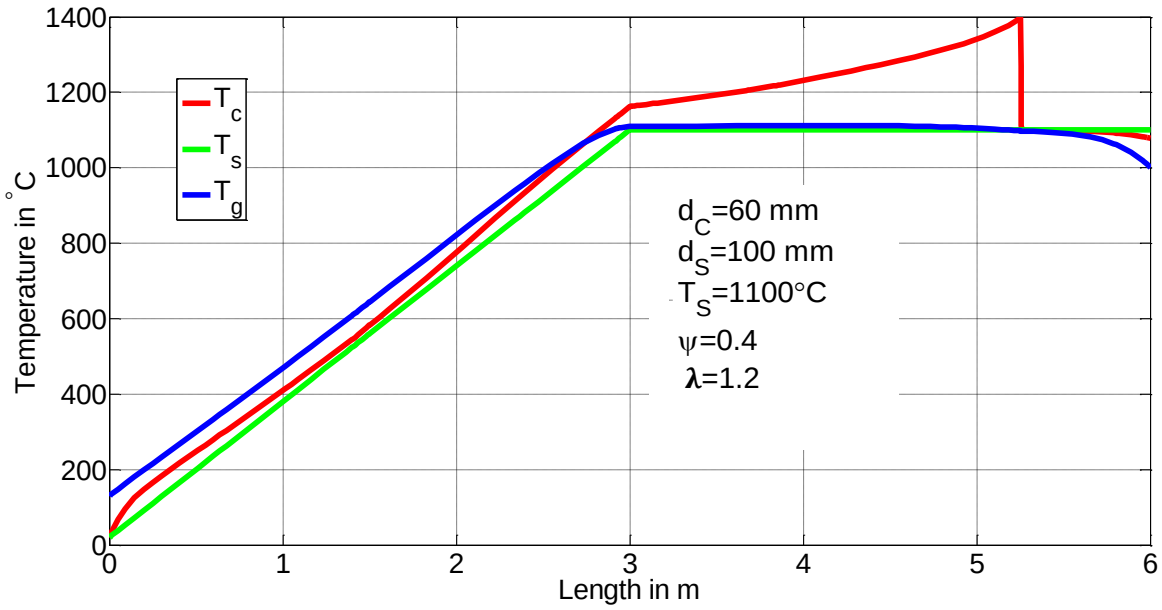

Figure 5.8-a: Temperature distribution profile along kiln length (λ=1.2)

Figure 5.8-b suggests that if the stone particles enter at the ambient temperature for λ=1.1. In this case, the reaction coefficient has a strong effect on the combustion process as low temperature and the flue gas temperature exceeds the solid temperature. In order to determine the effect of combustion temperature at a constant rate, the simulation is performed at different temperature.

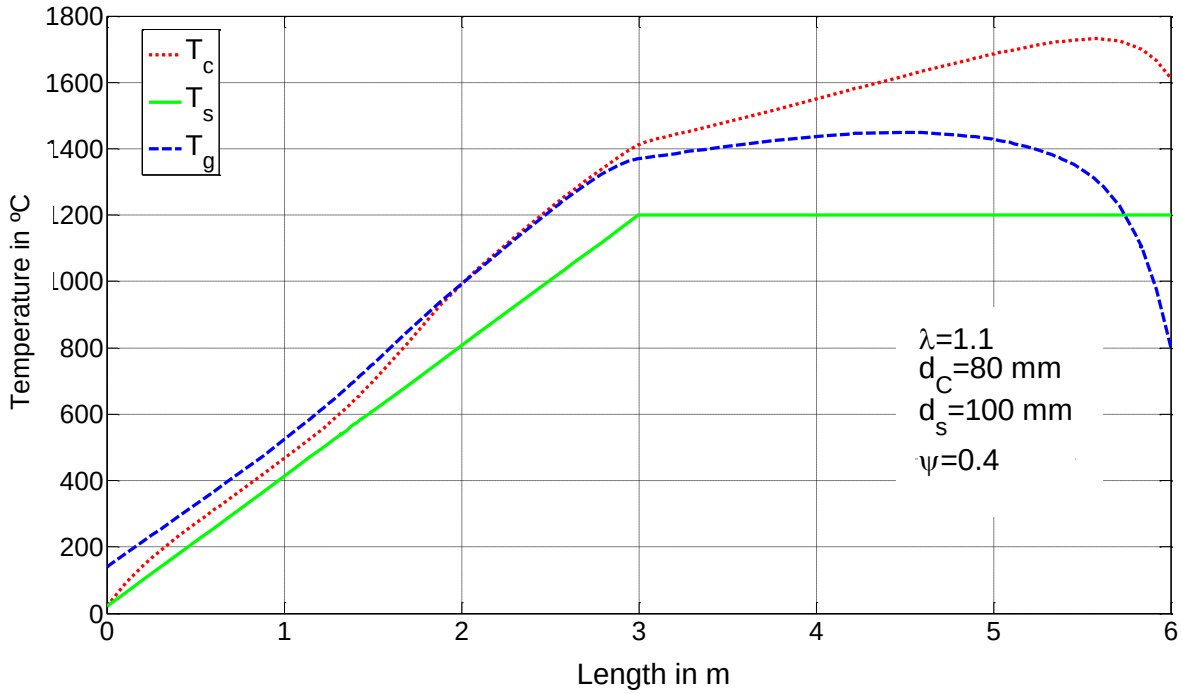

Figure 5.8-b: Temperature distribution profile along kiln length (**λ**=1.1)

The rate of change of the mass coke of as a function of kiln length is shown in Figure 5.9. The maximum rate of change of mass of direct oxidation is at the kiln length of 4 m for **λ**=1.2 and 4.5 m for **λ**=1.1. After reaching the maximum, the rate of change of mass due to oxidation decreases because of an increase in coke surface area. At this maximum position, the concentration of oxygen is around 16%.

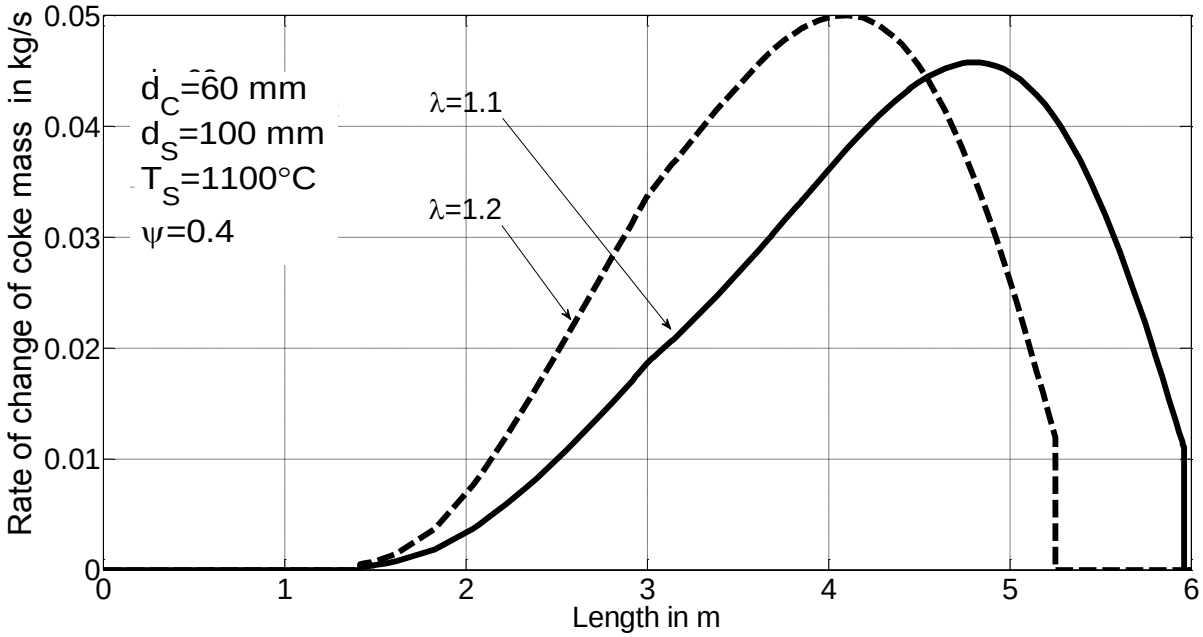

Figure 5.9: Rate of change of mass of the coke particles along kiln length

In Figure 5.10 represents the strong influence of initial stone temperature on the combustion process. When the stone particles enter with a constant temperature of 1100°C ($T_{s(z=0)}$ =1100°C), the combustion of the coke particles takes place at the beginning of the kiln length. When the stone particles enter with a constant temperature at 20°C ($T_{s(z=0)}$ =20°C), no conversion process takes place till the temperature reached around 600°C. After that, conversion starts slowly. In order to determine the effect of initial stone temperature on combustion length, the simulation is performed without and with the preheating zone. This combustion temperature is determined by two factors which are the size of coke particles and excess air number. The initial temperature of particles has a big influence on the combustion length.

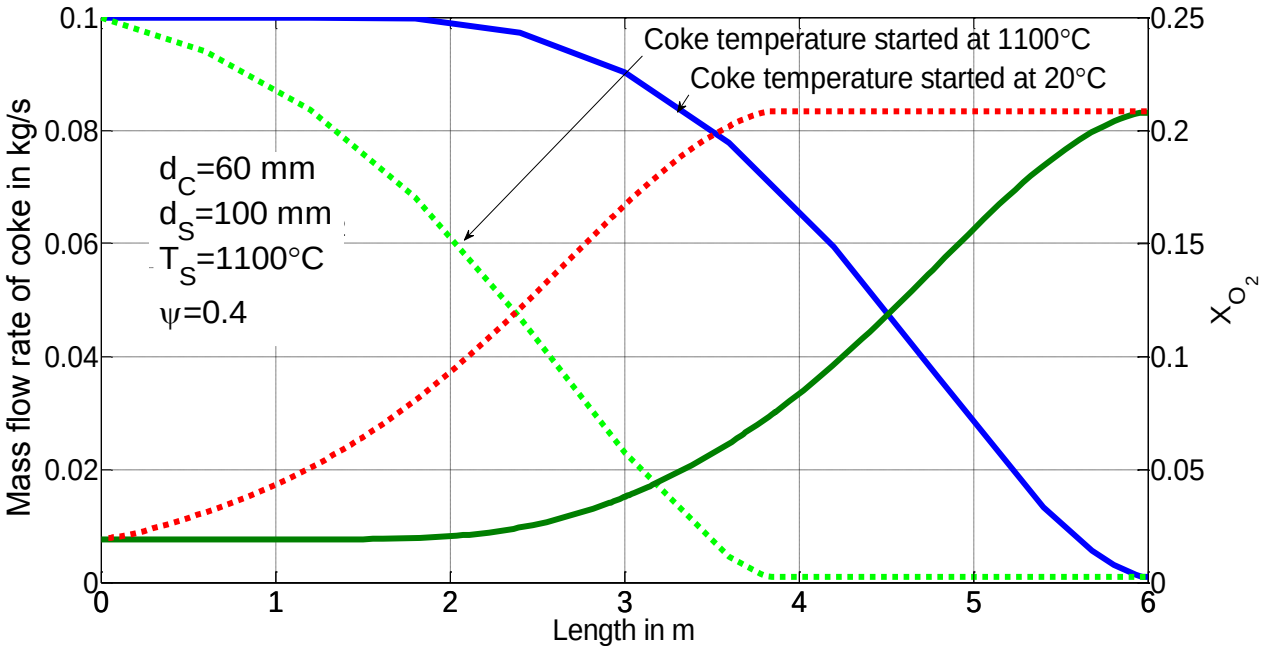

Figure 5.10: Mass flow rate of coke from top to bottom along kiln length

(Effectiveness of the preheating zone)

5.8 The influence of the heat radiation

In order to study the influence of heat transfer by radiation, the following model was developed. Figure 5.11 shows the change of mass with effective temperature as a function of kiln length. At the higher temperature process, heat transfer by radiation does not have much influence on the change of mass of the

coke. Thus radiation heat transfer can be neglected when the operating temperature is high. On the other hand, the influence of radiation can reduce the temperature of the particles.

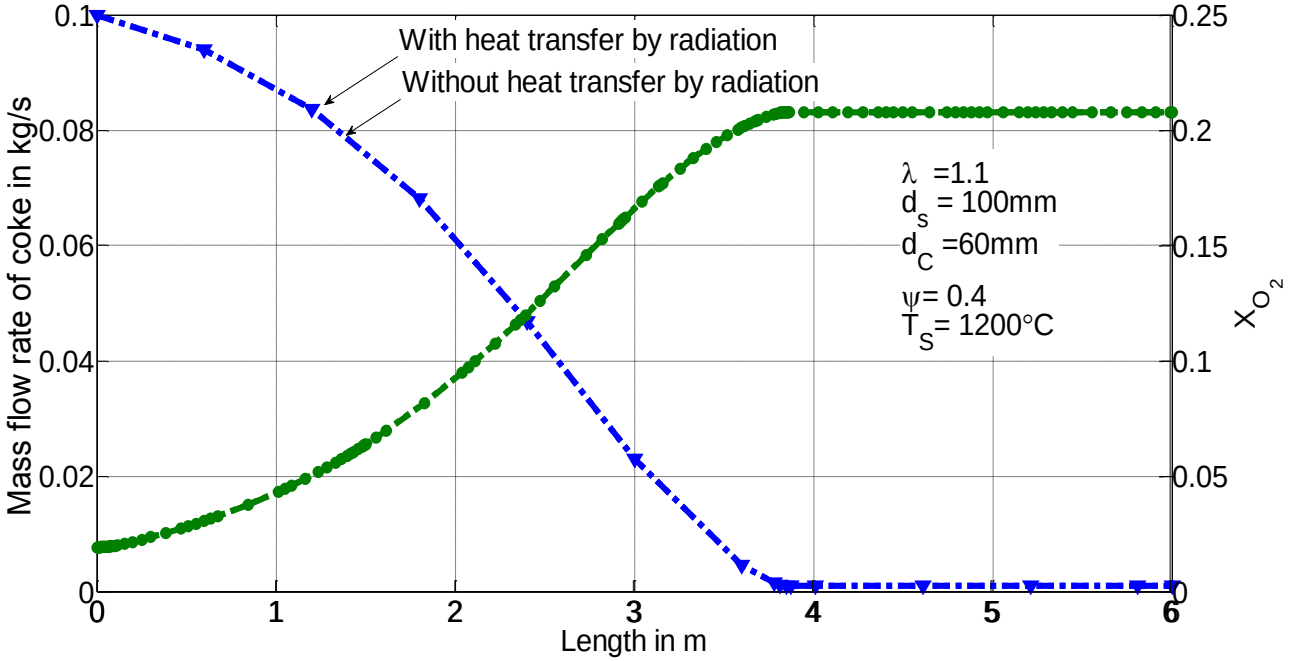

Figure 5.11: Change of mass flow along kiln length
(with the effect of heat transfer by radiation)

The rate of change of mass at different temperature process as a function of kiln length is shown in Figure 5.12. The rate of change of mass increases along the kiln length with the direction of the gas flow and it reaches the maximum when the concentration of oxygen is around 13%. After this maximum, the conversion rate of the oxidation decreases because the increase of the coke surface area.

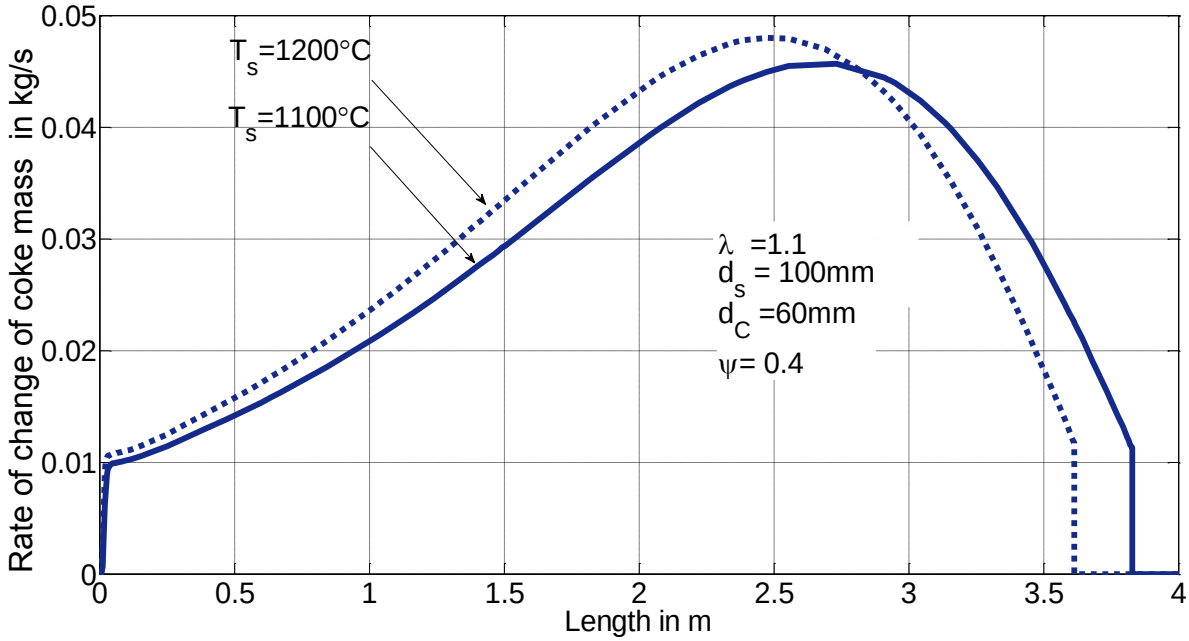

Figure 5.12: Rate of change of mass of the coke particles along kiln length

Figure 5.13-a shows the temperature profile of the gas and coke predicted by the model with different excess air number while the stone temperature is considered as a constant at 1100 °C. At the bottom of the kiln (z=L), the preheated air enters at a temperature of 800°C. After the conversion rate decreases, the gas temperature is increased. When heat transfer by radiation takes into account, the gas temperature is higher than the coke temperature.

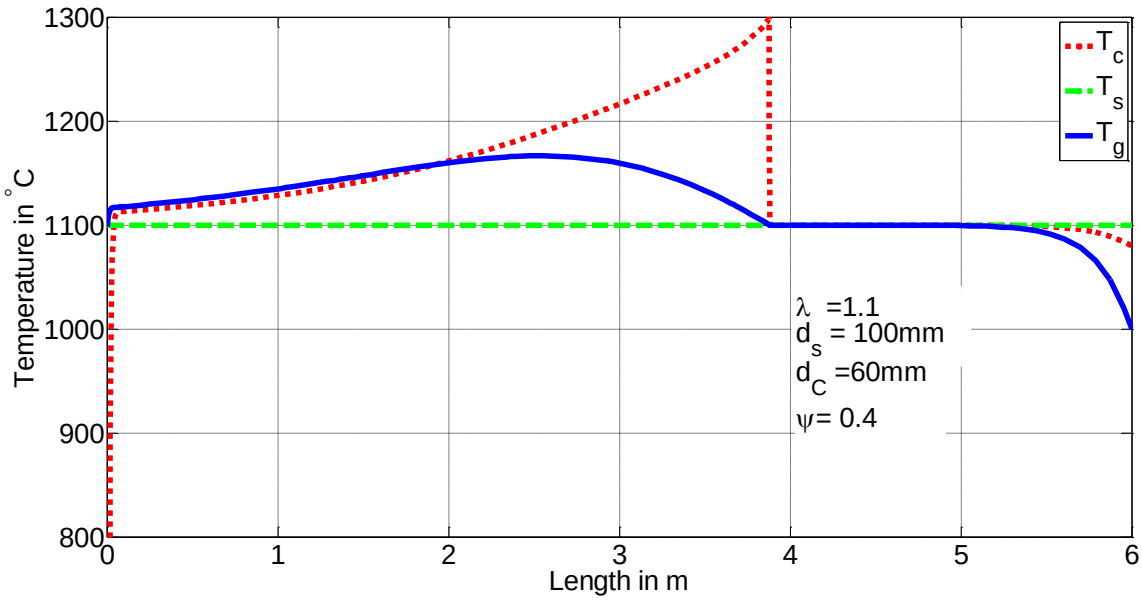

Figure 5.13-a: Temperature distribution profile along kiln length

Figure 5.13-b represents the close view of the temperature profile of Figure 5.13-a. As seen in this figure, the maximum difference between the gas temperature and the stone temperature is around 70°C and the gas temperature reaches a maximum of 1170°C and drops to 1120°C while leaving towards the kiln top.

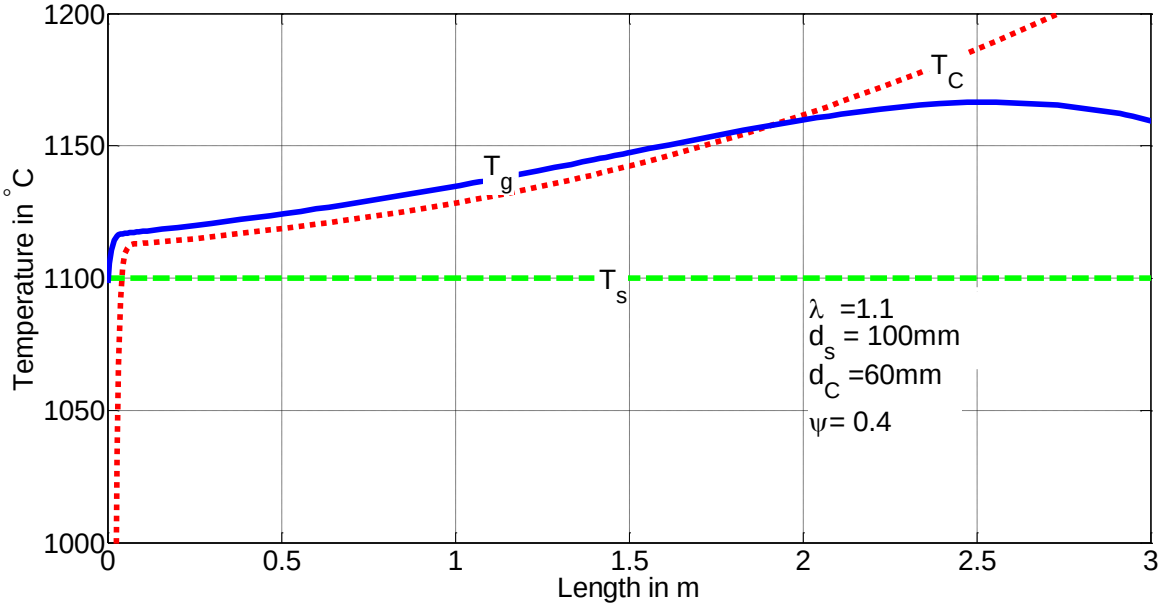

Figure 5.13-b: Close view of temperature distribution profile of Figure 5.13-a

5.9 Case of λ⩾1 with Boudouard effect

Coke reacts with oxygen to form CO and CO diffuses forwards and combines with the incoming oxygen in the gas phase to form CO_2 .The cycle is repeated again to obtain continuous combustion. On the other hand, if the reaction rate is very fast, all the oxygen is consumed as it reaches the particle surface. During the combustion of the coke particles, CO_2 reacts with coke to produce CO which diffuses towards the gas to react with oxygen. CO_2 thus formed diffuses back to the particles' surfaces to undergo the heterogeneous reduction reaction at the coke particle surface. The typical reaction mechanism follow: carbon dioxide is absorbed at the reactive surface before it reacts with carbon to produce carbon mono-oxide and later the carbon mono-oxide is desorbed from the surface [26].

Figure 5-14 shows the change of mass including the Boudouard reaction as a function of kiln length with the effective temperature when the excess air number is one. The coke combustion reaches 100% burning at the length about 3 m for 1200^{o}C and about 3.5 m for the temperature of 1100^{o}C respectively. Complete combustion of the coke was achieved while the excess air number was one and both direction oxidation and Boudouard reaction were considered.

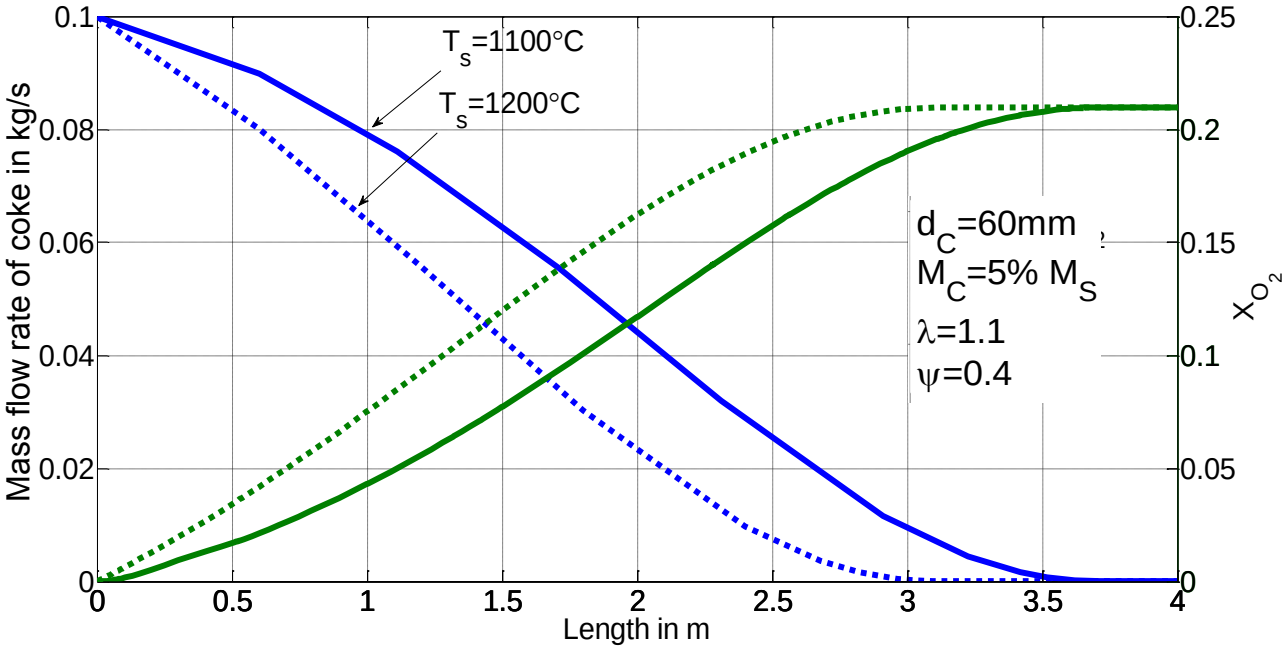

Figure 5.14: Influence of the temperature on mass flow rate of the coke particles

Figure 5.15 shows the effect of temperature on the change of mass of coke including Boudouard reaction at **λ**=1.1. The mass change is related to the initial mass of the particle. After the start of oxidation, the rate of change of mass increases in the direction of the gas flow as the temperature increased. At a solid temperature 900^{o}C, the combustion length is about 2.5 m, however, when the solid temperature is 1200^{o}C, the combustion length is reduced to about 1.8 m. Until the maximum oxidation is achieved, the conversion due to the Boudouard reaction is negligible. Carbon oxidation increases with temperature as the reaction coefficients are a strong function of temperature.

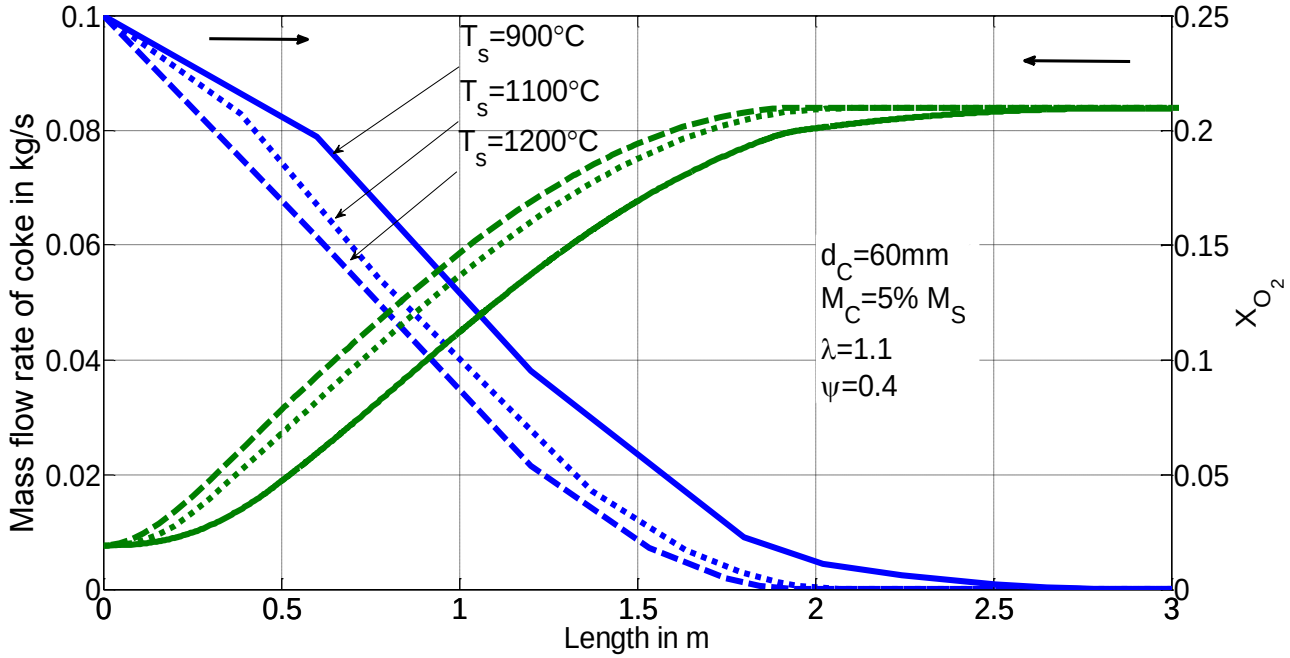

Figure 5.15: Influence of the temperature on mass flow rate of the coke particles

5.10 Case of λ<1 with Boudouard effect

Coke is charged from the top(L=0) and oxygen from opposite end. During the combustion of the coke particles, CO_2 reacts with coke to produce CO which diffuses into the gas phase to react with oxygen. Figure 5.16-a shows the change of mass of coke as a function of kiln length with the influence of excess air number. At about 5 m, oxygen reacts with carbon when **λ**=0.8 and at 4.2m when **λ**=0.9. At 1.8 m, oxygen is burnt out completely for **λ**=0.8 and at 0.7 m for **λ**=0.9 as seen in Figure 5.16. Both have the same rate of change when the oxygen concentration is around 10%.

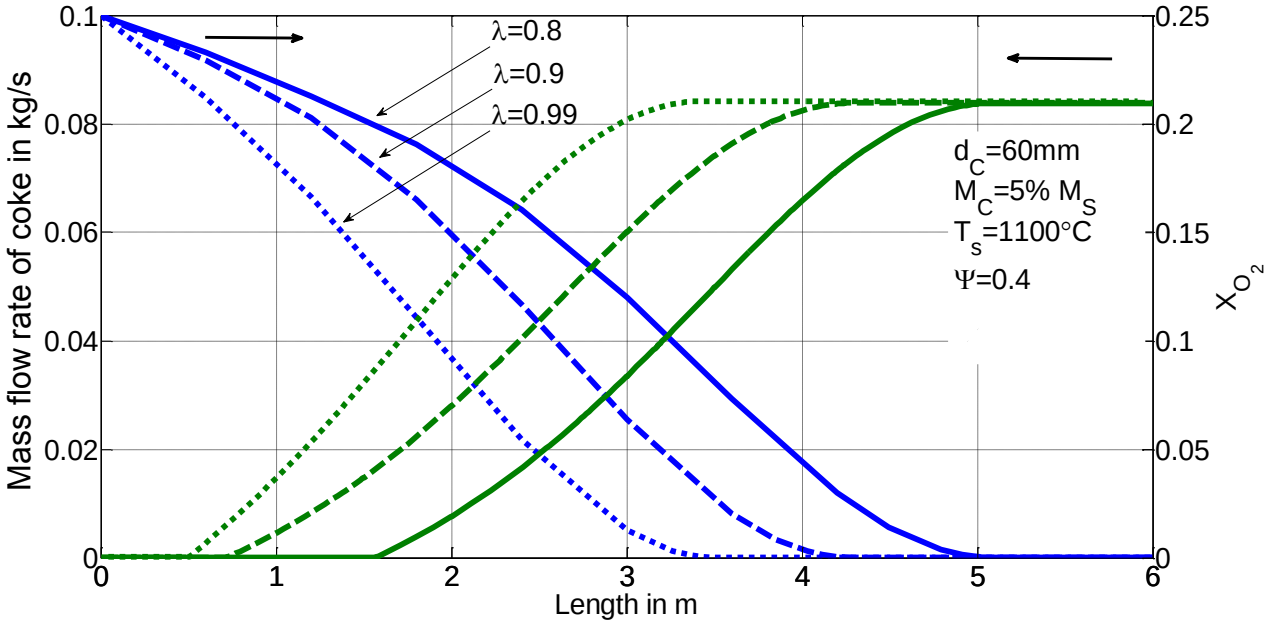

Figure 5.16-a: Mass flow rate of coke particles with different excess air number

Figure 5.16-b represents rate change of mass flow which includes direct oxidation and the Boudouard reaction. After the start of the oxidation, the conversion rate increases in the direction of the gas flow. The reason is that the specific surface area of the coke increases. However, the partial pressure of oxygen decreases. Therefore, a maximum is reached. After this maximum, the conversion rate of the oxidation decreases, because the decrease of the partial pressure has a stronger effect on the increase of the specific surface area of coke.

Until the maximum of the oxidation is reached, the conversion due to the Boudouard reaction is negligible. For **λ**=0.8, the conversion rate of oxidation and Boudouard becomes equal at the length of about 2.2m. At this position the concentration of oxygen is 2% and the concentration of carbon dioxide is 18%. The same concentration values apply for **λ**=0.9. The concentration of carbon dioxide must be about 10 times higher than that of oxygen for both conversion rates to be equal. This shows that the Boudouard reaction is much slower than the oxidation reaction.

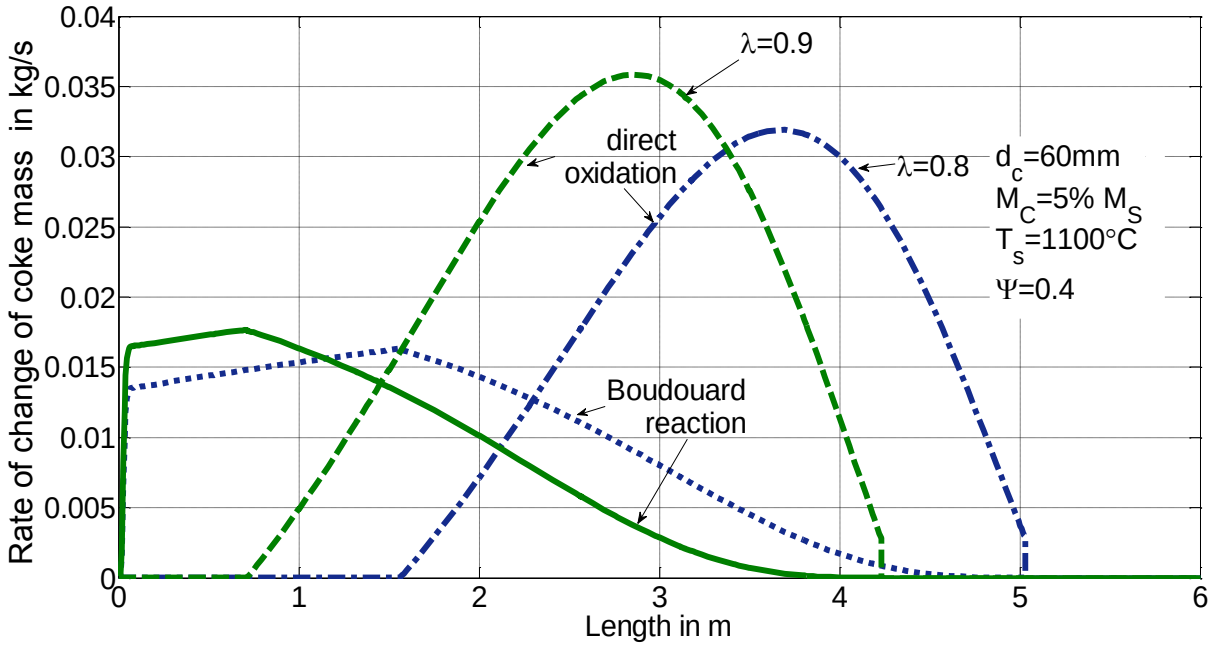

Figure 5.16-b: Rate of change of mass of the coke particles with direct oxidation and Boudouard reaction (T_s= 1100°C)

Figure 5.16-c shows the change of mass of coke with oxygen concentration as a function of kiln length at low temperature process (T_s=

1000°C). The Boudouard length is increased when the constant stone temperature is 1000°C (see Figure 5.16-d).

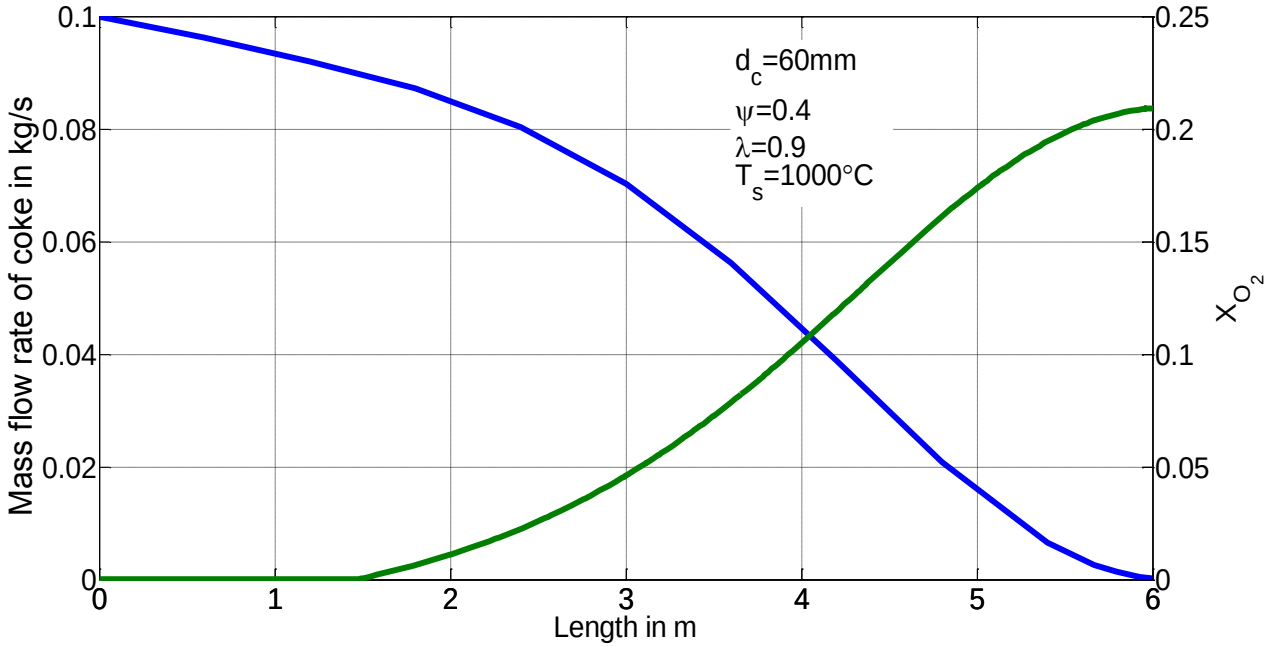

Figure 5.16-c: Mass flow rate of coke particles with oxygen concentration (T_s= 1000°C)

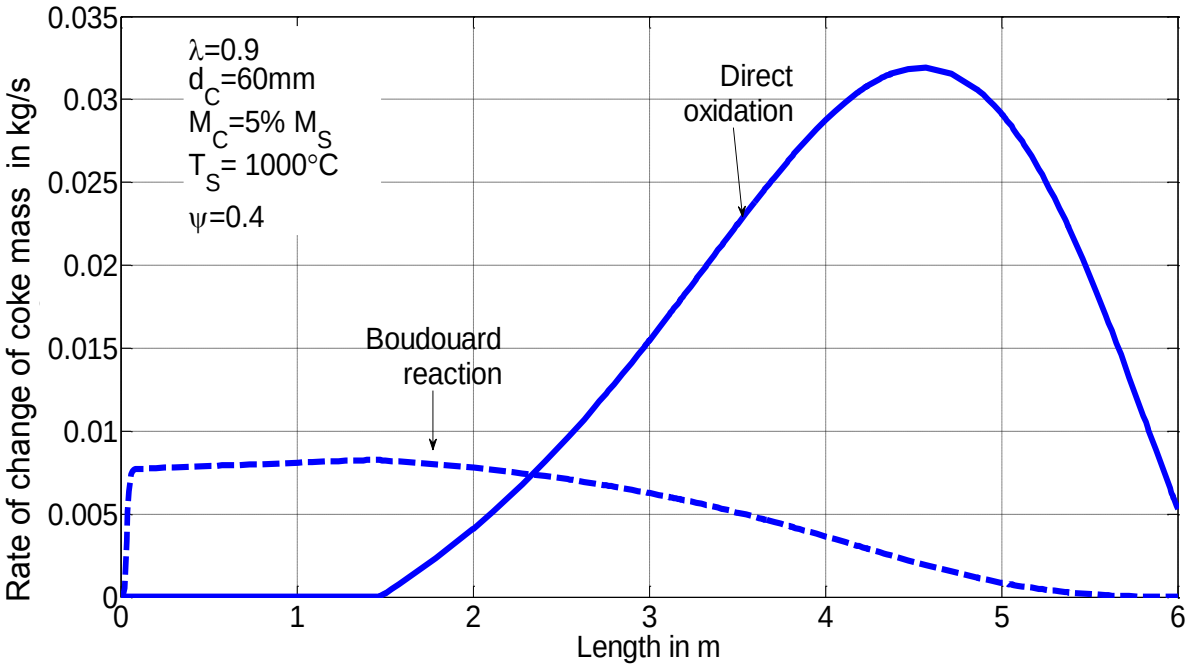

Figure 5.16-d: Rate of change of mass of the coke particles with direct oxidation and Boudouard reaction (T_s= 1000°C)

In order to study the influence of stone temperature on coke combustion for **λ**=0.8, the simulation has been carried out at two different stone

temperatures. Figure 5.17-a and 5.17-b show the predicted profiles of the coke and flue gas temperatures as a function of length. The flue gas temperature is higher than the coke temperature when the Boudouard reaction is encountered. Under the same conditions with an increase in the stone temperature to 100°C, the combustion length changes from 4.9 m to 5.2 m when **λ**=0.8.

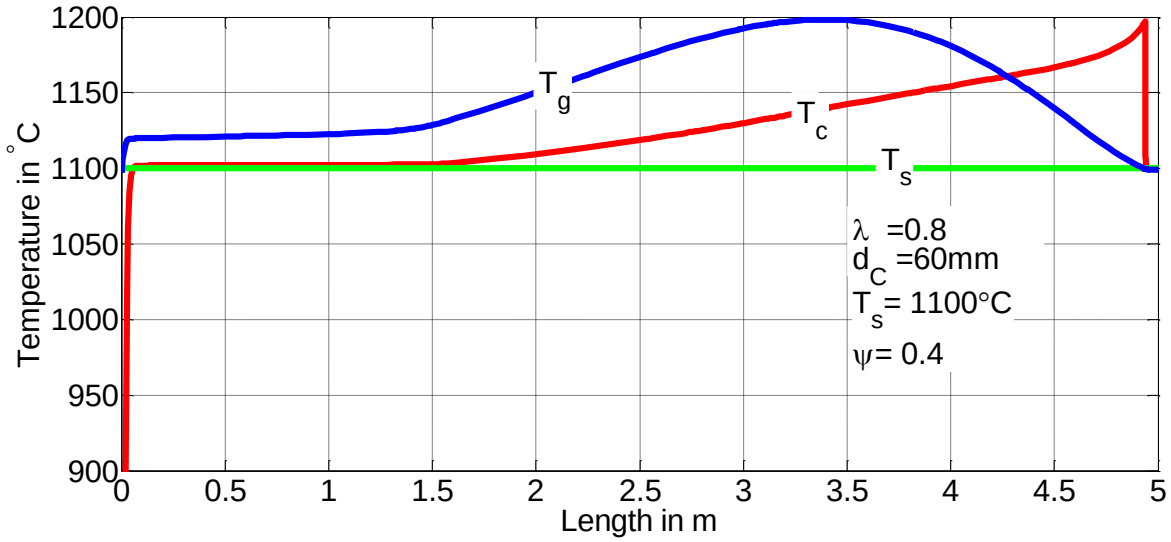

Figure 5.17-a: Temperature profile along kiln length with constant stone temperature (T_s=1100°C)

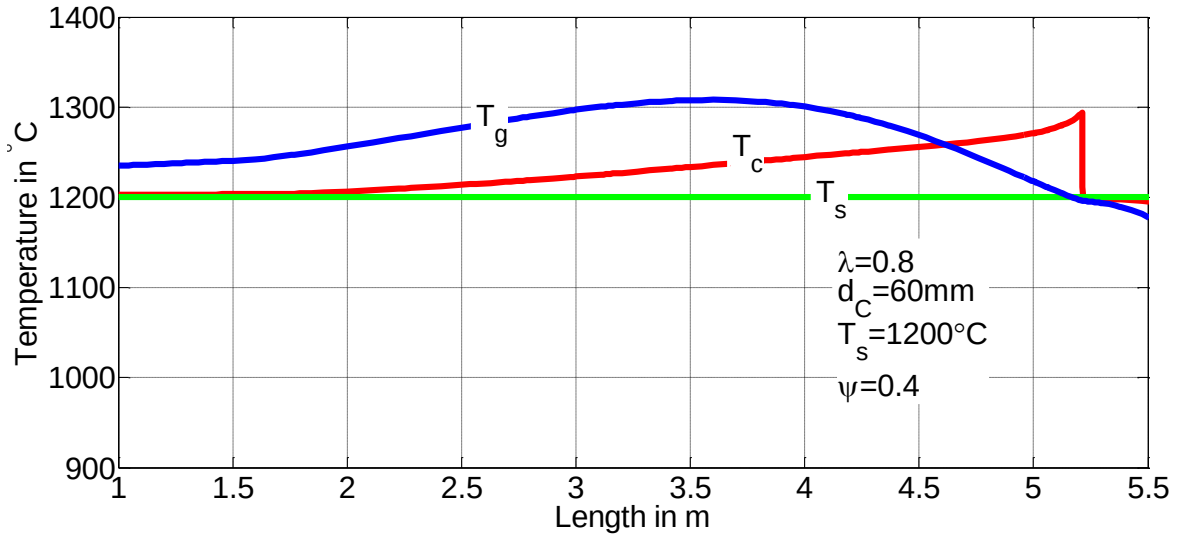

Figure 5.17-b: Temperature profile along kiln length with constant stone temperature (T_s=1200°C)

As an example, Figure 5.18-a, 5.18-b and 5.18-c show the predicted profiles of the coke and flue gas temperatures as a function of length at **λ**=0.9 with three different stone temperatures. It can be seen from the figures that while stone temperatures is lower than 1000^{o}C, the length for the Boudouard reaction is effective. The maximum gas temperature may reach up to 1050 ^{o}C when λ=0.9 at a constant stone temperature of 950^{o}C. While the constant stone temperature increases, the combustion length decreases and the Boudouard reaction length is short.

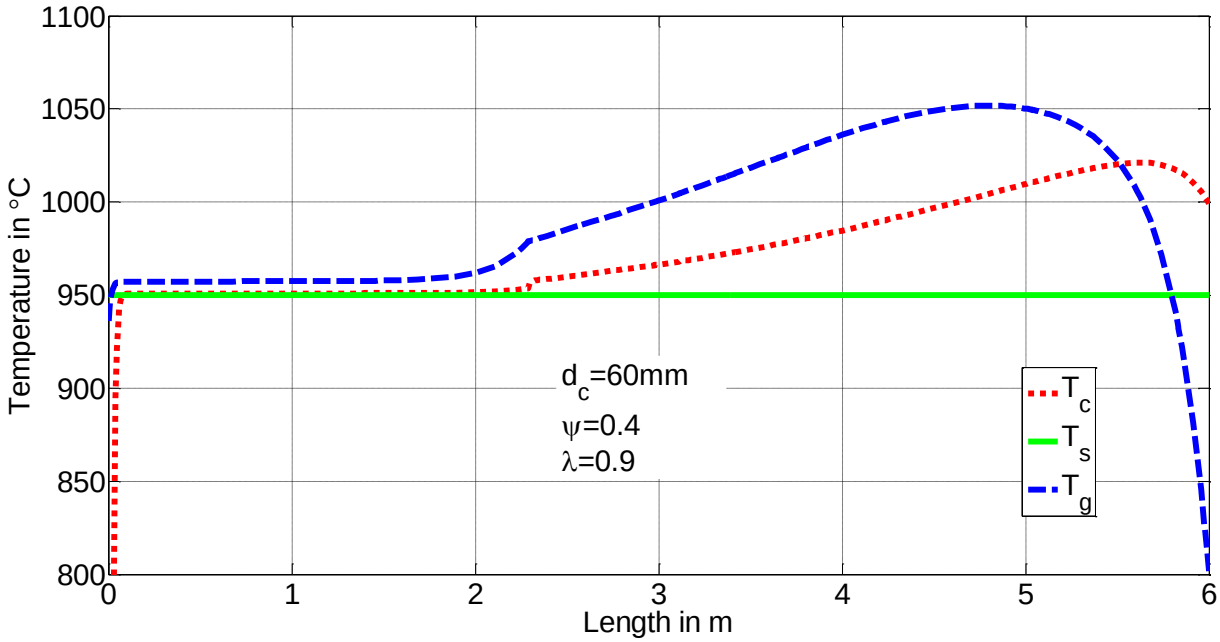

Figure 5.18-a: Temperature profile along kiln length with constant stone temperature (T_s=950^{o}C)

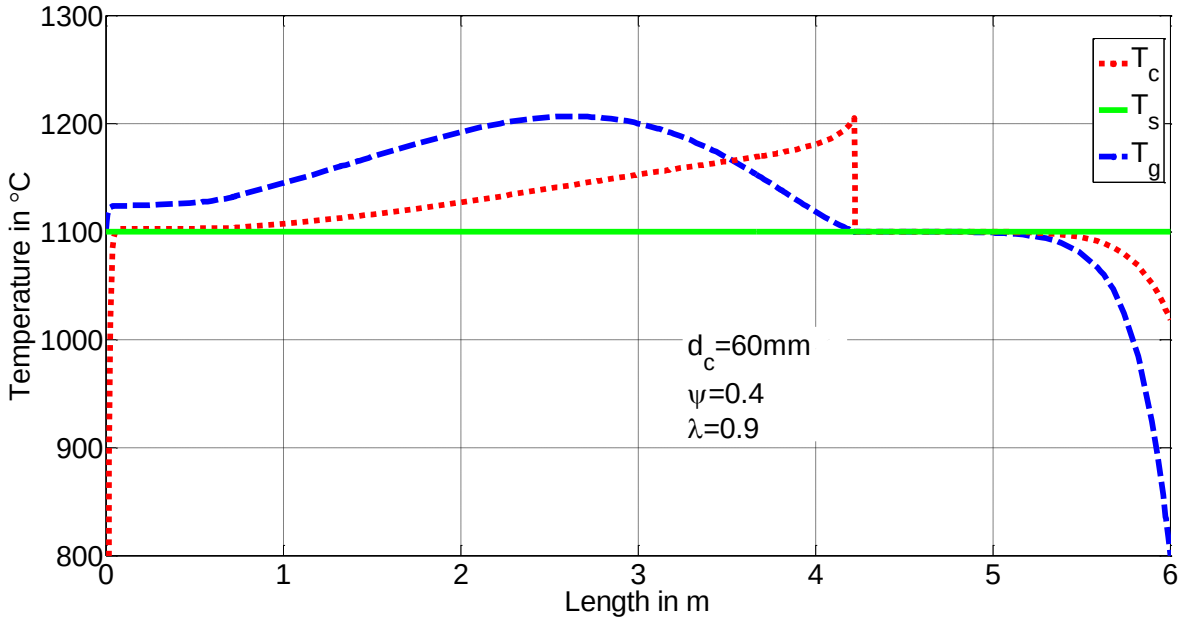

Figure 5.18-b: Temperature profile along kiln length with constant stone temperature (T_s=1100°C)

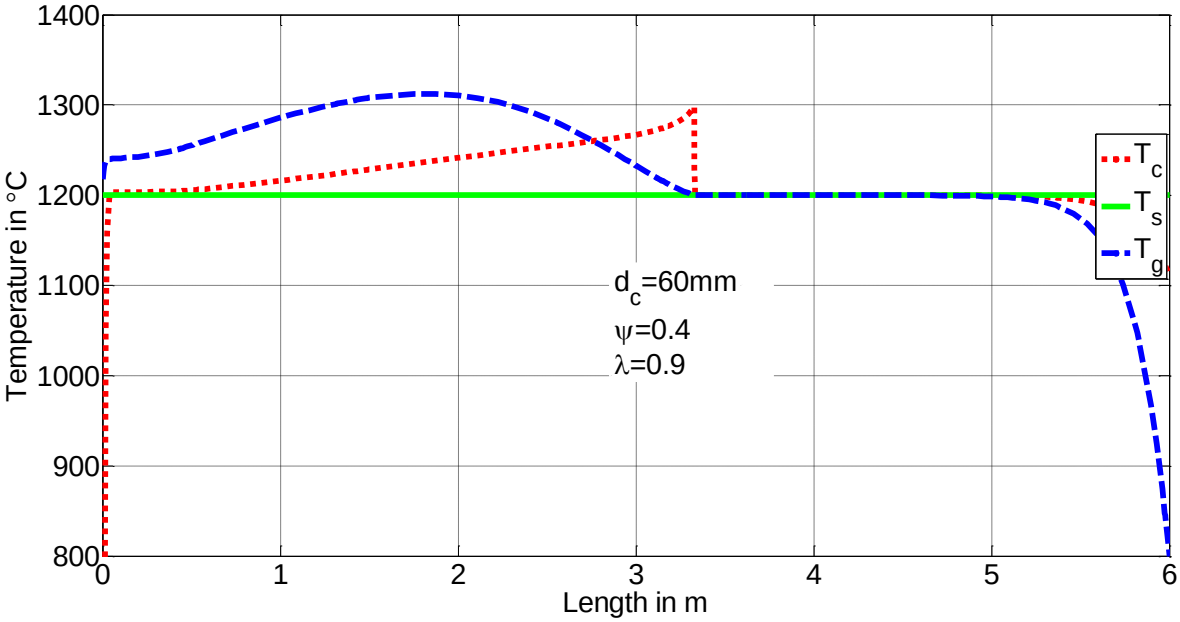

Figure 5.18-c: Temperature profile along kiln length with constant stone temperature (T_s=1200°C)

The concentration of gas components (O_2, CO_2 and CO) is predicted by the model. The oxygen concentration in gases decreases due to its consumption by combustion. When the oxygen decreases with the direction of gas flow along the kiln length, the concentration of carbon dioxide increases as seen in Figures

5.19-a, 5.19-b and 5.19-c. When oxygen is almost exhausted, carbon dioxide reacts with carbon to form carbon monoxide. The concentration of carbon dioxide reaches a maximum when the concentration of oxygen is zero. After this point, carbon monoxide produced by the Boudouard reaction cannot be burned to carbon dioxide, thus the concentration of carbon monoxide is increasing together with a decrease in both carbon dioxide concentration and temperature due to the endothermic nature of the Boudouard reaction. Nevertheless the temperature of flue gases is too high to stop the Boudouard reaction and it proceeds until exiting to the top of the kiln.

For **λ**=0.9, the concentration of oxygen and the concentration of carbon dioxide are the same when the kiln length is 1.1 m at a temperature 1500^{o}C and 1.4m at a temperature 1400^{o}C. The same conditions apply for different temperature in Figure 5.19-b and 5.19-c. It can be seen that the combustion length is decreasing with the higher temperature process at the same excess air number. The Boudouard length increases with the decreasing temperature process.

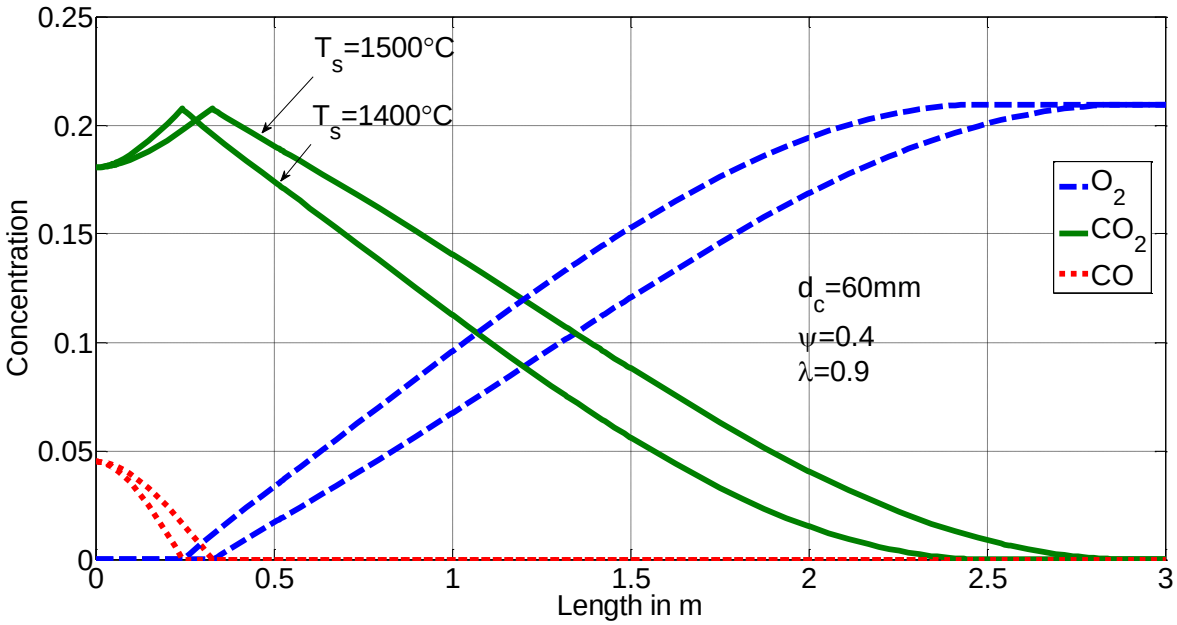

Figure 5.19-a : Concentration of gases at λ= 0.9 with different stone temperature (T_s=1400^{o}C and 1500^{o}C)

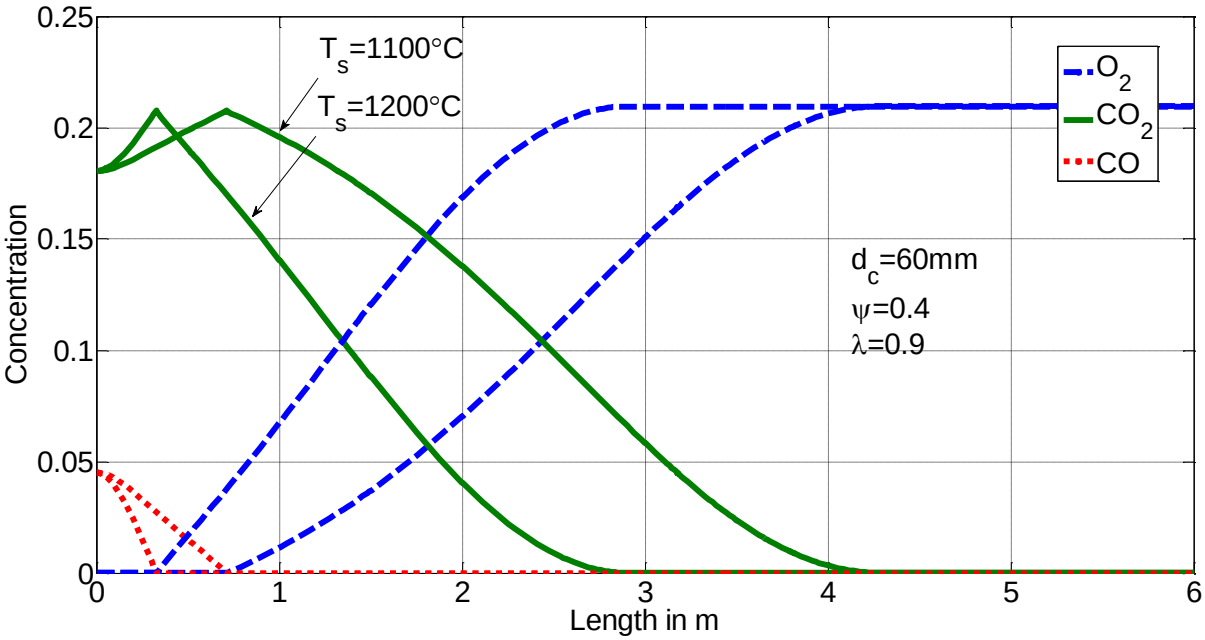

Figure 5.19-b : Concentration of gases at λ= 0.9 with different stone temperature (T_s=1100^{o}C and 1200^{o}C)

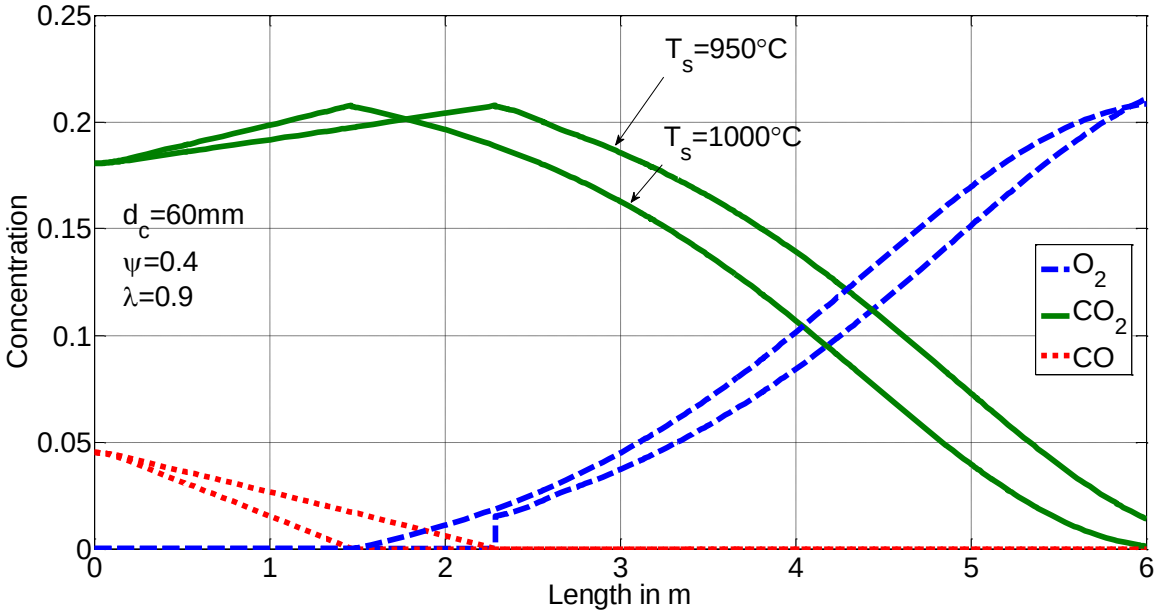

Figure 5.19-c: Concentration of gases at λ= 0.9 with different stone temperature (T_s=950^{o}C and 1000^{o}C)

5.11 Influence of initial stone temperature when λ<1

Figure 5.20 shows the influence of initial temperature as a function of kiln length at λ<1 condition. All the solid particles enter from the kiln top at the ambient temperature ($T_{c(z=0)}$ =20^{o}C and $T_{s(z=0)}$ =20^{o}C) and preheated air enters from the

bottom of the kiln $T_{g(z=L)}$ =800 ^{o}C. When the particle temperature rise up to 600^{o}C at the length of 2.2 m, the coke particles started to burn slowly with carbon dioxide as oxygen concentration is completely burnt out. The coke particles burnout completely after the kiln length of 6 m at λ= 0.9.

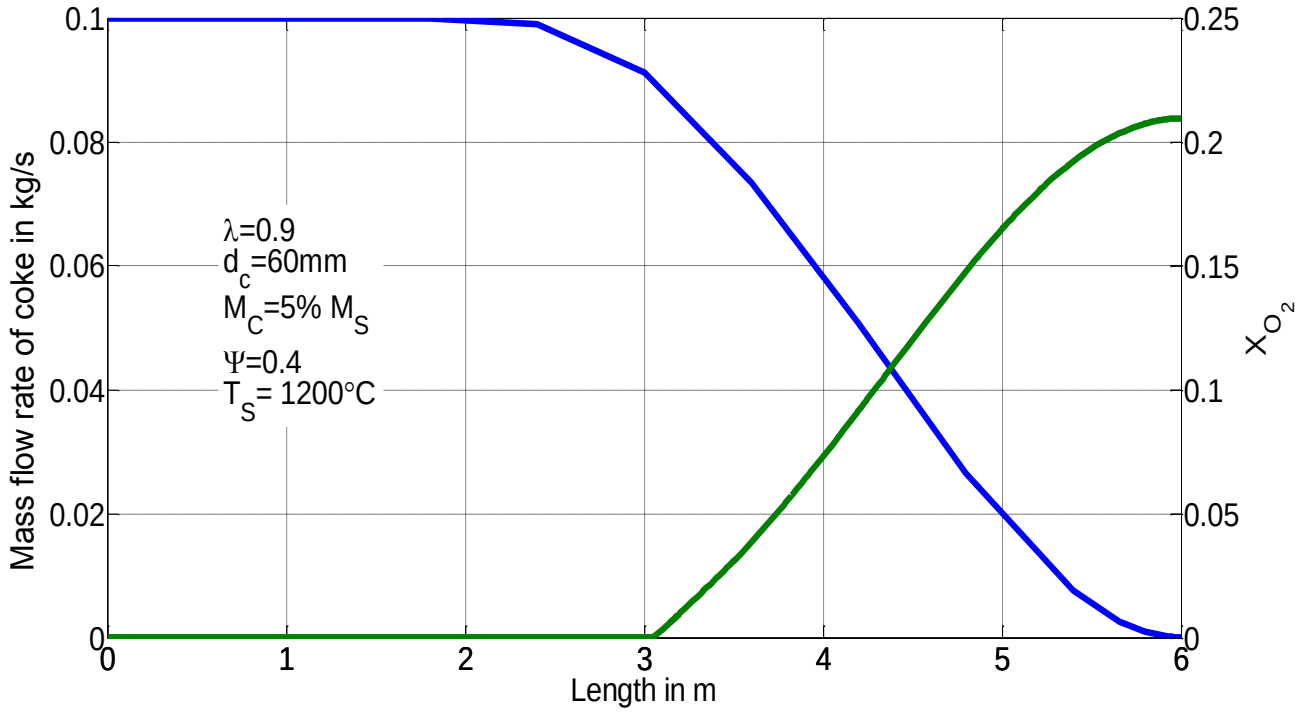

Figure 5.20: Mass flow rate of coke along kiln length

Figure 5.21 shows the gas concentration profile (O_2, CO_2 and CO) for λ=0.9 as a function of kiln length. In order to study the influence of temperature, the model is simulated with the same conditions at λ=0.9. When the oxygen decreases due to combustion, carbon dioxide is produced. CO_2 reacts with carbon again and CO is produced. The carbon monoxide increases because there is no oxygen concentration after 3 m when the coke reacts with carbon dioxide. Then the Boudouard length takes place.

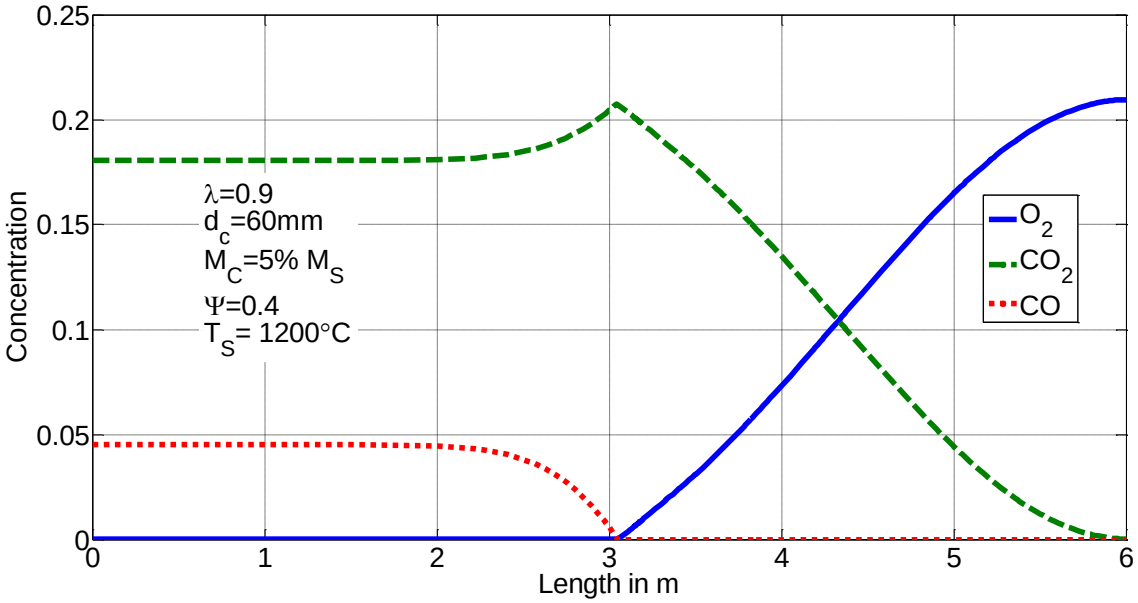

Figure 5.21: Concentration of gases at λ= 0.9 at stone temperature 1200 ^{o}C

Figure 5.22 shows the predicted temperature profile for coke and gas at λ=0.9. The coke and stone temperature starts from 20^{o}C from the top of the kiln $T_{c(z=0)}$ =20 ^{o}C and $T_{s(z=0)}$ =20 ^{o}C, whereas the preheated air enters at 800^{o}C from the bottom of the kiln(z=L). The solid particles are heated by the hot gas, leaving the reaction zone in countercurrent flow. Before 1m of the kiln length, the coke temperature is higher than the stone temperature as no burning occurs. After that the coke and stone temperature is nearly the same as when the conversion started. The gas temperature is higher for most of the kiln length except when the coke surface area reaches its maximum.

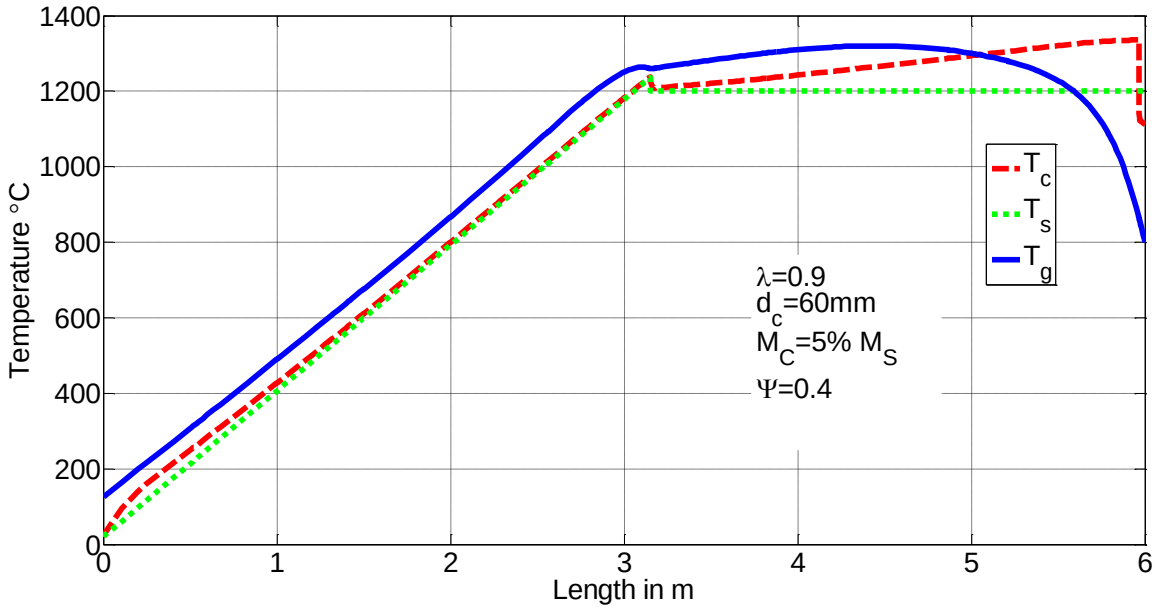

Figure 5.22: Temperature profile along kiln length

5.12 Influence of mass flow rate

In this section, the model has been applied to study the influence of the mass flow rate. The mass flow of the stone is doubled from 55 ton/day/m^2 to 110 ton/day/m^2, the combustion length increased. Figure 5.23 shows the two different mass flow rates as a function of kiln length. A total coke particle is assumed to be 5% of the solid particle. When the mass flow of solid particles is doubled, the combustion length increases from 3.1 m to 5.2 m (1.7 times). From the simulation, as the mass flow rate of stone is doubled, the gas temperature decreased and the combustion length increased.

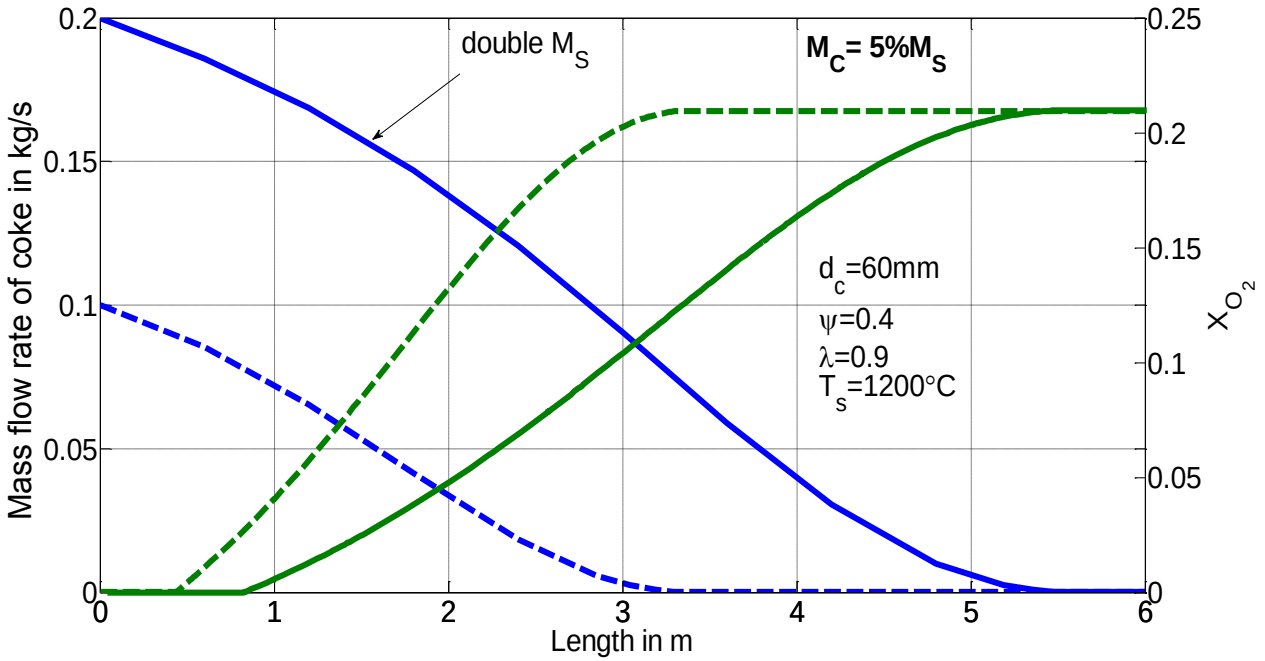

Figure 5.23: Influence of the mass flow rate on kiln length

5.12 Influence of amount of coke

Figure 5.24 shows the change of mass with an increasing of the amount of coke particles from 5% to 10% of the total solid particles inside the shaft kiln. When the amount of coke increases, the change of oxygen concentration due to combustion for both cases is nearly identical.

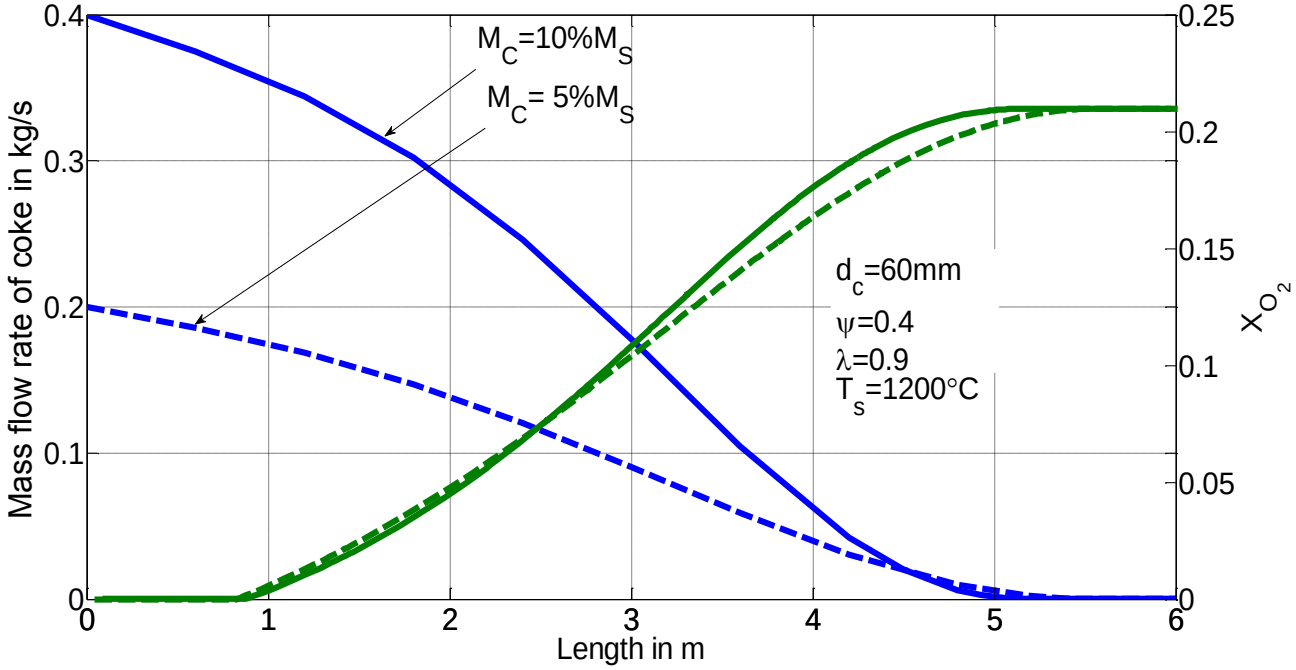

Figure 5.24: Mass flow rate of coke with the influence of the amount of coke

Figure 5.25 shows the conversion of coke particle as a function of kiln length. At the beginning, the burning of coke starts immediately and the conversion of coke is faster at the beginning and at the end. Since λ= 0.9 is used in the model, the concentration of oxygen is completely burnt out before leaving to the top of the kiln. The flow of coke is doubled, the conversion starts slowly and the combustion length is around 5 m. According to the simulation, it can be said that the flow rate is proportional at 1.7 power of length.

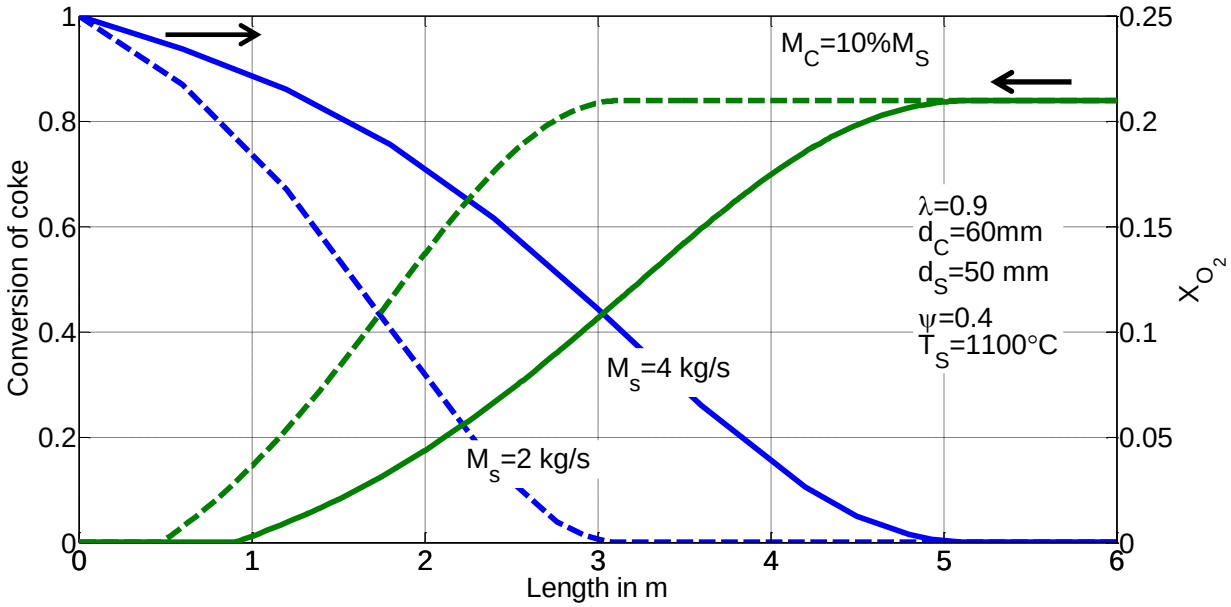

Figure 5.25: Conversion of coke particle with different flow rate

Figure 5.26-a and 5.26-b represent the rate of change of mass flow according to direct oxidation, the Boudouard reaction and total rate of change at different temperature. Until the maximum of the oxidation is reached, the conversion due to the Boudouard reaction is negligible. For **λ**=0.9, the conversion rate of oxidation and Boudouard becomes equal at the length of about 1.8 m for T_s= 1200^{o}C and 2.3 m for T_s=1000^{o}C. At this position the concentration of oxygen is 2% and the concentration of carbon dioxide is 18%. This shows that the Boudouard reaction is much slower than the oxidation reaction.

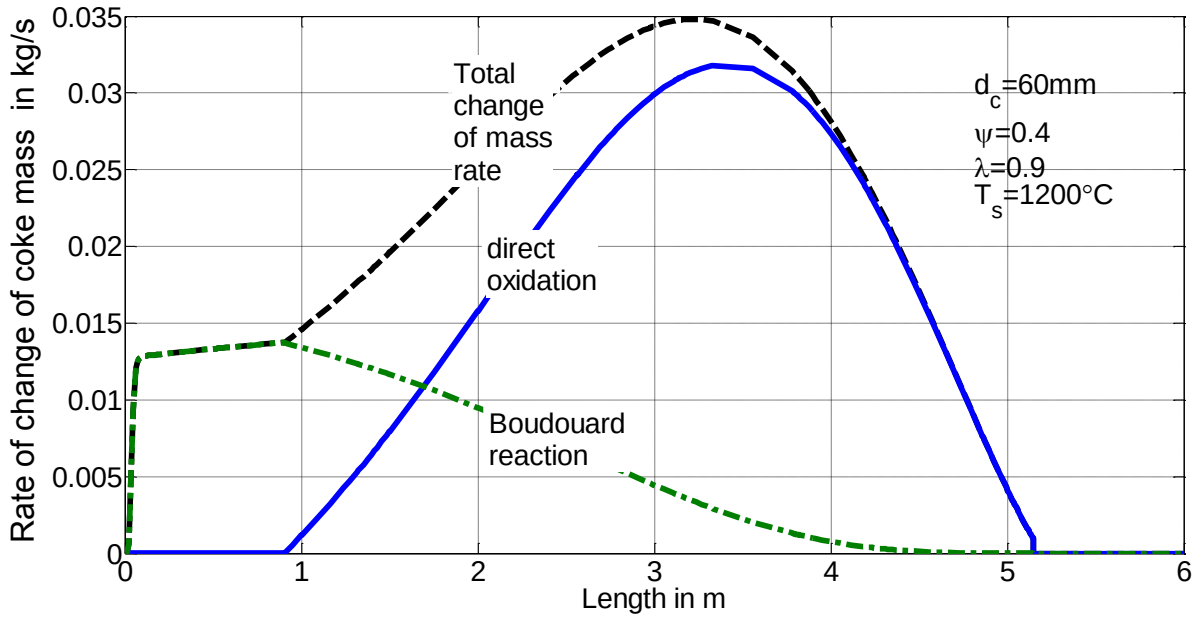

Figure 5.26-a: Rate of change of mass of the coke particles (T_s=1200°C)

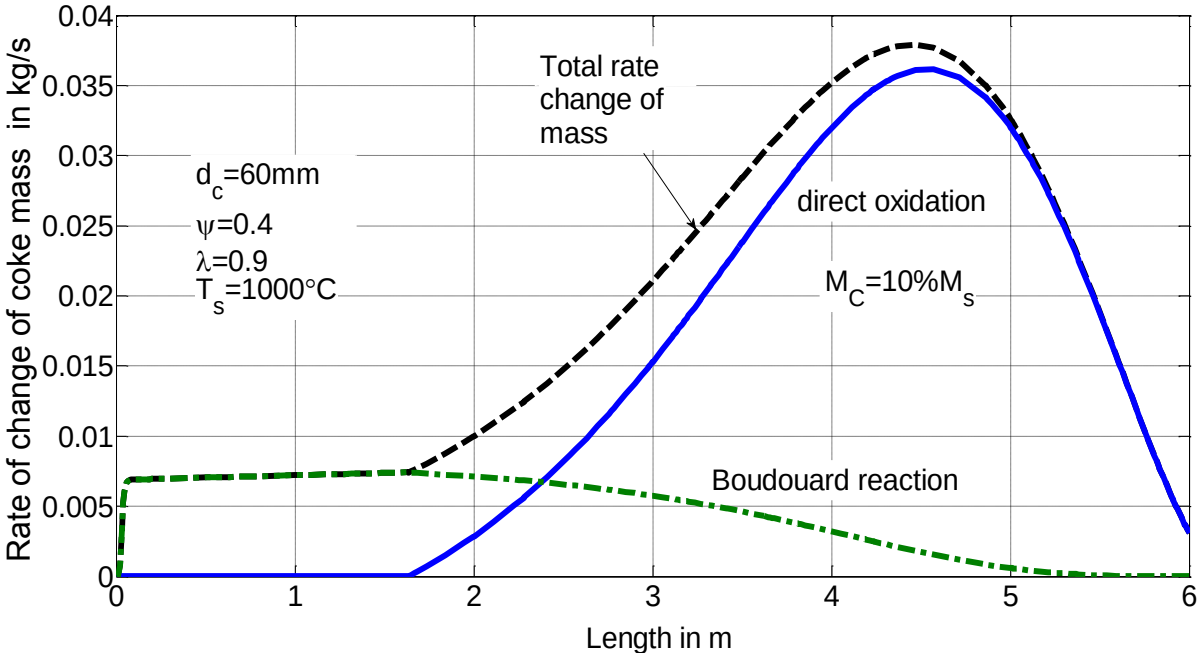

Figure 5.26-b: Rate of change of mass of the coke particles (T_s=1000°C)

Different simulations are possible by changing the particle diameter, the ambient temperature and the flow velocity of combustion gas. However, in order to develop a more comprehensive model to predict coke combustion in all conditions, the effects of conversion, particle porosity and stone temperature should be considered.

5.13 Conclusion

Starting from the assumption that the stone temperature is a constant, combustion behavior with the influence of excess air number, particle size and the initial stone temperature is analyzed. As coke particle size increased, the duration of combustion and gas and coke temperature also increased. A special case with an excess air number of less than one is also simulated. The Boudouard reaction length also depends on process temperature as well as excess air number. This shows that the Budouard length increases as the process temperature decreases as the stone temperature decreases within a range from 1400^{o}C to 950^{o}C. When the excess air number is less than one, the gas temperature is higher than the coke temperature (Boudouard effects). If the excess air number decreased 20%, the direct oxidation reaction decreases 10% and Boudouard increases by nearly 18% at the process temperature of 1100ºC. By increasing the ratio of coke fuel to solid particles, the combustion length changes and the Boudouard length also increases. This is due to the increase in the number of particles. The difference between the lowest and the highest new value of reaction coefficient for the Boudouard reaction influences with the combustion length of 13%.

6 Modelling of coke combustion with process temperature

6.1 The model

In this chapter, the model has been analyzed to predict the temperature of the coke, gas and stone, the influence of the initial stone temperature and conversion profiles. In order to study the influence of the temperature, stone temperature is calculated in the model. In earlier investigation, it is assumed that the stone temperature is constant. It solves for the diffusive heat and mass transport coupled with chemical reaction of reactants and products in a coke sphere. With temperature changing, the gas contents in shaft kiln can change and it will effects on the combustion process.

6.2 Energy balance on stone particle

To determine the stone temperature, energy equation for stone has been formulated. The equations are used the same as the set of the equation which described in chapter 5. It is assumed that the stone gets the energy from gas and coke. The energy balance equation for stone is described as following and all depends on the length of the kiln, z:

For the stone

$$d\left[\dot{\mathrm{M}}_{\mathrm{s}}.\,\mathrm{c}_{\mathrm{p},s}.\,\mathrm{T}_{\mathrm{s}}\right] = \propto_{\mathrm{s}}.\,\mathrm{dA}_{\mathrm{s}}.\left(\mathrm{T}_{\mathrm{g}} - \mathrm{T}_{\mathrm{s}}\right) + \varepsilon_{c}.\,\sigma.\left({\mathrm{T}_{\mathrm{c}}}^{4} - {\mathrm{T}_{\mathrm{s}}}^{4}\right).\,\mathrm{dA}_{c}. \qquad (6\text{-}1)$$

The change of enthalpy of stone is equal to the convective heat transfer between gas and stone plus the radiation heat transfer between solid and stone. Here $\dot{\mathrm{M}}_{\mathrm{s}}$ is the mass flow rate of the stone, $\mathrm{c}_{\mathrm{p},s}$ is the stone specific heat capacity, T_{s} is the stone temperature, T_{g} is the gas temperature, $\propto$ is the heat transfer coefficient, A_{s} is the surface area of the stone inside the furnace, $\boldsymbol{\varepsilon}$ is the emissivity and σ is the Stephan-Boltzmann constant.

6.3 Results and discussions

6.3.1 Influence of excess air number

The influence of the excess air number on the change of mass of coke according to oxygen concentration is simulated. When the excess air number is 1.05, the conversion of coke slowly changes before 1 m. The combustion length gives approximately 5.1 m for λ= 1.05 and around 6 m for λ= 1.02 when the initial condition is $T_{s(z=0)}$ =700 ^{o}C $T_{c(z=0)}$ =20 ^{o}C and $T_{g(z=L)}$ =800 ^{o}C. The higher excess air number, the shorter is the combustion length and the higher is the residual of the oxygen concentration. With the increasing of excess air number, the combustion length decreased.

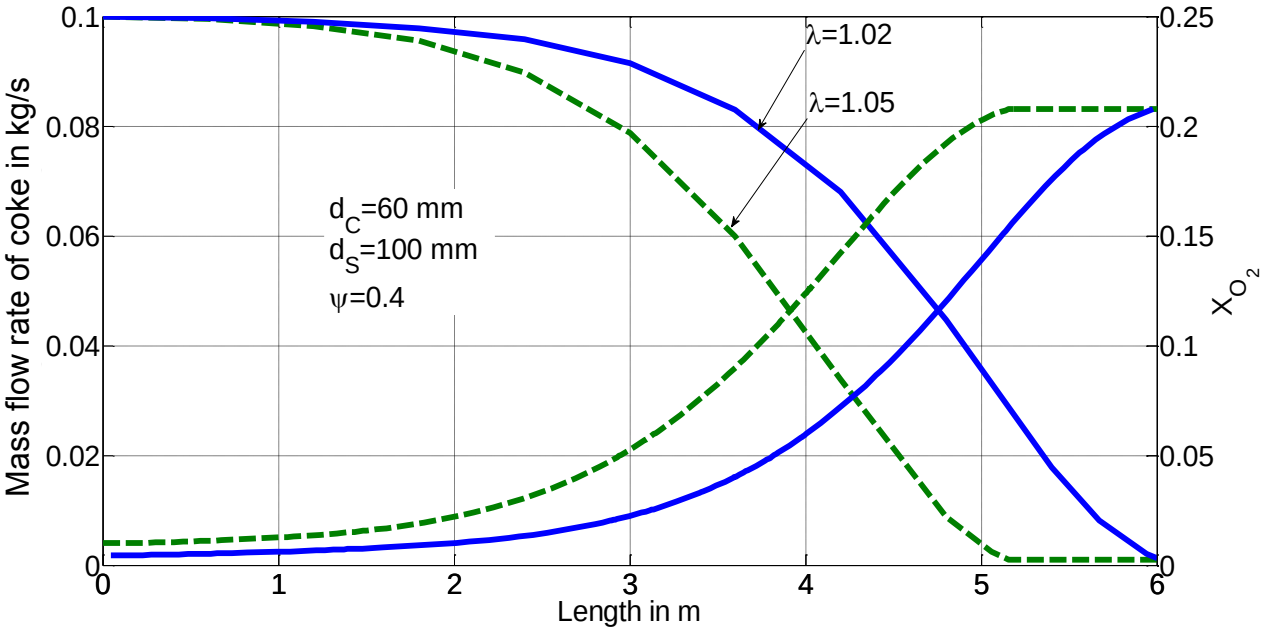

Figure 6.1: Mass flow rate of coke with the influence of excess air number

Figure 6.2 shows the temperature profile of the gas, coke and stone predicted by the model with different excess air number. Solid particles charged from top of the kiln and $T_{s(z=0)}$ =700 ^{o}C and $T_{c(z=0)}$ =20 ^{o}C is assumed. At the bottom of the kiln (z=L), the preheated air entered with a temperature of 800^{o}C. The temperature increases with the solid coke fuel combustion as the surface area of coke increased. The stone temperature increases from the energy from coke particle and the maximum of stone temperature reached 1400^{o}C.

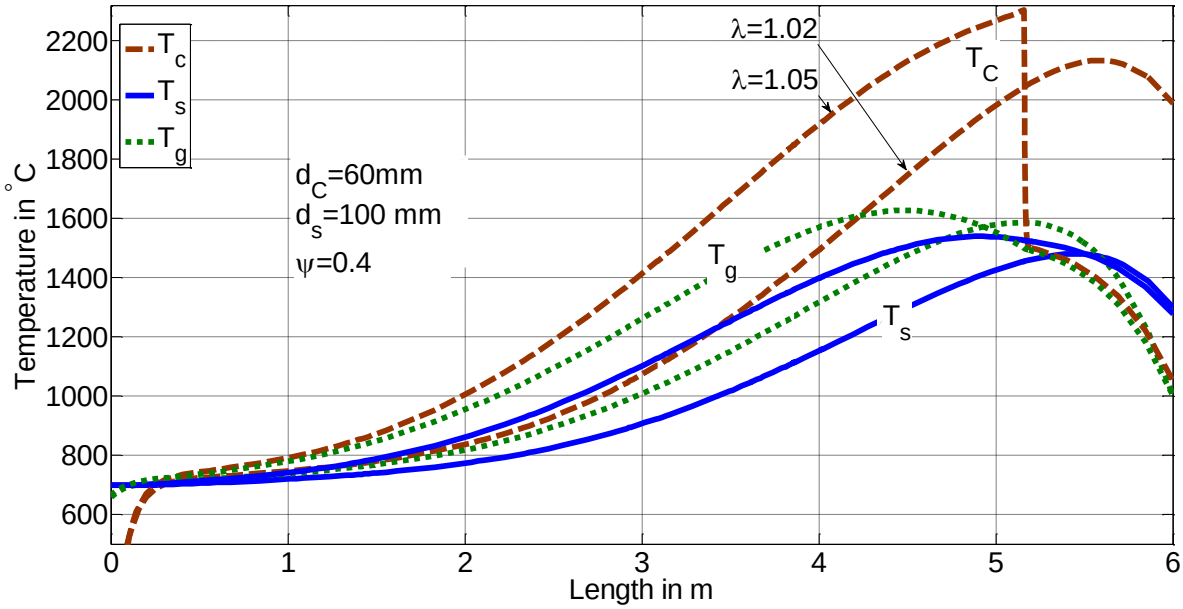

Figure 6.2-a: Influence of the stone temperature at different excess air number

Figure 6.2-b and 6.2-c shows the gas and stone temperature profile predicted by the model with different initial stone temperature. Solid particles charged from top of the kiln and $T_{s(z=0)}$ =700 °C and $T_{c(z=0)}$ =20 °C is assumed. Depending on the initial temperature, the stone temperature may vary when the combustion take place, however, they have same temperature after leaving from the kiln

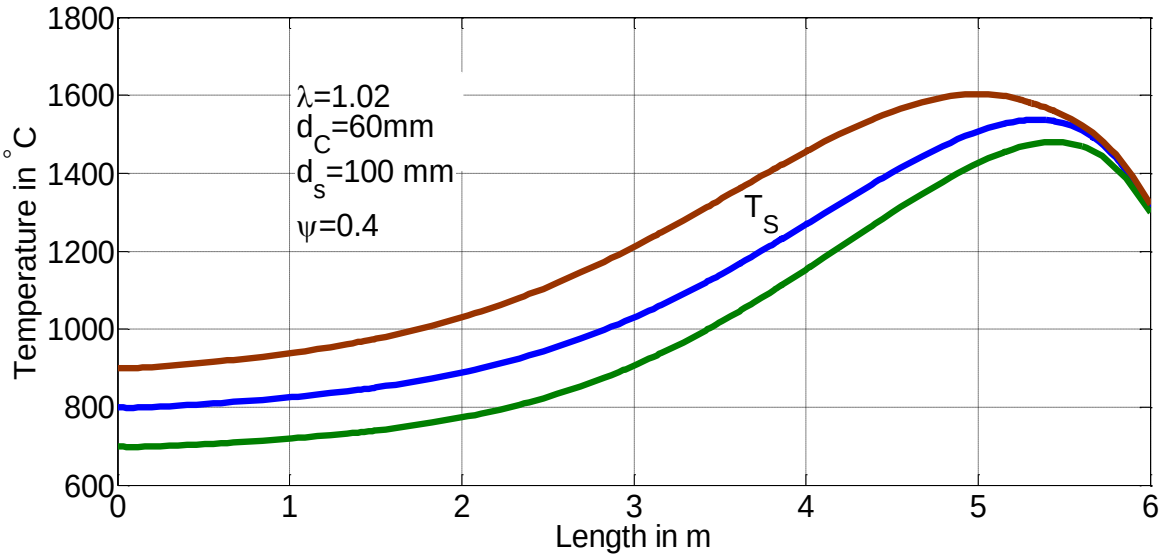

Figure 6.2-b: Stone temperature with the influence of initial stone temperature

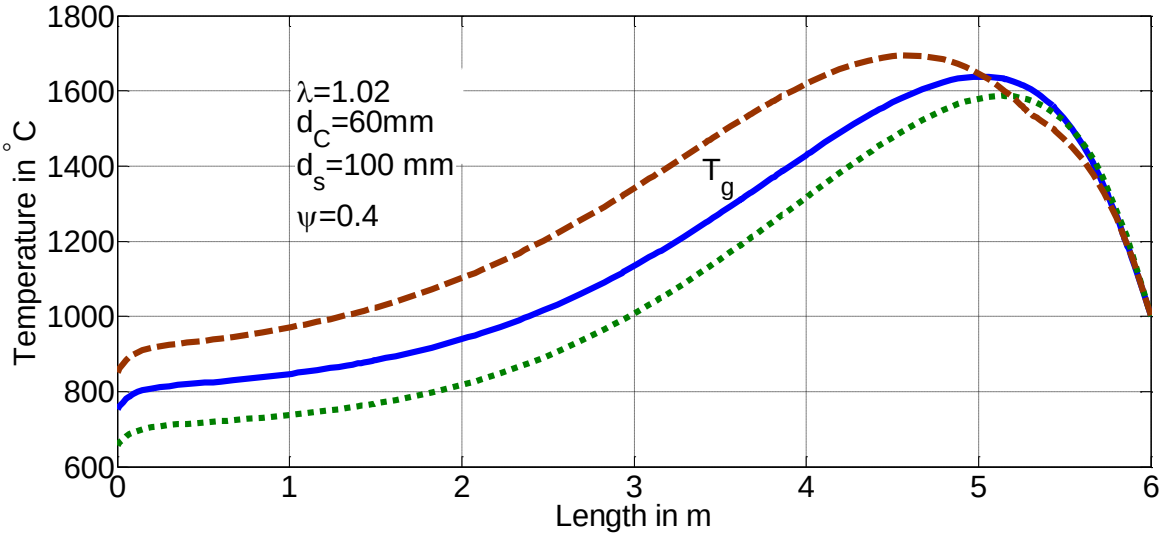

Figure 6.2-c: Influence of the initial stone temperature on gas temperature

6.3.2 Initial stone temperature

The influence of the initial stone temperature on the change of mass of coke according to oxygen concentration is compared. When the excess air number is 1.05, the conversion of coke slowly changes before 1 m. Mass flow of coke starts changes at approximately 0.7 m from the top to the bed, leading to a decreasing oxygen concentration as combustion occurs. The combustion length gives approximately 5.2 m for $T_{s(z=0)}$ =700 °C and around 5.1 m for $T_{s(z=0)}$ =900 °C .

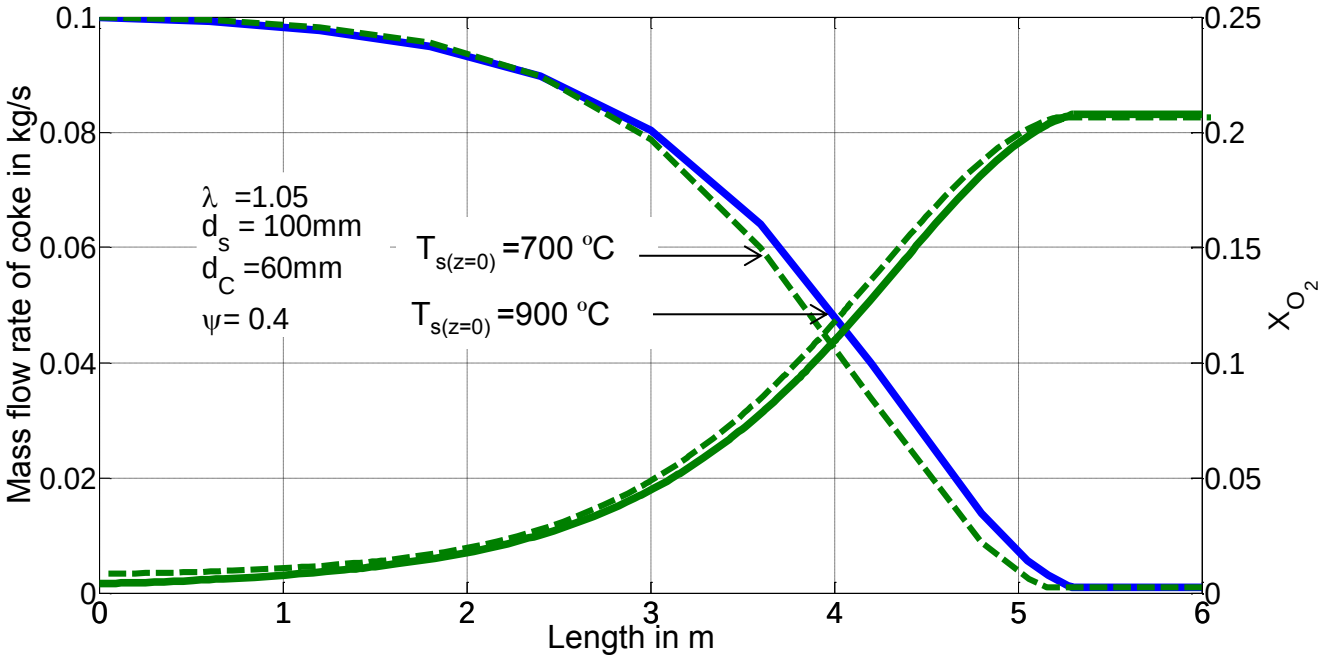

Figure 6.3: Mass flow rate of coke with the influence initial stone temperature

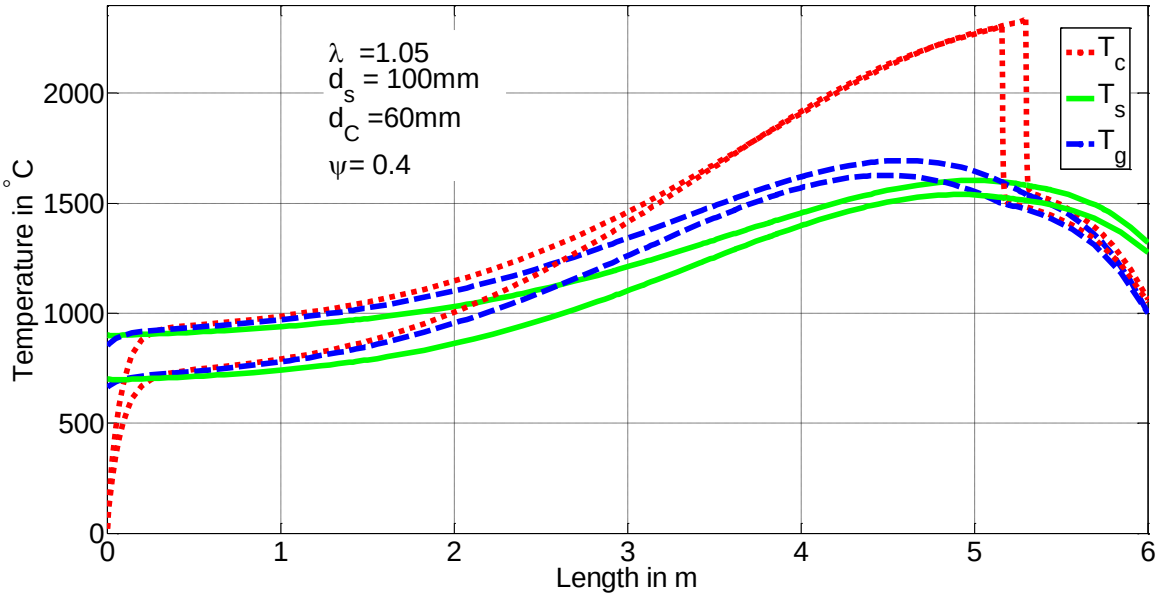

Figure 6.4: Temperature profile with the influence of initial stone temperature

6.3.3 Influence of stone particle size

The influence of the size of stone particles in the kiln operations is investigated. The mass flow rate of the stone keeps constant at 55 ton/day/m^2. By increasing the diameter of the stone, the number of the stone particle decreases inside the shaft kiln. However, Figure 6.5-a shown that there is no influence of the stone particle size on the mass change of coke when d_c=60 mm as a function of kiln length. The combustion length is the same on different stone particle size.

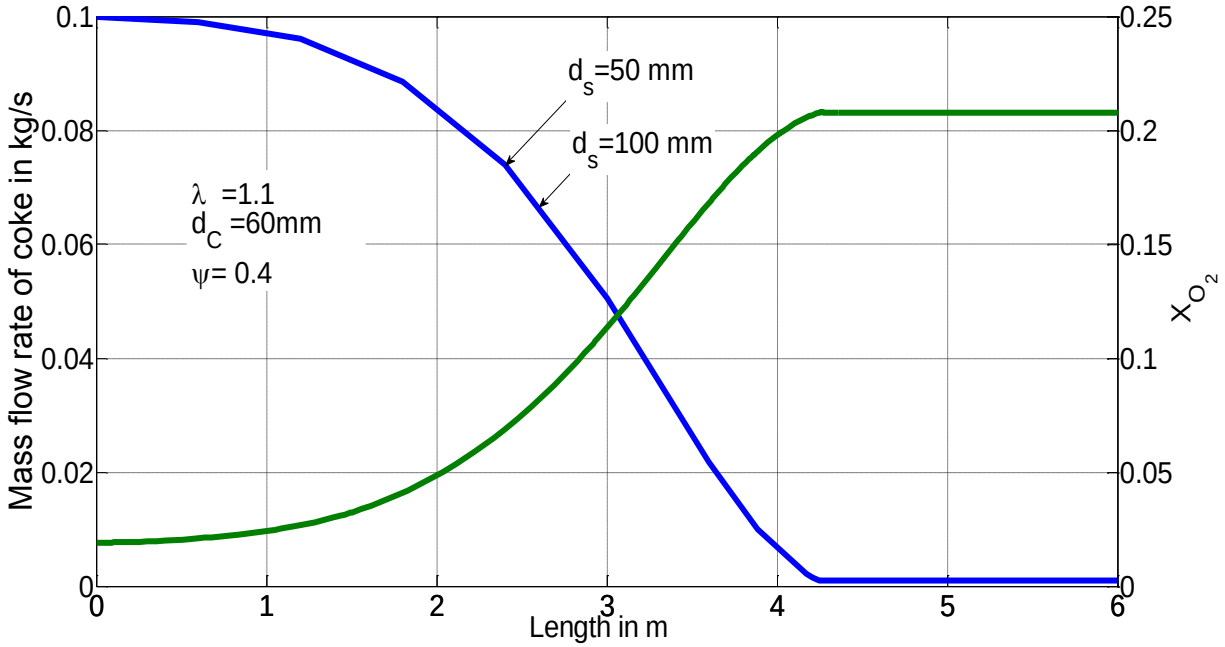

Figure 6.5-a: Influence of stone particle size on the change of mass of coke

Figure 6.5-b shows the stone diameter effect on the rate of change of mass of coke. At the beginning of the combustion, the rate of change of mass of coke is increases with the increasing of the stone particle size. Until the maximum of the oxidation, for **λ**=1.1, at the position of 1.2 m, the rate of change of mass is for both size of stone particles.

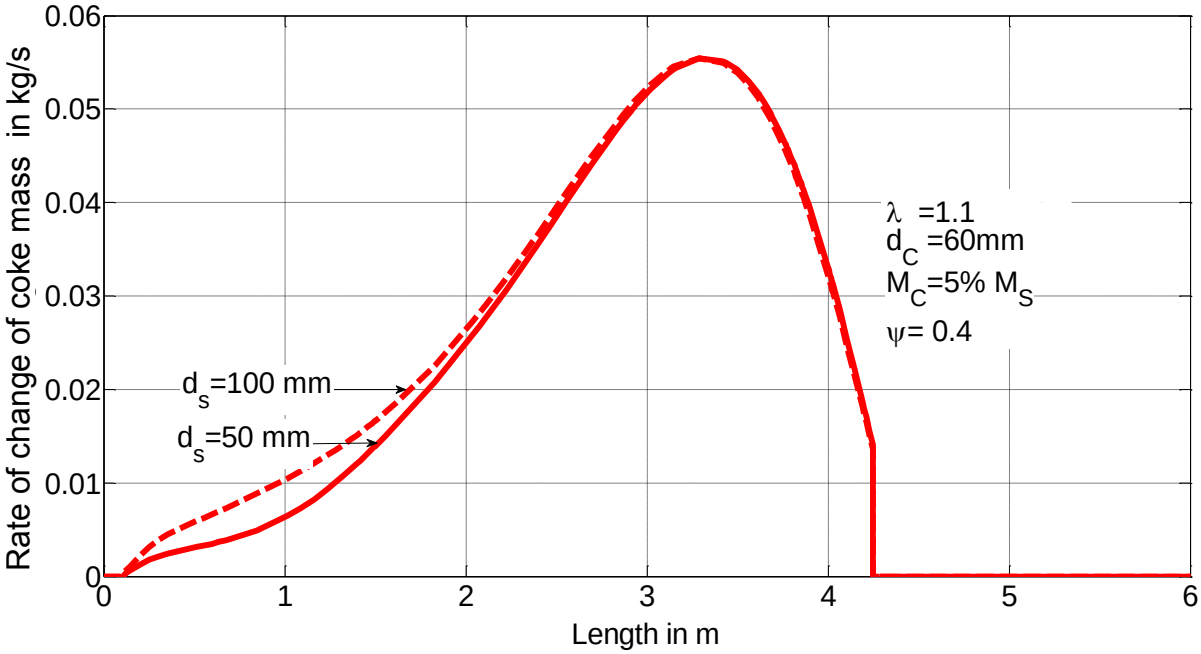

Figure 6.5-b: Influence of stone particle size on rate of change of mass

Figure 6.6-a shows the conversion profiles of coke particles with different size of stone particles. It can be seen that the changing of stone particle size is not much influence on the conversion of coke. However, the stone temperature and gas temperature are increased significantly with the decreasing of the size of stone particles.

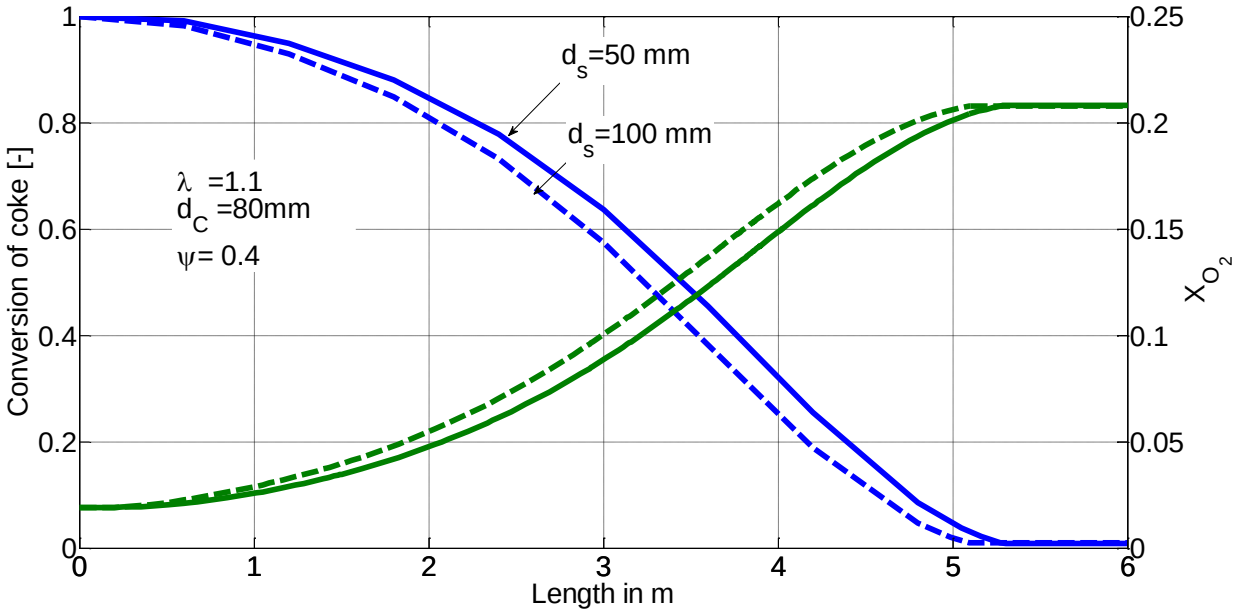

Figure 6.6-a: Influence of stone particle size with the conversion degree

(d_c=80 mm)

Figure 6.6-b shows the stone diameter effect on the rate of change of mass of coke for a diameter of coke, 80 mm. Unlike d_c=60 mm, the combustion length is increases with the decreases of the stone diameter. After the maximum of the oxidation, the rate of change of mass of coke is decreases with the direction of the gas flow with an increasing of the stone particle size.

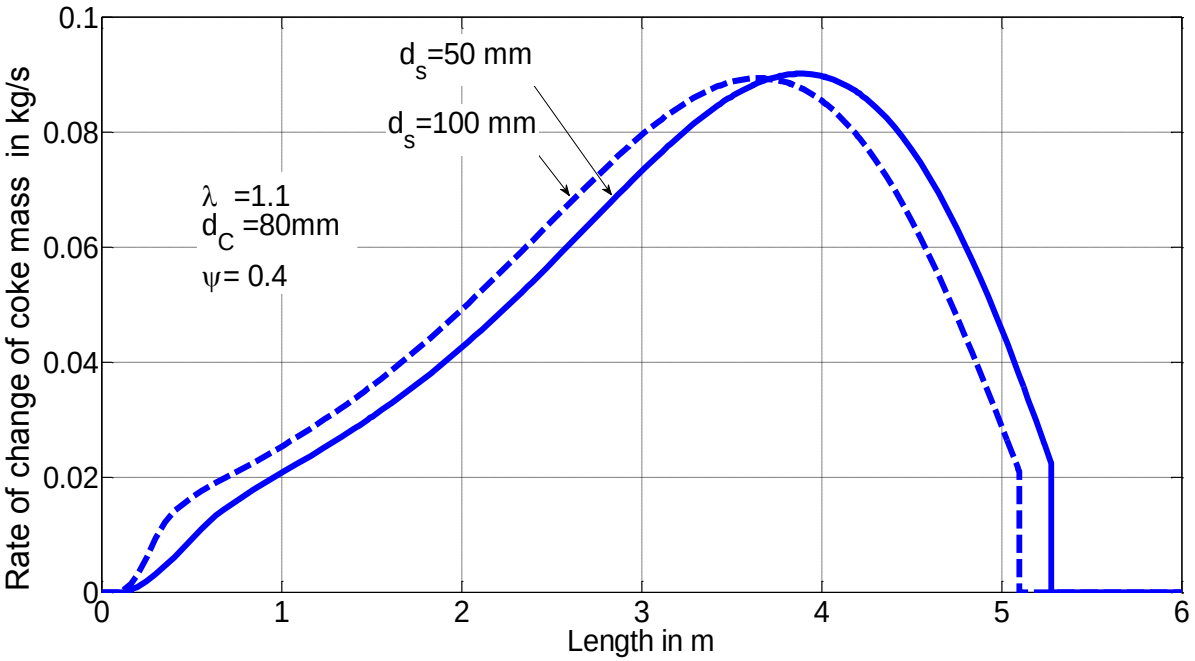

Figure 6.6-b: Influence of stone particle size on rate of change of mass

(d_c=80 mm)

Figure 6.7 and 6.8 show the predicted temperature for stone, gas and coke with the effect of the stone diameter. The initial stone temperature considered $T_{s(z=0)}$ = 700°C. The stone temperature increased because of the combustion process and reached to the maximum when the specific surface area of coke is a maximum. The temperature of the stone increased with the decreasing of stone particle size.

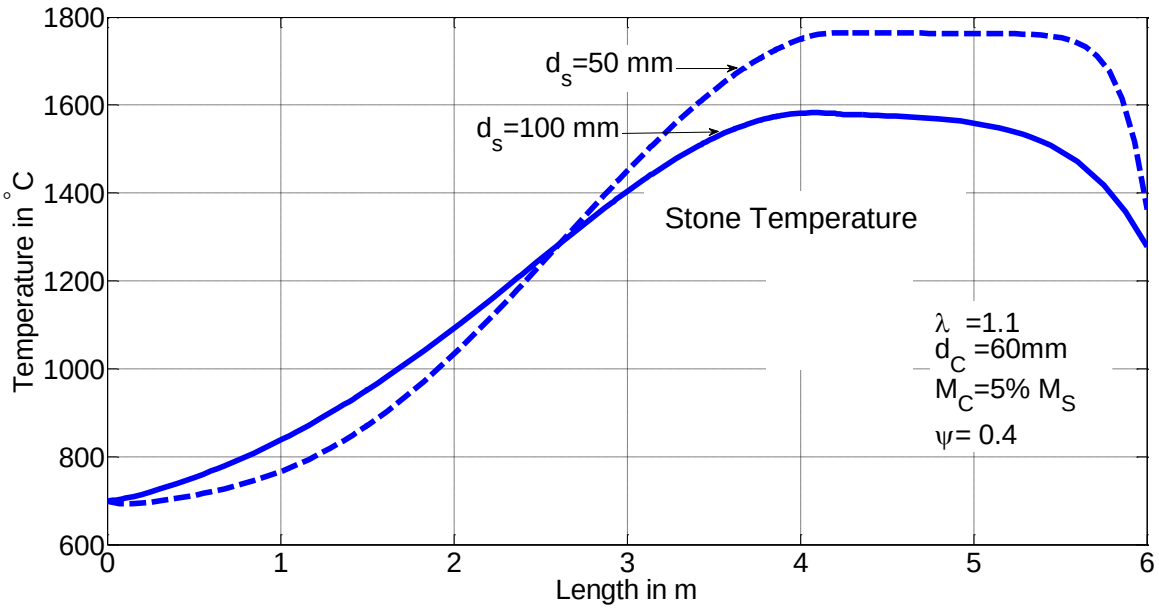

Figure 6.7: Influence of stone particle size on the predicted stone temperature

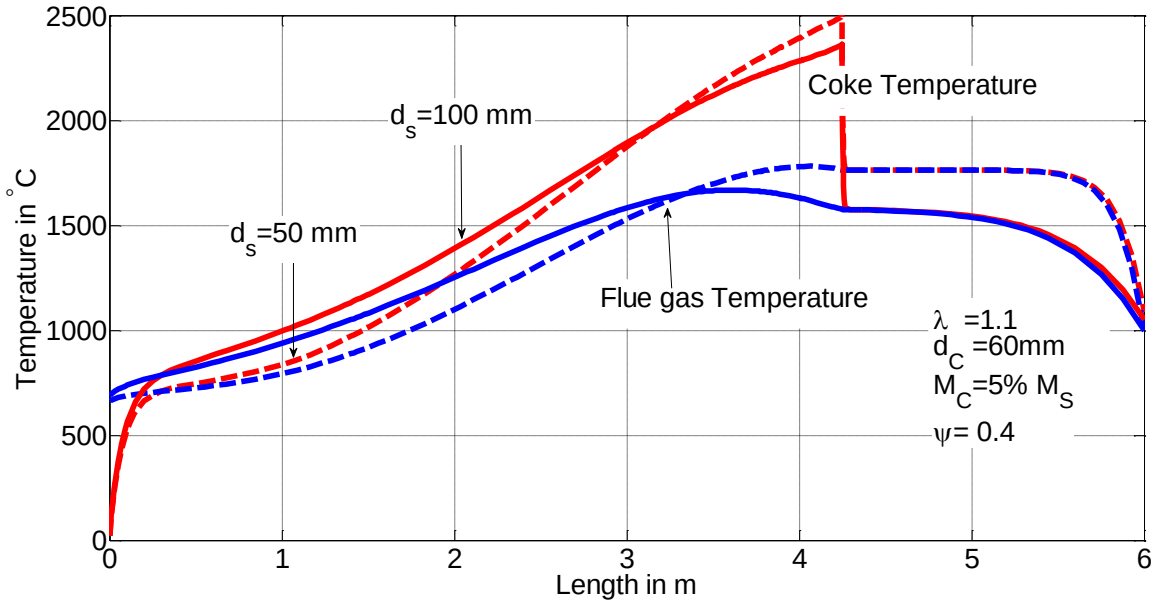

Figure 6.8: Influence of stone particle size on the predicted gas and coke temperature

6.4 Summary

The developed mathematical model contains the other input data of stone temperature. The model can predict the gas, coke and stone temperature, the mass flow rate of coke and gas profiles inside the kiln. The models are compared to initial stone temperature with different size of stone. One can see that the influence of the size of stone particles gave small influence on combustion length but different stone temperature. Determination of the physical properties of the stone from different origins would give different results.

7 Conclusion

The effect of different parameters on the combustion process has been presented through different models in the present work. Coupled heat and mass transfer associated with this process is studied including the effects of endothermic as well as exothermic, heterogeneous and homogeneous chemical reactions. The analytically predicted the combustion time depends on the type of coke and its size, the velocity from the injected air, and the excess air number. The model for particle size distribution inside the kiln is introduced and it was capable of predicting the combustion time. Models developed are shown to be suitable for describing the typical coke behavior in many industrial applications.

1-D model for describing the combustion behavior of coke particle is developed. Smaller the coke particle is, the faster the combustion time would be. However, this leads to a lower temperature of the particles. The model describes chemical reaction, heat and mass transfer between gas and solid. According to the temperature profiles, the diameter of coke particle has a strong influence on temperature. From the simulation results, it can see that if the temperature difference between gas and solid particles is higher, this would lead to higher energy consumption. The influence of reaction coefficient is very small when the process begins with high temperature. This result shows that the reaction mechanism is supported for the low temperature process.

Experiments are performed to get the reaction coefficient due to Boudouard reaction. Using this data, combustion length is predicted for excess air number less than one. The influence of the Boudouard reaction on the combustion time and the length of combustion zone in mixed feed shaft kilns are discussed as a function of excess air number, temperature and size. It is shown that the combustion zone is shifted to the bottom of kiln with decreasing excess air number. This model serves as basic to model the limestone calcination in mixed feed kilns. The heat of the oxidation must be coupled with the endothermic

calcination. Then the real profile of the coke and limestone can be calculated. The real temperature of the coke particles additionally influences the length of the Boudouard zone. This indicates that the assumptions made are reasonable for the model to describe the most important phenomena in the kiln.

With the increasing of initial stone temperature, the combustion length varied, however, the particles size has the inverse effect on combustion length. The simulation shows the different effects of changing parameter under different operating conditions.

The developed model is suitable to study the influence of different operating conditions (excess air number, throughput, size of particle, reactivity) of the kiln. Using the present model, it would be easier to optimize the industrial kiln. Similarly, the results can be present for better understanding on coke combustion system under the shaft kiln condition.

References

[1] M.K.M. El-Fakharany, , “Process Simulation of Lime Calculation in Mixed Feed Shaft Kilns”, Ph.D. Dissertation, Otto von Guericke University of Magdeburg,Germany ,2012.

[2] F. Herz, B. Hallak, E. Specht, “ Experimental study of the combustion of lumpy coke and anthracite particles”, Industrial Furnaces and Boilers(INFUB), Gaia(Porto)-Portugal, 2015.

[3] Masoud Pahlevaninezhad., “The effects of kinetic parameters on combustion characteristics in a sintering bed”, Energy 73 (2014) 160-176

[4] Verma,C.L., “Simulation of lime shaft kilns using mathematical modelling”; Cement-Lime-Gypsum 12(1990), pp.576-582

[5] Ulzama, M.S “A theoretical analysis of single coal particle behavior during spontaneous devolatilization and combustion”, Ph.D. Dissertation, Otto von Guericke University of Magdeburg, Germany, 2007.

[6] S.Ergun, “Fluid flow through packed columns” Chem. Engng. Prog. 48 , p.p. 89/94.

[7] B. Hallak, E. Specht, R. Gröpler, and G. Warnecke, “Simulation of limestone calcination in -normal shaft kilns – mathematical model,” *ZKG Int.*, vol. 68, no. 9, pp. 66–71, 2015.

[8] K.Jin, F.Yanhui, Z.Xinxin, “Simulation of transport phenomena in coke oven with staging combustion”, Applied Thermal Engineering, Vol. 58, Septermber 2013, Pages 354-362.

[9] M. Brauer, “Grundlagen der Einphasen-und Mehrohasenstromungen” Sauelander Verlag, Aarau u. Frankfurt 1971.

[10] Y.Yamazaki, Kenichi,H,“ The effect of Matallic Iron Particle on Coke-Matrix after Coke CO_2 gasification reaction”, Journal of Thermal Science and Technology. Vol.6, No.2, 2011

[11] E. Specht, Wärme- und Stoffübertragung in der Thermoprozesstechnik-Grundlagen,Berechnungen,Prozesse. Essen:Vulkan-Verlag, 2014.

[12] B. Hallak, F. Herz, E. Specht, and G. Kehse, “Energy consumption and CO2 content in the flue gas of normal shaft kilns. Part 1: Influence of the air excess number,” *ZKG Int.*, vol. 67, no. 11, pp. 60–66, 2014.

[13] B. Hallak, F. Herz, E. Specht, and G. Kehse, “Energy consumption and CO2 content in the flue gas of normal shaft kilns. Part 2: Influence of the limestone quality and the process parameters,” *ZKG Int.*, vol. 67, no. 12, pp. 38–41, 2014.

[14] D. Hai Do, “Simulation of Lime Calcination in Normal Shaft and Parallel Flow Regenerative Kilns,” Ph.D. Dissertation, Otto-von-Guericke-Universität, Magdeburg, Germany, 2012.

[15] F. P. Incropera and D. P. DeWitt, “Introduction to Heat Transfer, ” 2011.

[16] W. Lipinski and A. Steinfeld, “Heterogeneous thermochemical decomposition under direct irradiation,” *Int. J. Heat Mass Transf.*, vol. 47, no. 8–9, pp. 1907–1916, Apr. 2004.

[17] B.Agnieszka, “Dynamic Process Simulation of Limestone Calcination in Normal Shaft Kilns”, Ph.D. Dissertation, Otto von Guericke University of Magdeburg,Germany ,2006.

[18] H.Sun “Numerical Analysis of Reaction in Cupola Melting Furnace” ISIJ International, Vol.44 (2004), No.1, pp. 27-36.

[19] A. Koekemor, “ Effect of material type and particle size distribution on pressure drop in packed beds of large particles: Extending the Ergun equation”, Fuel 158(2015) 232-238.

[20] C.Zua, L.Ying Wenn, “ Interaction mechanism between coal combustion products and coke in raceway of blast furnaces”, Journal of Iron and Steel Research, Vol.24, Issue 1, January 2017, Pages 8-17.

[21] S. Andrej, J. Oman, “ Annular shaft kiln for lime burning with kiln gas recirculation”, Applied Thermal Engineering, Vol 28, Issue 7, May 2008, Pages 785-792.

[22] Y.K. Rao and Jalan B.P., “A Study of the Rates of Carbon-Carbon Dioxide Reaction in the Temperature Range 839 to 1050 0C,” Metallurgical Transactions 3 (1972), pp. 2465.

[23] H.J.Grabke, “Oxygen Transfer and Carbon Gasification in the Reaction of Different Carbons with CO2, Carbon” 10 (1972), pp. 587.

[24] H.Cheng, Reiser B.D. and Dean S., On the Mechanism and Energies of Boudouard Reaction at FeO (1 0 0) Surface: 2CO→C+CO2, Catalysis Today 50 (1999), pp. 579.

[25] S.Luo, H. Singbo, " Combustion kinetics of the coke on deactivated dehydrogenation catalysts", Vol.129, January 2015, Pages 156-161

[26] D.Hai Do and E.Specht, "Numerical simulation of heat and mass transfer of limestone decomposition in normal shaft kiln" ASME/JSME 2011 8th Thermal Engineering Joint Conference (AJTEC2011) March 13-17, 2011, Honolulu, Hawaii, USA.

[27] Landolt and Börnstein, Thermodynamic Properties of Inorganic Materials: PureSubstances, New Series. Berlin: Springer, 2002.

[28] N.N. Viswanathan, M.N.Srinivasan, "Process simulation of cupola". ISIJ International, vol.38, pp. 1062-1068,1998.

[29] H.S.Fogler, "Elements of Chemical Reaction Engineering", 4th.ed. Prentice Hall PRT, 2005.

[30] R.He, T.Suda, T.Fujimori, "Effects of particle sizes on transport phenomena in single char combustion". Heat and Mass Transfer, vol.46, pp.3619-3627,2003.

[31] G.Sandaka, "Calcination behavior of lumpy limestones from different origins", Ph.D. Dissertation, Otto von Guericke University of Magdeburg,Germany ,2015.

[32] A. Kasai, T.Murayama and Y.Ono, "Measurement of effective thermal conductivity of coke", ISIJ International, vol.33, No.6, pp.697-702,1993.

[33] S.Robert, T.Tadeusz, "1D Mathematical Model of Coke Combustion", IAENG Inernational Journal of Applied Mathematics, 45:3, IJAM_45_3_10.

List of Publications

- ✓ Conference paper titled "**Combustion Behavior of Coke in Shaft Kilns with Hypostoichiometric Air Flow** "has been published in **11th European Conference on Industrial Furnaces and Boilers (INFUB)**.

Curriculum Vitae

Name	Nyein Nyein Linn
Nationality	Myanmar
Date of birth	07.01.1985
Place of birth	Namtu, Shan state, Myanmar
Father	U Shin Pu
Mother	Daw Annie
Marital status	Single

2002-2006	Bachelor of Engineering in Mechanical Engineering Government Technological Unviersity (Lashio), Myanmar
2007-2009	Demostrator, Mechanical Engineering Department, Government Technological Unviersity (Myitkyina), Myanmar
2009-2011	Master of Technology, Thermal Engineering Institut Teknologi Bandung, Indonesia.
2012-2014	Assistant lecturer, Mechanical Engineering Department, Mandalay Technological University, Pateingyi, Myanmar
2014-2017	Ph.D study, Institute of Fluid Dynamics and Thermodynamics, Otto-von-Guericke-University Magdeburg, Germany.
Contact	nyein0906@gmail.com, +95-9440424713(Myanmar)